OPTICAL ANALYSIS FOR LASER HETERODYNE COMMUNICATION SYSTEM

T. A. Nussmeier
Hughes Research Laboratories
3011 Malibu Canyon Road
Malibu, California 90265

March 1974
Final Technical Report
Contract NAS 5-21898

Prepared for
GODDARD SPACE FLIGHT CENTER
Greenbelt, Maryland 20771

1. Report No.	2. Government Accession No.	3. Recipient's Catalog No.
4. Title and Subtitle OPTICAL ANALYSIS FOR LASER HETERODYNE COMMUNICATION SYSTEM		5. Report Date March 1974 6. Performing Organization Code
7. Author(s) T.A. Nussmeier S.H. Brewer		8. Performing Organization Report No.
9. Performing Organization Name and Address Hughes Research Laboratories 3011 Malibu Canyon Road Malibu, California 90265		10. Work Unit No. 11. Contract or Grant No. NAS 5-21898
12. Sponsoring Agency Name and Address		13. Type of Report and Period Covered 27 Nov. 1972 through 26 Nov. 1973 Final Technical Report 14. Sponsoring Agency Code

15. Supplementary Notes

16. Abstract

A new computer program has been developed to predict the effects of optical aberrations on transmitters and receivers used in heterodyne communication systems. Two independent optical trains for the received signal and the local oscillator are specified and evaluated. A value of heterodyne signal power is evaluated and normalized with respect to an ideal value to provide a quantitative value for receiver degradation. Values of local oscillator illumination efficiency, optical transmission, detection efficiency and phase match efficiency are also evaluated to isolate the cause of any unexpected degradations. The program has been used for a tolerance analysis of a selected system designed for space communications, and for evaluation of several other systems. Results of these analyses are presented.

17. Key Words (Suggested by Author(s))	18. Distribution Statement
Heterodyne Communications Numerical Analysis Optical Abbreviations aberrations Space Applications	

19. Security Classif. (of this report)	20. Security Classif. (of this page)	21. No. of Pages	22. Price*
UNCLASSIFIED	UNCLASSIFIED	177	

* For sale by the National Technical Information Service, Springfield, Virginia 22151

TABLE OF CONTENTS

LIST OF ILLUSTRATIONS

SECTION I

INTRODUCTION AND SUMMARY

1.1 INTRODUCTION

The development of laser communication systems for space is a vital step toward providing the nation with the capability for synchronous relays, deep space probes, and ground stations. The special properties of laser systems make such links possible without the need for large antenna structures, and the need for high power as required by microwave systems. Such a capability is particularly required, within this decade, to furnish wideband data links from low altitude satellites with high resolution sensors to earth synchronous communication terminals from which the information may then be relayed to ground stations.

Spaceborne communication systems must necessarily operate near theoretical thresholds. The demands against weight, prime power, information rate, cost, reliability, and other factors do not allow a large safety margin to compensate for overlooked degradations. For this reason and others, the present computer program, LACOMA (LAser COMmunicator Analysis program), has been developed to accurately simulate optical configurations of heterodyne communication systems and to evaluate the effects of aberrations, distortions and misalignments on the heterodyne performance of these systems. The program has been developed with the communication engineer in mind. It has been designed to be easy to program and easy to interpret. Output is specified in terms of antenna gain to allow results to be directly applied to system calculations. Absolute power values are also printed out to provide actual signal levels for evaluation.

1.2 COMPARISON WITH OTHER OPTICAL COMPUTER PROGRAMS

LACOMA represents a major advance in the optical analysis of laser heterodyne communication systems. It also represents an advance in general optical system analysis since it includes the effects of gaussian pupil functions. Some of the optical analysis programs with which LACOMA might be compared are:

1. POLYPAGOS – Aerospace Corporation
2. SLAP (Spectral Lens Analysis Program) – PAGOS Corporation
3. MTF – D. Grey Associates
4. ACCOS-GOALS – Scientific Computations Inc.

These represent a cross section of the generally available optical analysis programs and will serve as benchmarks to compare LACOMA.

LACOMA is a direct descendant of SLAP which is in turn an updated version of POLYPAGOS, so that one would logically expect more similarities between these programs. An overview of the programs is provided by the tabular check sheet of Table 1-1. A major difference between these programs is the Fourier transform algorithms. LACOMA (also SLAP and POLYPAGOS) utilizes an algorithm which permits the specification of number and location of the output points for the computed spread function (ASF, PSF) results. For a given optical system or telescope, LACOMA allows sampling of the Airy disc via grid sizes from 2 x 2 to 101 x 101 or any other arrays between these extremes. This is not possible with the algorithms used by the other programs. Not included in the table is a cost comparison. If it were possible to set up a cost or running time comparison, the Gray-MTF might show somewhat better due to its heavy emphasis on machine language programming for the CDC 6600. The ACCOS-GOALS would probably score as the most costly. Some of the tabulated categories are subjective such as the ease of input, but they reflect more than a single view.

TABLE 1-1.

Comparison of Optical Computer Programs

Feature	LACOMA	SLAP	POLY-PAGOS	MTF-GREY	ACCOS/ GOALS
Heterodyne Power	X				
Detector Power	X	X	X	X	
Multiple Detectors	X				
Multiple Beams	X				
Optimization Capability					X
Interactive Operation					X
Gaussian Input Pupil	X				
Transmittance					
Output Grid Selection	X	X	X		
Deformed Surfaces	X	X	X		
Perfect Surface	X	X	X		
3-D Tilts and Decentrations	X	X	X	X	X
Geometrical Analysis		X	X		X
Generalized Aperture Description	X	X			
Ease of Input	X	X	X		X

T1199

LACOMA constitutes a new tool in the optical communications field. It is unique in its ability to perform an accurate analysis of the laser communication system.

1.3 RECOMMENDED ADDITIONS FOR INCREASED VERSATILITY

LACOMA has been shown to be a unique and useful tool in the analysis of heterodyne systems (see Section III). During the course of using the program, it was often tempting to use it as a design tool. This led to an investigation into the possibility of modifying the present program to combine the features of design and analysis. The result of this study led to the following list of recommended additions, some of which would provide some design or optimization capability, and others that would enhance the analysis function.

a. Optimization – Conventional optimization techniques will not necessarily produce optimum optics for laser communication systems, especially for the transmitter and local oscillator. A gaussian beam amounts to an aperture weighting function which should be included in the optimization process. Also, ideally, the received signal optics and local oscillator optics should be optimized on the basis of their combined beams. It is recommended that work in the optimization area occur in stages.

(1) Focus optimization – optimization of best focus position for a given system configuration.

(2) General optimization Phase I – Development of algorithms and approach to optimization for transmitter and receiver.

(3) General optimization – Phase II – Development of optimization program based on algorithms and approach spelled out in Phase I.

b. Tolerance Analysis – Automatic determination of tolerance budgets necessary to maintain specified level of performance. This can be a separately addressable subroutine of an optimization program.

c. Perturbed Focal Surface — Revisions to permit tilted, decentered, curved focal surface without dummy surfaces.

d. Return Option for Tilted-Decentered Surfaces — To automatically restore coordinate system after tilt and/or decentration without dummy surfaces.

e. Aberrated Entrance Pupil — Accommodation of aberrations of entrance pupil due to tilts-decentrations, input beam inclination.

f. Potato Chip Aspheres — Generalize deformed surface options to include more generally deformed surfaces due to thermal-mechanical stresses or potato chip aspheres.

g. Pseudo-diffraction Intensity Function — Geometrical analysis to be used for evaluation of systems without involving full scale diffraction-heterodyne analysis.

h. Transmittance — Subroutine to compute losses due to absorption losses, Fresnel reflection losses, antireflection films, multilayer thin films.

Polarization — extension to determine orthogonal polarization components of beam.

i. Graphics — Isometric and contour representation of wave function, pupil function, spread functions, etc.

Interactive graphics — for analysis and optimization.

j. Fresnel Diffraction — Modification of diffraction integrals of LACOMA to permit computation of amplitude or intensity function out of Fraunhofer plane.

k. Thermal-mechanical Structural Analysis — Extension of LACOMA to interface with thermal-mechanical analysis programs such as STARDYNE, NASTRAN, etc., to perform overall system analysis.

Some of the listed modifications are contained in other programs as seen in Table 2-1, while others, such as transmittance, are unique. Transmittance in particular should be considered for LACOMA, since this parameter affects the amplitude distribution across the exit pupil, which, in turn, can make a significant difference in phase distribution across the focal plane, and can also cause a shift in the location of the

focal plane. Other modifications that are considered particularly appropriate to heterodyne systems are focus optimization, perturbed focal surfaces, and the related Fresnel diffraction modification.

1.4 SUMMARY

Section II of this report is designed to be a self-contained user's manual. An engineer familiar with heterodyne optical systems should be able to utilize LACOMA with this manual and a minimal amount of help from computer personnel.

Section III contains an analysis of the sample system, the optical mechanical subsystem developed for NASA under contract NAS-5-21859. This analysis includes a "perfect" reference system, several runs for the system with no distortions or errors, and finally analyses with tilts and distortions that might be introduced by manufacturing tolerances or by mechanical or thermal stress. This section has been arranged to provide a specific example for using LACOMA.

At the end of Section III, two additional analyses are summarized, one that establishes bounds on the field of view of heterodyne receivers, and a second that analyzes a telescope designed for a terrestrial system. This last example was selected because there is sufficient aberration to cause significant performance degradation, thus providing a means for illustrating the advantages of LACOMA over conventional optical programs.

Section IV contains a detailed discussion of the program. Specific equations and computational flow diagrams are discussed. Error sources and their probable magnitudes are covered at the end of this section.

SECTION II

LACOMA USER'S MANUAL

2.1 GENERAL PROGRAM DESCRIPTION

The program has been developed to allow prediction of laser communication system performance and to permit tradeoff analysis in the design of these systems. The program is set up to allow the optional analysis of transmitter or receiver optics.

For the transmitter, the program starts with the data for the specified laser beam and propagates the beam through the optical train to determine the far-field intensity function.

For the receiver, the program carries the received signal beam through the optical train to the detector. The local oscillator laser beam is also traced to the detector where the two beams are combined and the various quality criteria computed.

The computation for the receiver requires the entry of two sets of optical data — one for the received signal optics and another for the local oscillator optics. The program checks whether one or two sets of data have been entered (see Fig. 2-1). If there is only one set, it performs the transmitter analysis. Two sets of data precipitate the receiver analysis.

a. Transmitter — For a single set of optical data the program computes the gaussian beam profile and any specified quadratic phase on the input beam and traces it through the optical train, carrying the complex amplitude function through in the form of an amplitude array B (i, j), and the optical path difference array W (i, j) (see Fig. 2-2). At the exit pupil it computes the rms wavefront error σW and the normalized Strehl intensity I (σ) for the (systematic) system wavefront.

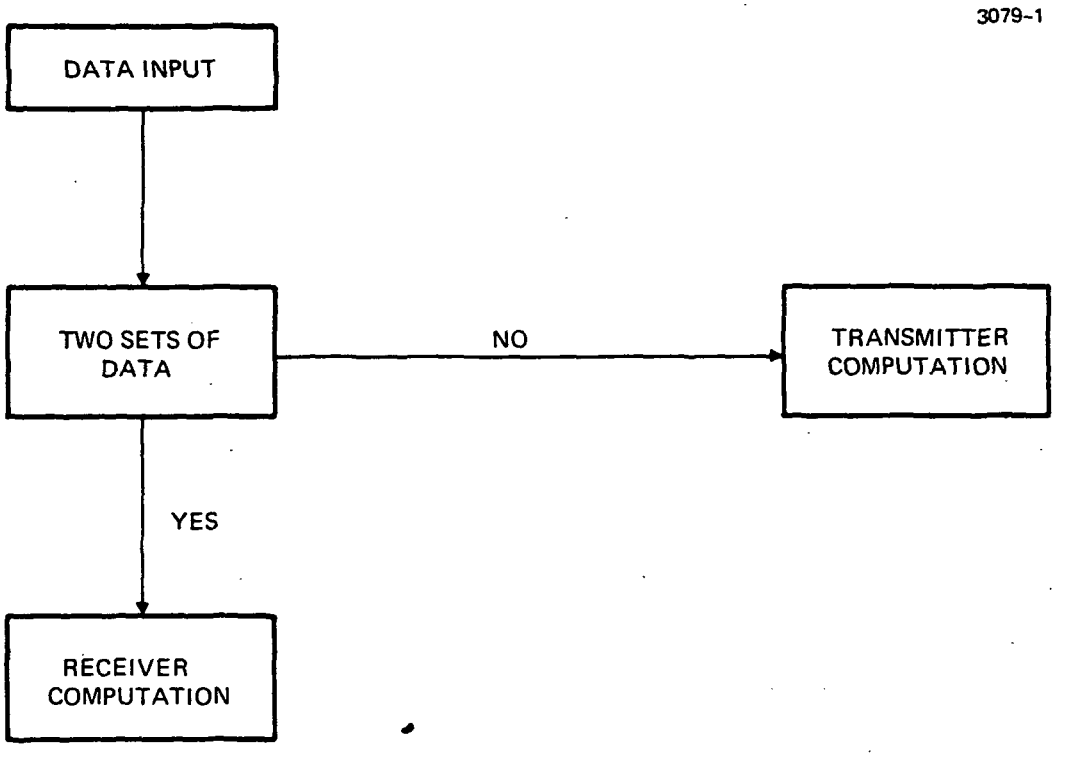

Fig. 2-1. Basic flow diagram.

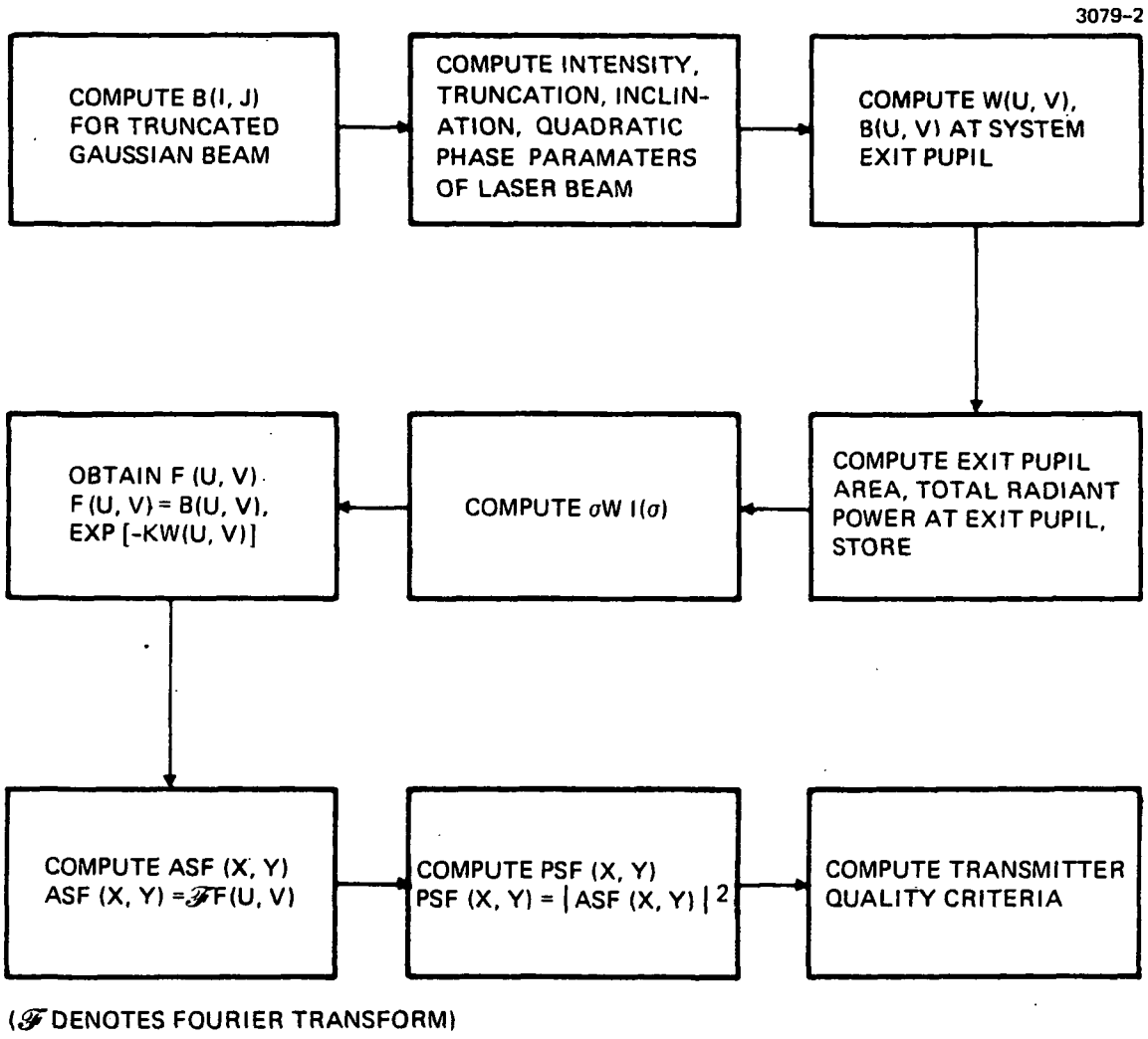

Fig. 2-2. Transmitter computation flow

It forms the pupil function F (u, v) (≡ complex amplitude array at the exit pupil).

$$F(u,v) = B(u,v) \cdot \exp\left[-KW(u,v)\right] \qquad (2\text{-}1)$$

$$K = \frac{2\pi_i}{\lambda}$$

u, v = pupil coordinates

The Fourier transform of F(u, v) yields the far-field amplitude spread function ASF(x, y)

$$ASF(x,y) = \mathscr{F}\, F(u,v) \qquad (2\text{-}2)$$

$\mathscr{F}$ denotes Fourier transform.

Squaring the modulus of the complex amplitude spread function gives the far-field intensity or point spread function PSF (x, y)

$$PSF(x,y) = \left|ASF(x,y)\right|^2 \qquad (2\text{-}3)$$

b. Transmitter Quality Criteria – The far-field intensity function is itself a measure of the transmitter performance. This is augmented by the computation and output of: the peak far-field intensity value, optical transmission, maximum antenna gain, and the overall transmitter efficiency.

- Peak intensity – This is simply the peak value of the far-field intensity function and is included in the quality criteria in case the investigator chooses not to print out the entire far-field intensity function.

- Optical Transmission – This is the ratio of the exit pupil power P_e to the total laser power P_o

$$\text{Optical Transmission} = \frac{P_e}{P_o} \qquad (2\text{-}4)$$

Transmission losses accounted for here are those due to vignetting and obscuration.

- Maximum Antenna Gain — This is computed for the exit pupil area A_e.

$$\text{Maximum Antenna Gain} = \frac{4\pi A_e}{\lambda^2} \tag{2-5}$$

- Overall Transmitter Efficiency — This value relates the computed peak far-field intensity of the transmitter to that for an ideal transmitter with the same input power and effective exit pupil area

$$\text{Overall Transmitter Efficiency} = \frac{I_r R^2 \lambda^2}{A_e P_e} \tag{2-6}$$

I_r = Transmitter peak intensity

R = Range

c. Receiver — When two sets of optical data are entered, the program performs the receiver analysis. The optical data are entered sequentially. That is, there is a total of N surfaces entered where

$$N = N_1 + N_2$$

The first set of N_1 surfaces represents the received signal optical train and the following N_2 surfaces are for the local oscillator optical train. The program (Fig. 2-3) computes the received signal pupil function $F_1(u, v)$.

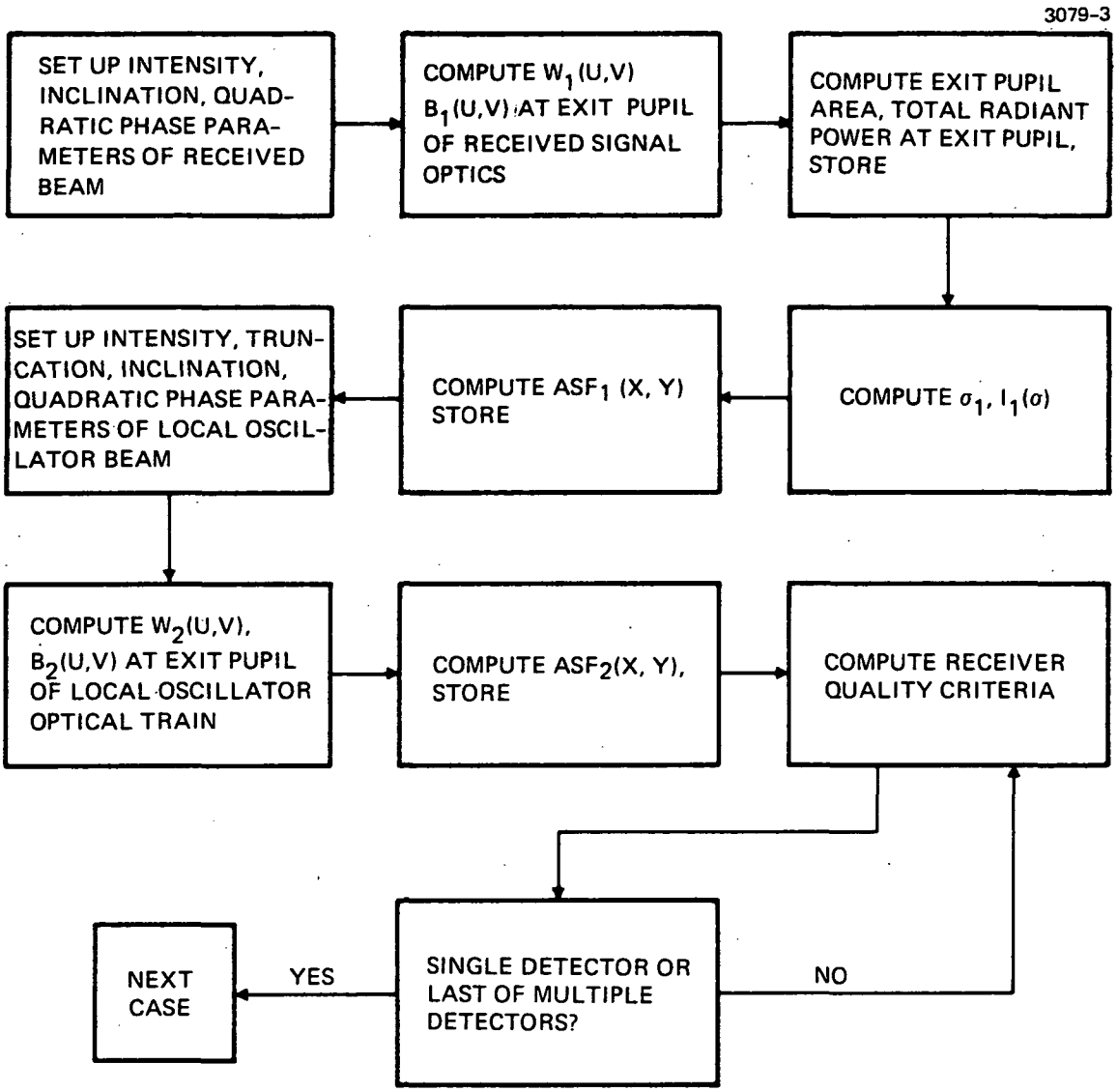

Fig. 2-3. Receiver computational flow.

$$\text{Nonheterodyne Detection Efficiency} \equiv \frac{P_D}{P_o} \qquad (2\text{-}12)$$

- L.O. illumination Efficiency — This efficiency compares the heterodyne power $\bar{P}_h$ for the two given signals with no phase error with the optimum heterodyne power value for two signals of corresponding power

$$\text{L.O. Illumination Efficiency} = \frac{\bar{P}_h}{\sqrt{P_D P_L}} \qquad (2\text{-}13)$$

- Maximum Antenna Gain — This is the theoretical gain for the effective entrance pupil area A of the received signal optical train.

$$\text{Maximum Antenna Gain} = \frac{4\pi A}{\lambda^2} \qquad (2\text{-}14)$$

- Receiver Efficiency to i.f. — Assuming a quantum efficiency of 1, this efficiency relates the square of the heterodyne power P_h^2 to the product of the total received power P_o and the L.O. power P_L, and is a measure of overall receiver performance.

$$\text{Receiver Efficiency to i.f.} = \frac{P_h^2}{P_o P_L} \qquad (2\text{-}15)$$

2.2 DATA DISCUSSION

The program performs analyses on laser communication system optics as summarized in Section 2-1 with the detailed computational procedure described in Section IV of this document. The analyses performed by the program are briefly listed here.

Paraxial Analysis (Section 4.1)

Ray Trace-Optical Path Difference (Section 4.3)

Amplitude and Point Spread Function (Section 4.8)

Receiver Quality Criteria (Section 4.9)

Transmitter Quality Criteria (Section 4.10)

Numerous options are available for handling of the data, choice of computations, output data, etc. Two data arrays IPRØG and IDETEC control the major functions and are discussed in detail.

Some optical system parameters and/or configurations which can be accommodated by LACOMA include:

- Catoptric systems
- Catadioptric systems
- Dioptric systems
- Spherical surfaces
- Aspheres
- Cylindrical surfaces
- Toroidal surfaces
- Surfaces with slight cylindrical error or warpage
- Periodic surface errors
- Misaligned (tilted, and/or decentered) systems
- Composite vignetting and obscuration
- Afocal systems (via perfect imaging lens)

Any of the analyses can be performed for any of the system parameters or configurations.

a. Data Requirements – A certain minimum amount of data must be entered to obtain any results. These minimum data requirements can combine with built-in data or default conditions to give a complete system analysis. These data are listed here with their associated program variable names and text references.

Data	Variable Name	Text Reference
Number of surfaces	N	2.6, Fig. 2-1
Surface curvature	RHOS (ρ_s)	2.6, 4.1, 4.3, Fig. 2-1, 4-1
Surface-surface spacing	TS (t_s)	2.6, 4.1, 4.2, 4.3, Fig. 2-1, 4-2
Refractive index	XMUS (μ_s)	2.6, 4.1, 4.3, Fig. 2-1
Entrance pupil semi-diameter	BETA0 (β_o)	2.6, 4.1, Fig. 2-1

With these data input, quality criteria will be obtained for a transmitter or receiver depending on the entry of values for N(1) only or N(1) and N(2). The computations will be performed under the following default conditions.

(1) Plane wavefront input-uniphase energy

(2) Analysis performed at paraxial image position

(3) Axial analysis only — no inclination of input beam

(4) Entrance pupil at first surface

(5) No misalignment

(6) No vignetting or obscuration

(7) All surfaces rotationally symmetric spheres or aspheres

(8) Wavelength = 0.010611385 (mm)

(9) Data assumed input in millimeters

(10) For receiver — single circular detector, centered on optical axis, detector radius = radius of AIRY disc for uniformly illuminated unobscured aperture of specified semi-diameter.

(11) Pupil array = 51 x 51

(12) Spread function array = 51 x 51

(13) Detector array = 21 x 21 (round)

(14) Output data = Paraxial analysis, wavefront statistics, quality criteria

(15) Gaussian beam truncation point assumed $1/e^2$ intensity point.

b. Data Discussion — System parameters and program options effected by the default conditions are listed below. The relevant variable names available to override the default conditions are given in parentheses with page references for descriptions of the variables.

(1) Input wavefront or object distance — Section 4.1, 4.7

XLINV (Lo^{-1})

MAG

(2) Image (or detector) location — Section 4.2

IFLG1

TS(N-1) (t_{N-1})

TS (N) (t_N)

(3) Inclination of input beam — Section 4.7

H

(4) Entrance Pupil location — Section 4.1

M

(5) Misalignment — Section 4.6

DLTAX (Δx)

DLTAY (Δy)

DLTAZ (Δz)

THTAX (θx)

THTAY (θy)

THTAZ (θz)

(6) Vignetting or obscuration — Section 4.4

BETASX (β_{sx})

BETASY (β_{sy})

BETAPX (β_{px})

BETAPY (β_{py})

VZERØ (V_o)

VPI (V_π)

GZERØ (G_o)

GPI (G_π)

UZERØ (U_o)

(7) Special surfaces — Section 4.3

RHØ1 (ρ_1)

RHØ2 (ρ_2)

CC (b)

CRS (a)

PHI (ϕ)

AMP (C_1)

FREQ (C_2)

C3 (C_3)

USI (U_s)

VSI (V_2)

(8) Wavelength — Section 4.8

VLAMDA (λ)

(9) System units of length – All Dimensional Data Must Be Input In Same Units as Wavelength.

(10) Detector Parameters — Section 4.8

IDETEC

NDET

(11)	Pupil Array	Section 4.7
	NXY	
(12)	Spread function array	Section 4.7
	NFRS	
	DELFS	
(13)	Detector Array	
	IDETEC	Section 4.8
	DELFS	
(14)	Output Data	
	IPRØG	
(15)	Gaussian beam parameters	Section 4.7
	ZØMEGA (ω_o)	
	PZERØ (P_o)	

2.3 SETTING UP THE DATA DECK

The data deck consists of the following:

- Title Card – one card with any combination of characters in columns 1 to 80.
- First Data Card – The first card must contain $INP in columns 2 to 5, followed by a blank. Data may begin on this card or the next.
- Data Cards – As many as necessary with data in cols. 2 to 80.
- End of data card – the last card must contain $END in cols. 2 to 5.

The details of the input format of these cards are discussed in the Input Format, Section 2.5.

The details of the individual data are given in Input Parameters, Section 2.6.

2.4 DATA PREPARATION PROCEDURE

For the receiver analysis, two sets of data are entered sequentially. The first N(1) surfaces are the received signal optics. These are immediately followed by N(2) surfaces representing the local oscillator optics. A total of N(1) + N(2) surfaces are entered, surface No. 1 is the first surface of the received signal optics, surface No. N(1) is the last (detector) surface for the received signal optics, surface No. (N(1) + 1)) is the first surface of the local oscillator optics and surface No. (N(1) + N(2)) is the last (detector) surface for the local oscillator optics. The system parameters for the received signal optics versus the LO optics are defined by two component arrays with the first component representing the received signal optics in all cases.

Examples: The sample case entitled "RECEIVER TEST CASE #2", (Appendix D) indicates surface data for a total of twenty surfaces. Also input are

- N(1) = -12, -8, where the negative signs indicate that data is input in radius form rather than curvature, the first twelve surfaces are the received signal optics and the following eight are the LO optics, thus accounting for the twenty surfaces.
- BETA0(1) = 53.975, 2.621, the received signal optics semi-diameter is 53.975 mm and that for the LO is 2.621 mm.

Notice that, as discussed in Input Format, Section 2.5,

N(1) = -12, -8,

is the same as

N(1) = -12, N(2) = -8,

and

BETA0(1) = 53.975, 2.621,

is the same as

BETA0(1) = 53.975, BETA0(2) = 2.621,

The program indication of whether a transmitter or receiver is being analyzed is based on the value of N(2)

If N(2) = 0 → Transmitter analysis

If N(2) ≠ 0 → Receiver analysis.

It is recommended that the user refer to the facsimile input sheet, Fig. 2-4. All of the variables are shown on this sheet. The user can look at each variable, decide whether it applies to his problem, enter an appropriate value if it does and move on to the next variable. This procedure guarantees that no data is overlooked. Notice that the variables may occur in any order in the data deck which may or may not correspond to the order in which the variables appear on the facsimile input sheet.

2.5 INPUT FORMAT

Input data consists of two groups, both of which must be present for each case, in the following order:

a. One title card — any combination of blanks, letters, numerals, and the characters + -, = / $ ( ) . * in columns 1 to 60.

b. One or more cards of numerical data in colums 2 to 80, which are read in by means of the NAMELIST input feature, as described below.

```
$INP N(1) = , , M(1) = , , BETAO(1) = , , XLINV(1) = , , MAG(1) = , ,
IFLG1(1) = , , H(1) = , , RHOS(1) = , , , , TS(1) = , , , ,  XMUS(1) = , , ,
SKAPA(1) = , , , DFORM(1,1) = , , , RADS(1) = , , , RHO1(1) = , , ,
RHO2(1) = , , ,  PHI(1) = , , , AMP(1) = , , , FREQ(1) = , , , USI(1) = , , ,
VSI(1) = , , , C3(1) = , , , CRS(1) = , , CC(1) = , , THTAX(1) = , , ,
THTAY(1) = , , THTAZ(1) = , , DLTAX(1) = , , DLTAY(1) = , , DLTAZ(1) = , ,
BETAPX(1) = , , , BETAPY(1) , , , BETASX(1) = , , , BETASY(1) = , , ,
VZERO(1) = , , , VPI(1) = , , GZERO(1) = , , , GPI(1) = , , UZERO(1) = ,
VLAMDA = , NFRS = , DELFS = , NXY = , PZERO(1) = , , ZOMEGA = ,
IPROG(1) = , , , IDETEC(1,1) = , , , NDET = , FLAG = ,
$END
```

Fig. 2-4. Facsimile input sheet.

NAMELIST REQUIREMENTS

a. Column 1 must be blank on all cards.

b. The first card of the data must contain $INP in columns 2 to 5, followed by a blank space. Variable values may begin on this card or on the next card. The termination of a data set is indicated by the characters $END in columns 2 to 5. The appearance of the character $ anywhere else will cause an error.

c. Variable names

1. Single-valued variables are input in the form

(name) = (value)

Example: NPTS = 16, DX = 0.02,

2. Commas follow every numerical value.

3. Arrays may be put in as single elements with the subscript or by listing the consecutive values:
Examples: A(1) = 3, A(4) =-1.69, A(5) = 32.1,

or

A = 3, 0., 0., -1.69, 32.1,

4. Double-subscripted arrays must be input columnwise.
Example: A 4 x 3 matrix A may be input in the order

$A = a_{11}, a_{21}, a_{31}, a_{41}, a_{12}, a_{22}, a_{32}, a_{42}, a_{13},$

a_{23}, a_{33}, a_{43}

5. A string of consecutive elements in an array may be entered by giving the name and subscript of the first element.
Example: To input elements 19 through 23 of array A, write

$A(19) = a_{19}, a_{20}, a_{21}, a_{22}, a_{23}$

d. Value formats

1. Whole numbers may be input with or without a decimal point. Exponents (power of ten) may be indicated by an E followed by the power, or the E may be omitted and a signed integer used for the power.

   7.46×10^{6} may be written 7.46E6, 7.46E+6, 7.46+6, or 7.46+06:

   7.46×10^{-6} may be written 7.46E-6, 7.46-6, or 7.46-06

2. No plus signs are necessary for positive values or exponents. Negative values or exponents are indicated with a minus sign.

   Example: -4.396×10^{-8} becomes -4.396E-8 or -4.396-8

3. Double precision numbers take a D instead of an E to indicate the exponent. If a double precision number contains less than nine significant digits, it must have a D plus exponent for proper conversion.

   Examples: 3.141592653587973 is written just like that, while 3.14159 becomes 3.14159D0.

4. Identical consecutive values of an array may be abbreviated by writing an integral multiple and an asterisk(*) in front of the value.

   Example: if $A_1 = A_2 = 2$, and $A_3 = A_4 \ldots = A_{33} = -4$,

   write

   A = 1., 2., 31*-4,

e. Errors

1. If the $INP followed by a blank does not appear as the first punches in the first card (excluding column 1), the computer will ignore that card and continue reading, trying to find $INP in the next cards. This process continues until $INP is found or there are no more cards. No error message is given if the wrong cards are being read and rejected.

2. If a variable name is misspelled, the computer will give an error trace, terminate execution, print the following message: "Namelist name not found."

f. Order multiple cases

1. Variables may appear in any order.

2. Not all data need appear in any set. On successive cases where it is desired to change just a few values, only those variables need be input, with the rest retaining their values from previous cases.

3. Values are all zero initially, unless otherwise specified. Thus, it is necessary to input only nonzero values. If runs are stacked, however, any data not written over will carry over from the preceding run.

4. The same variable name may appear two or more times in a data set. The value physically last in the deck will override any previous values. Thus, it is not necessary to repunch cards to change numbers, just place a card with the changed value (and variable name with proper subscript, if any) somewhere following the old value.

2.6 INPUT PARAMETERS

Variable Name	Description, Comments, Text References
N(I)	One-dimensional array of length (2), specifying number of surfaces. Count the image surface but not the entrance pupil or object. A negative sign affixed to N indicates input of RADS (radius) instead of RHØS (curvature). If N(2) = 0, transmitter analysis is to be performed. If N(2) ≠ 0, N(1) specifies the number of surfaces in the received signal optics and N(2) is the number of surfaces in the local oscillator optics.
M(I)	One-dimensional array of length (2) for surface number of aperture stop. M(1) ≡ surface number of received signal (or transmitter) aperture stop. M(2) ≡ LO aperture stop surface number. Default values: M(1) = 1, N(2) + 1.
BETA0(I)	One-dimensional array of length (2) for semi-diameter of entrance pupil. BETA0(1) → received signal or transmitter. BETA0(2) → LO.
XLINV(I)	One-dimensional array of length (2) specifying inverse of radius of incident wavefront at entrance pupil. XLINV(1) → Received signal or transmitter. XLINV(2) → L.O. Default values: XLINV(1) = 0., 0.,
MAG(I)	One-dimensional array of length (2) specifying magnification of output versus input wavefront radius. $MAG = -R_N/R_o$ where $R_N \equiv$ output wavefront radius $R_o \equiv$ input wavefront radius

and the sign conventions on R_o, R_N are standard.

MAG(1) → Received signal or transmitter.

MAG(2) → L.O.

Default: MAG(1) = 0., 0.,

IFLG1(I) One-dimensional array of length (2) controlling location of image (or detector).

IF IFLG1 = 0 $T'_{N-1} = BF + T_N$

IF IFLG1 = 1 $T'_{N-1} = T_{N-1} + T_N$

where

T'_{N-1} ≡ spacing used in analysis as spacing from surface (N-1) to image

BF ≡ Paraxial back focus

T_{N-1} ≡ input value TS(N-1)

T_N ≡ input value TS(N)

IFLG1(1) → Received signal or transmitter

IFLG1(2) → L.O.

Default: IFLG1(1) = 0, 0,

NOTE: For IFLG1 = 1 and $T_N \neq 0$, T_{N-1} will not revert to its previous value when running consecutive cases.

H(I) One-dimensional array of length (2) specifying obliquity in radians of input beam.

H(1) Received signal or transmitter

H(2) L.O.

Default: H(1) = 0., 0.,

RHØS(I) One-dimensional array of length (101) for the spherical curvature (or base curvature of an asphere) for the I^{th} surface when N is positive. The sign convention to be applied to RHØS is that the curvature of a surface is positive when the center of curvature lies to the right of the surface.

RADS(I) One-dimensional array of length (101) for the spherical radius (or base radius of an asphere) for the I^{th} optical surface. The sign convention for RADS is the same as that for RHØS.

N must be entered negative when data is input into this array.

RADS(I) = 0 defines a plane surface.

TS(I) One-dimensional array (101) for the axial separation between surface I and I + 1.

The sign convention for TS is that TS is positive for spacings measured from left to right.

XMUS(I) One-dimensional array (101) for the index or refraction of the medium between surfaces I and I + 1.
A sign change between XMUS (I-1) and XMUS(I) indicates a reflection at surface I.

Default: XMUS(I) = 1.

DFØRM(J,I) Two-dimensional array (5, 101) for aspheric deformation coefficients of the 2(J+1) power terms at surface I
DFORM(1,I) ≡ $\overline{\alpha}$
DFORM(2,I) ≡ $\overline{\beta}$
DFORM(3,I) ≡ $\overline{\gamma}$
DFORM(4,I) ≡ $\overline{\delta}$
DFORM(5,I) ≡ $\overline{\epsilon}$

The aspheric expression is

$$\zeta = \frac{\rho Q^2}{1 + (1 - \kappa \rho^2 Q^2)^{\frac{1}{2}}} + \bar{\alpha} Q^4 + \bar{\beta} Q^6 + \bar{\gamma} Q^8 + \ldots$$

where

$Q^2 = x^2 + y^2$

$x, y \equiv$ surface intercept points

$\rho \equiv$ RHØS = base curvature

$\kappa \equiv (1 - \epsilon^2) =$ conic coefficient – SKAPA

SKAPA(I) One-dimensional array (101) for conic coefficient of surface I

where

SKAPA $\equiv \kappa = 1 - \epsilon^2$

$\epsilon \equiv$ conic eccentricity

$$\epsilon = \frac{S_2 + S_1}{S_2 - S_1}$$

$S_1 =$ distance from first focus to conic

$S_2 =$ distance from conic to second focus

RHØ1(I) One-dimensional array (101) for base curvature of aspheric (acircular) cylinder. Input in addition to RHØS(I). RHØ1 is used for tracing exact rays through surface I while RHØS is used in the paraxial ray trace, determining the first order parameters of surface I.

RHØ2(I) One-dimensional array (101). Toric rotation curvature of surface I. RHØ2 used (with RHØ1) for exact ray trace. RHØS used in paraxial analysis. The optical axis and the axes of RHØ1 and RHØ2 are mutually orthogonal.

CRS(I) — One-dimensional array (101). Constant of rotational symmetry at surface I. CRS(I) = 1., for rotationally symmetrical surface of curvature RHØ1(I). CRS(I) = -1. identifies surface I as a "perfect" surface.

CC(I) — Cylindrical constant. When CC(I) = 0 and CRS(I) = 0. surface is cylinder with curvature RHØ1 or RHØ2 depending on which is nonzero. If RHØ1 and RHØ2 are nonzero, surface is toric.

PHI(I) — One-dimensional array (101). Angular rotation of cylindrical axes. For PHI(I)=0 the axis of the RHØ1 cylinder is parallel to the y axis and the axis of the RHØ2 cylinder is parallel to the x axis.

AMP(I) — One-dimensional array (101). Amplitude term for periodic surface error function at surface I.

FREQ (I) — One-dimensional array (101). Frequency component associated with sinc function portion of periodic surface error. A surface of semidiameter BETA0 will exhibit NZ sinc function zeroes between the center and the edge for

$$\frac{NZ}{BETA0} \leq FREQ < \frac{NZ+1}{BETA0}$$

C3(I) — One-dimensional array (101). Frequency component associated with cosine function portion of periodic surface error. A surface of semidiameter BETA0 will exhibit NC complete cycles between the center and the edge for

$$\frac{2NC}{BETA0} \leq C3 < \frac{2\,(NC+1)}{BETA0}$$

USI(I)	One-dimensional array (101). Displacement in x direction of origin of periodic surface error at surface I.
VSI(I)	One-dimensional array (101). Displacement in y direction of origin of origin of periodic surface error at surface I.
DLTAX(I)	One-dimensional array (101) for displacement Δx of coordinate system at surface I.
DLTAY(I)	One-dimensional array (101) displacement Δy of coordinate system at surface I.
DLTAZ(I)	One-dimensional array (101), displacement Δz of coordinate system at surface I.
THTAX(I)	One-dimensional array (101) for angular rotation or tilt θx in radians around the y axis at surface I. If THTAX(I) input greater than 2π, it is assumed to be degrees.
THTAY(I)	One-dimensional array (101), angular rotation or tilt θy in radians (or degrees if $\theta y > 2\pi$) around the x axis at surface I.
THTAZ(I)	One-dimensional array (101), angular rotation in radians (degrees if $\theta z > 2\pi$) around the z (optical) axis at surface I.
BETAPX(I)	One-dimensional array (101), semiaperture of obscuration in x direction at surface I.
BETAPY(I)	One-dimensional array (101), semiaperture of obscuration in y direction at surface I. If both BETAPX and BETAPY are entered, the obscuration is rectangular. If only one is entered, the obscuration is circular (i.e., BETAPX = 12., BETAPY = 0.,).

BETASX(I) One-dimensional array (101), semiaperture of vignetting in y direction at surface I.

If BETASX and BETASY are both nonzero, the clear aperture is rectangular. If only one is nonzero, the clear aperture is circular.

NOTE: Normally, only those rays are traced which lie inside BETASX, BETASY and outside BETAPX, BETAPY. If anegative sign is attached to any of the four values at surface I, the logic is reversed so that only rays are traced which fall inside BETAPX, BETAPY or outside BETASX, BETASY. This produces the effect of an annular obscuration.

VZERØ(I) One-dimensional array of length (2). Allows representation of percent vignetting of upper edge of entrance pupil. Expressed as fraction so that VZERØ = 0.5 reduces clear aperture of upper edge to BETA0/2. VZERØ = 0. or 1. represent no vignetting.

VZERØ(1) → Received signal (or transmitter)

VZERØ(2) → L.O.

Default: VZERØ(1) = 0., 0.,

VPI(I) Same as VZERØ but for lower edge of entrance pupil.

GZERØ(I) One-dimensional array (2). Entrance pupil obscuration parameter. Distance from center of entrance pupil to edge of upper obscuring aperture.

GZERØ(1) → Received signal or transmitter

GZERØ(2) → L.Ø.

Default: GZERØ (1) = 0., 0.,

GPI(I) — One-dimensional array (2). Same as GZERØ but for lower edge of obscuring aperture.

UZERØ(I) — One-dimensional array (2). Radius of obscuring aperture. Arc of radius UZERØ passes through GZERØ (concave downward) and through GPI (concave upward). No rays are traced below the arc through GZERØ or above the arc through GPI. For a circular, centered obscuration UZERØ = GZERØ, UZERØ must be nonzero if GZERØ and/or GPI are entered.

UZERØ(1) → Received signal or transmitter

UZERØ(2) → L.O.

Default: UZERØ(1) = 0., 0.,

VLAMDA — Spectral wavelength of operation of system being analyzed. All dimensional data (TS, BETA0, etc.) must be in same units as wavelength.

Default: VLAMDA = 0.010611385 (mm)

NFRS — Integer input specifying number of intervals or output points for which spread function (ASF, PSF) arrays are computed. Dimensions of spread function array = (2·NFRS-1) x (2·NFRS-1) ·

NFRS ≤ 51.

Default: NFRS = 26

(giving spread function arrays = 51 x 51).

DELFS — Spread function interval size. Nominally 1/10 the Airy disc radius. Detector parameters are specified as integer multiples of this value.

Default: $\text{DELFS} + \frac{0.61 \cdot \lambda \cdot \text{FL}}{10 \cdot \text{BETA0}}$

where FL and BETA0 are respectively the focal length and semiaperture for the received signal or transmitter optics.

NXY — Integer input specifying number of grid points over entrance pupil semidiameter. The total pupil array is $(2 \cdot \text{NXY} + 1) \times (2 \cdot \text{NXY} + 1)$

$\text{NXY} \leq 50$

Default: NXY = 25

(giving pupil array = 51 x 51).

PZERØ(I) — Receiver — PZERØ(1) = Radiant power density at entrance pupil of received signal optics. If PZERØ(1) input negative, PZERØ(1) = total radiant power incident (uniformly) on entrance pupil. PZERØ(2) = total radiant power in truncated gaussian beam of L.O. laser. Transmitter — PZERØ(1) = total radiant power in truncated gaussian transmitter laser beam.

Default: PZERØ(1) = 1., 1.,

ZØMEGA — Radius of $1/e^2$ intensity point of transmitter or L.O. gaussian laser beam.

Default-transmitter: ZØMEGA = BETA0(1)

Default-receiver: ZØMEGA = BETA0(2)

IPRØG(I) — One-dimensional array of integer flags for various program options.

Default: IPRØG(1) = 1, 0, 0, 0, 0, 0,

IPRØG(1) = 0 - Paraxial analysis only

= 1 - compute receiver or transmitter quality criteria

IPRØG(2) = 0 - Pass

= 1 - Output receiver ASF arrays or transmitter PSF array.

IPRØG(3) = 0 - Compute receiver quality criteria with detector centered on optical axis, received signal and L.O. beams shifted due to effect of input beam obliquity, misalignments, IMC error, etc.

= 1 - Center received signal and L.O. chief rays on detector

= 2 - Center respective peaks of ASF for received signal and L.O. on detector.

IPRØG(4) = 0 - Pass

= 1 - Print un-normalized transmitter PSF

IPRØG(5) = 0 - Pass

= 1 - Print OPD (w(u, v)) arrays

IPRØG(6) = 0 - Pass

= 1 - Print pupil function

NDET — Integer input specifying number of detectors to be analyzed.

Default: NDET = 1,

IDETEC(I, J) — Two-dimensional array (5, 5) defining parameters of detectors to be included in analysis.

IDETEC(I, J) = a, b, c, d, e,

I = a, b, c, d, e,

J = Detector number

IDETEC(1, J) = a = circular, rectangular flag

1 - circular detector

2 - rectangular detector

IDETEC(2, J) = b = Integer input specifying number of grid points across x dimension of detector. Total width Sx of detector in x direction is Sx = 2·b·DELFS

IDETEC(3, J) = c = Integer input specifying number of grid points across y dimension of detector. Total width Sy of detector in y direction is Sy = 2·c·DELFS. For circular detector c = 0 and Sx = circular diameter.

IDETEC(4, J) = d = Integer input specifying number of grid points by which detector center is to be displaced from the optical axis in the x direction. Detector displacement = Dx, and Dx = d·DELFS.

IDETEC(5, J) = e = Integer input specifying number of grid points by which detector center is to be displaced from the optical axis in the y direction. Detector displacement = Dy and Dy = e·DELFS

Default: a = 1
b = 10
c = 0
d = 0
e = 0

NOTE: Any combination of b and d; c and e; or off-axis chief ray shift causing the detector to fall outside the spread function array (NFRS) will abort the run.

FLAG — An integer flag used to reinitialize data. Primarily used between consecutive runs to wipe out all data from a previous run. This is submitted as an independent data deck with title card, $INP card with FLAG = 1, and $END card. Stacking this between two data decks accomplishes the initialization for the second set of data.

2.7 INTERPRETATION OF OUTPUT DATA

The amount of output data printed is controlled by the IPRØG flags. The system parameters as input will always be printed; the paraxial ray traces and computed first order parameters will always be printed. For the full transmitter or receiver analysis the full set of quality criteria will always be printed.

a. Paraxial Data

- Entrance pupil position T(0) = , the value printed here is the distance from the paraxial entrance pupil to the first surface. A negative value indicates that the entrance pupil lies to the right of the first surface.
- TEXIT — Paraxial exit pupil position, TEXIT = distance from surface (N-1) to paraxial exit pupil.
- XLINV — Inverse object distance as input or as computed from input of MAG.
- FOCAL LENGTH — computed paraxial focal length.

- BACK FOCAL LENGTH – computed paraxial back focal length = distance from surface (N-1) to paraxial focal plane.

- TS (N-1) – Spacing actually used in analysis as distance from surface (N-1) to image or detector surface. Depends on IFLG1, TS(N), etc.

- FL – when XLINV $\neq$ 0. FL = MAG/XLINV so that an input wavefront radius at the entrance pupil of $R_o = L_o$ = 1/XLINV will give an output wavefront radius of FL.

b. Chief Ray Data

- Field Angle – is the value input as H

- Chief Ray Coordinates – x, y, z are the coordinates of the intersection of the chief ray with the image surface.

- Direction Cosines – l, m, n for chief ray in image space.

- RW – Radius of reference wavefront to be used to compute OPD values over exit pupil.

- TR – Location of reference wavefront, TR = Axial distance from surface (N-1) to reference wavefront. For axial case TR = TEXIT.

- XTILT – For off-axis case, reference wavefront may be tilted or rotated XTILT = THTAX for reference wavefront.

- YTILT – = THTAY for reference wavefront.

- XDISP – with tilts and decentrations, the chief ray may become a skew ray so that it does not intersect the optical axis. XDISP is the distance from the chief ray to the optical axis at its point of closest approach.

  XDISP = DLTAX for reference wavefront.

- YDISP – Same as XDISP, YDISP represents distance from optical axis to chief ray at point of closest approach.

  YDISP = DLTAY for reference wavefront.

c. Wavefront Error Information

After all the OPD (W(u, v)) values have been computed over the reference wavefront, wavefront statistics are computed.

$$S1 = \sum_u \sum_v (W(u,v))^2$$

$$S2 = \sum_u \sum_v W(u,v)$$

- STD DEV $= \frac{1}{\lambda}\sqrt{\frac{S1}{N} - \left(\frac{S2}{N}\right)^2}$
- RMS $= \frac{1}{\lambda}\sqrt{\frac{S1}{N}}$
- Maximum un-normalized error = WMAX
- Minimum un-normalized error = WMIN
- Maximum normalized error = WMAX/λ
- Minimum normalized error = WMIN/λ

  WMAX = maximum value of W(u, v)

  WMIN = minimum value of W(u, v)

- Approximate Strehl ratio = I(σ)

  $I(\sigma) = 1. - (2 \cdot \pi \cdot \text{STD DEV})^2$

d. Spread Functions — (ASF and PSF) IPROG(2) = 1. — For the receiver analysis, selection of this option prints out the arrays FR and FI for the received signal and the local oscillator (ASF(x, y) ≡ FR(x, y) + iFI (x, y)).

labelled

"ASF (REAL), FOR RECEIVED SIGNAL" (FR1)

"ASF (IMAGINARY), FOR RECEIVED SIGNAL" (FI1)

"ASF (REAL), FOR LOCAL OSCILLATOR" (FR2)

"ASF (IMAGINARY), FOR LOCAL OSCILLATOR" (FI2)

"PHASE" is also printed where PHASE = ARCTAN (FI/FR).

The ASF values are normalized to 100 for compactness and the normalizing factor is printed. The ASF arrays will be (2·NFRS-1) x (2·NFRS-1) up to 72 x 72 beyond which only the central 72 x 72 points will be printed. If the array is smaller than 36 x 36, the entire array will be on a single page. Arrays larger than 36 x 36 will be printed one quadrant per page. The quadrants are related as per Fig. 2-5 with the 0, 0 point in the upper left hand corner of quadrant 4.

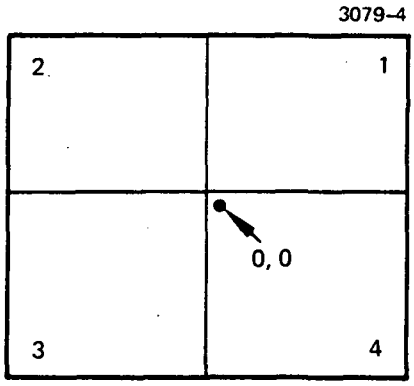

Fig. 2-5.
Output quadrants for ASF, PSF, pupil function.

PSF – The PSF or intensity value for a point in an array is $PSF(x,y) = (FR(x,y))^2 + (FI(x,y))^2$. The PSF array is printed for the transmitter. All the comments for the ASF printout apply here.

INTERVAL – This is the spacing between adjacent ASF or PSF points. INTERVAL = DELFS.

NUMBER INTERVALS = 2·NFRS-1

e. IPRØG(4) = 1. – This option causes the printing of the floating point tabulation of the transmitter PSF (intensity) values.

f. IPRØG(5) = 1. – This option causes the floating point tabulation of the OPD values to be printed.

g. IPROG(6) = 1. — This option prints the complex components of the pupil function normalized to 100. As with the ASF and PSF, the output may include only the central 72 x 72 of a larger array.

2.8 COORDINATE — SIGN CONVENTION SUMMARY

The coordinate system for ray tracing is a local coordinate system where the vertex of the surface being traced is the origin. The spacing TS combines with any misalignment parameters to transfer the coordinate system from surface to surface with the ray. Some key points regarding sign conventions and coordinates are summarized here.

- Surface parameters — A surface parameter with a positive sign causes the surface to be deviated to the right of the tangent plane, hence the negative sign indicates a deviation to the left of the tangent plane. Some of those parameters are:

  RHØS, RHØ1, RHØ2, RADS, DFØRM, AMP.

- Spacing — TS. A positive value for TS(I) specifies that surface I + 1 lies to the right of surface I.

- Finite object — nonuniphase input beam. A positive value for XLINV indicates that the entrance pupil lies to the right of the object point. The input wavefront is thus divergent. For MAG input positive for a system with a positive focal length, the input wavefront is divergent and the exiting wavefront is convergent.

- H-input beam obliquity — A positive H indicates an input beam incident on the entrance pupil from below the optical axis.

- Misalignments — DLTAX, DLTAY, DLTAZ, THTAX, THTAY, THTAZ — refer to Section 4.6.

- Detector — The optical axis is the reference here. For a centered system with no input beam obliquity, the detector, the received signal and the L.O. beam will be centered on the optical axis. If there is an input beam obliquity or misalignment in either the

received signal or the local oscillator, that beam will be shifted from the center of the detector while the other beam remains centered. The detector will always remain centered regardless of the shift in the beams unless the IPRØG(3) option is invoked or the detector is displaced via IDETEC(4, J) and/or IDETEC(5, J). Notice that IPRØG(3) centers the spread functions on the detector while IDETEC(4 and 5, J) shift the detector with respect to the optical axis without changing the location of the beams.

2.9 SAMPLE CASES

Computed results are included for four sample cases. There are two transmitter cases and two receiver cases. The descriptions of these cases are as follows:

a. "TRANSMITTER TEST CASE", Appendix A — This very simple case is an example of an analysis using a "perfect surface". Surface No. 1 is a dummy surface, surface No. 3 is the image surface and surface No. 2 is the perfect imaging surface. For this perfect system, the focal length and back focal length are equal at 100 mm. The transmitter quality criteria are determined at the (Fraunhofer) focal plane. The overall transmitter efficiency is 92% rather than approaching 100% because of the gaussian beam.

An examination of the data deck for this case would indicate the presence of data for a complete receiver. The transmitter analysis results from setting N(2) = 0.

b. "TRANSMITTER TEST CASE No. 1", Appendix B — This system consists of a meniscus lens represented by surfaces No. 2 and No. 3 and a paraboloidal mirror represented by surface No. 5. Surface No. 1 is a dummy located at the position of the laser input; surface No. 4 is a dummy at the mutual focus of the meniscus and paraboloid. The combination of the meniscus and paraboloid produces a perfectly collimated beam so that surface No. 6 is a perfect surface chosen to focus the beam at a distance of 8 km (back focal length — $8.00178987 \cdot 10^{6}$ mm). The laser beam defaults to a total power of

1 W. The $1/e^2$ radius is specified to be 0.925 mm (ZØMEGA = 0.925) and the far field intensity is sampled in increments of 50 mm (DELFS = 50.0). The reference wavefront has a radius of 7.9 km (RW = $7.93148013 \cdot 10^6$ mm) and is located 70 m to the right of surface No. 6 (TR = $7.03097397 \cdot 10^4$). The quality criteria are essentially self-explanatory with the added comment that the apparently low value for overall transmitter efficiency is due to the disparity between the $1/e^2$ radius (0.925 mm) and the truncation radius (BETA0 = 2.25).

c. "RECEIVER TEST CASE No. 1", Appendix C — The received signal optics for this system are for a real system. The local oscillator optics is a perfect surface of aperture and focal length to give an Airy disc about five times the diameter of that for the received signal. The peak value for the ASF(REAL) for the received signal (FR1) is 1304.5 while the peak value for the ASF (Imaginary) for the received signal (FI1) is 600.1 indicating that the peak intensity is $2.062 \cdot 10^6$ and that the focus can be improved (to reduce FI1). The ASF values for the local oscillator indicate good focus so that the peak intensity will be $2.004^2 = 4.0160$.

The ASF arrays are output for the two beams allowing an examination of the respective distributions. The FI arrays are converted to phase and exhibited since default conditions are relied on for the quality criteria. They are based on a circular detector of diameter equal to that of the Airy disc for a system of clear, uniformly illuminated aperture, and relative aperture = 8.0.

d. "RECEIVER TEST CASE No. 2", Appendix D — This data is for a typical set of received signal and local oscillator optics. The quality criteria are determined for the default case plus three other detectors:

(1) Detector No. 1 — Default case — circular, centered detector with diameter equal to the Airy disc.

(2) Detector No. 2 — Square, centered detector with sides equal to the diameter of the Airy disc.

(3) Detector No. 3 — Circular detector with same dimensions as Detector No. 1 but shifted from the beam center by a distance equal to the radius of the Airy disc.

(4) Detector No. 4 — Square detector with the same dimensions as Detector No. 2, but shifted from beam center by the Airy disc radius.

SECTION III

SAMPLE SYSTEM ANALYSIS

The system chosen for exercising this computer program is the optical mechanical subsystem (OMSS) developed for NASA under contract NAS 5-21859. This package is intended as an engineering model of a spaceborne data link and is one of the most advanced systems designed specifically for heterodyne communications work. The system has been designed and analyzed using existing optical computer programs and represents a nearly perfect optical system. As will be seen, the excellent performance predicted by a conventional program, ACCOS V is confirmed by LACOMA. Since the performance is nearly perfect, the differences between LACOMA and conventional programs are masked. An example of a less perfect system is presented at the end of this section to illustrate the advantages of LACOMA over programs that optimize intensity.

The OMSS consists of two focusing reflective surfaces, a parabolic primary and an elliptic secondary. This particular configuration provides essentially perfect performance when properly aligned, and, even in the presence of reasonable tilts and decentrations, performance is still excellent.

The analysis was carried out in three steps. First, a reference case using the same size optics with the same obscurations but with a "perfect" surface in the receive and the L.O. paths was analyzed to provide a measure of the best possible performance under the given restraints. The configuration of this system is shown in Fig. 3-1; the optical input data and the results are listed in Table 3-1.

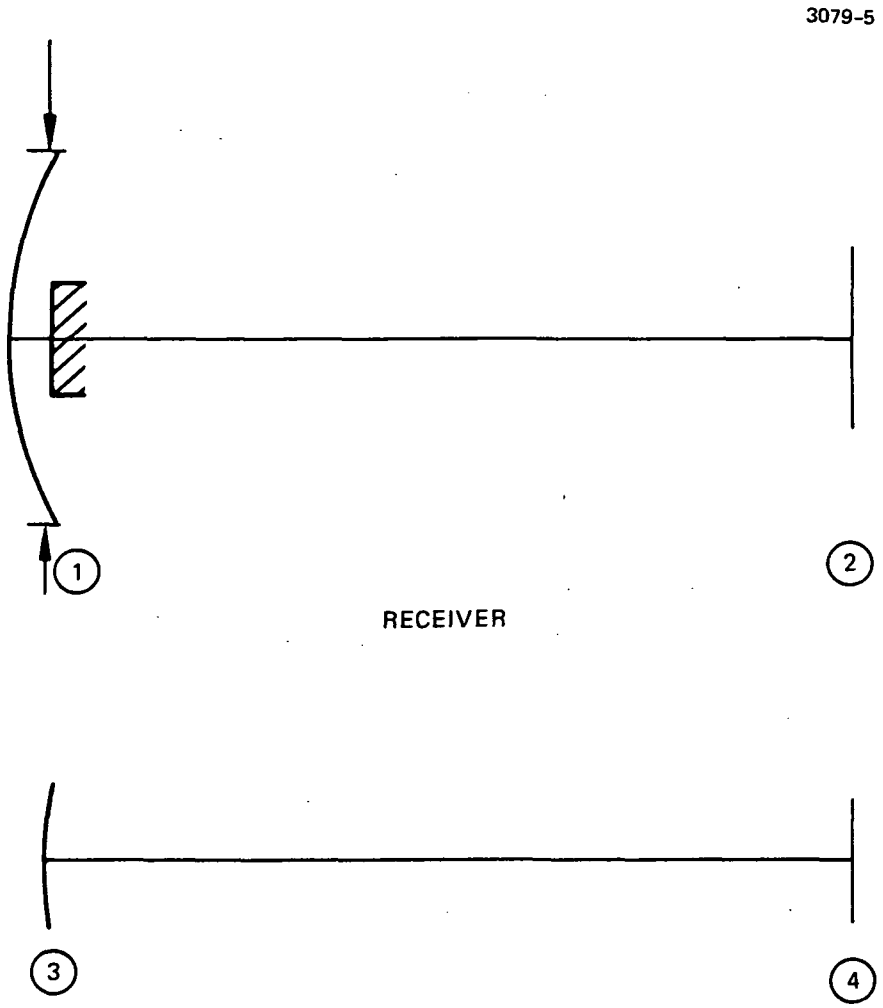

Fig. 3-1. Reference system optical schematic.

TABLE 3-1.

Reference System Specifications and Results

Specifications			
Receiver F/No.	F/8		
Entrance Pupil Diam	16.51 cm		
Obscuration Diam	3.20 cm		
L.O. F/No.	F/40		
Detector Diam	0.199 mm		
LACOMA Results			
Phase Match Efficiency		1.000	-0.00 dB
Optical Transmission		0.964	-0.16 dB
Direct Detection Efficiency		0.743	-1.29 dB
L.O. Illumination Efficiency		0.823	-0.84 dB
Theoretical Antenna Gain			93.78 dB
Receiver Efficiency to I.F.		0.504	-2.98 dB
Effective Antenna Gain			90.80 dB

T1200

The second step of the analysis was to evaluate the system without alignment errors to compare it with the reference case. Four configurations were evaluated; an on-axis case with and without a beamsplitter that will be used to add a beacon to the system, and an off-axis case also with and without the beamsplitter. The off-axis angle was chosen to equal the maximum angle encountered during the signal acquisition phase. The third step of the analysis was an evaluation of system sensitivity to manufacturing tolerances.

The optical configuration for the second and third parts of the analysis is shown schematically in Fig. 3-2. Several dummy surfaces were included to allow restoration of axes and to provide means to perturb optical elements without changing the basic constants of the system. The surfaces and their functions are listed below:

(1) Parabolic primary mirror

(2) Dummy used to restore tilts and displacements of the primary mirror, or to add spacing errors between the primary and secondary.

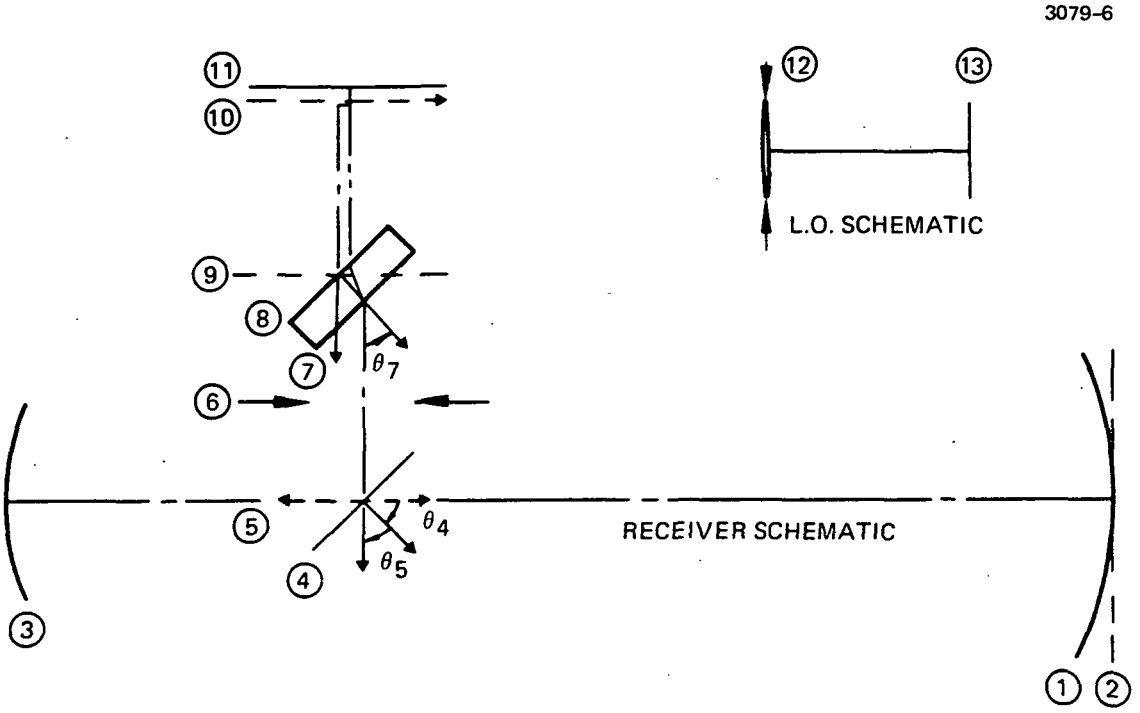

Fig. 3-2. OMSS optical schematic.

(3) Elliptical secondary mirror

(4) IMC mirror

(5) Dummy to restore the optical axis to 90^{o} after reflection from the IMC. The sum of the tilt angles of surfaces 4 and 5 must always equal 90^{o}.

(6) Aperture stop

(7) First beamsplitter surface

(8) Second beamsplitter surface

(9) Dummy to restore tilted axis introduced by surface No. 7

(10) Dummy to restore offset between optical axis and chief ray caused by the beamsplitter

(11) Detector plane for receiver path

(12) L.O. perfect surface and aperture stop

(13) Detector plane for L.O.

The constants to describe each surface for the nominal on-axis case are listed in Table 3-2. These values were determined during the OMSS design phase, and have been optimized for best Strehl ratio (diffraction focus). Note that there are three reflective surfaces in the system; both the refractive index and the direction of propagation (spacing) reverse sign at these surfaces.

Local Oscillator — At the time of this analysis, there was no final design data for the L.O. Accordingly, to avoid introducing degradation from this source, the basic design data was used to generate a "perfect" L.O. The planned L.O. will operate as a f/40 system with a gaussian beam distribution truncated at the $1/e^{2}$ points, and with no central obscuration. A perfect L.O. that meets these criteria is also shown in Fig. 3-2, and is specified in Table 3-2.

Figure 3-3 shows a printout of the data deck as it appeared after being input to the computer. Additional parameters shown in Fig. 3-3 are defined in Section II.

TABLE 3-2.

Input Data for Nominal OM Subsystem Surfaces

Surface	No.	Radius RADS	Spacing TS	Index XMUS	Obscuration BETAPX	Surface Modifications		Tilts THTAY	Displacements DLTAY	Entrance Pupil Radius BETA0
						CRS	SKAPA			
Primary	1	-820.0	(-)0	-1	16		0	0		82.55
Dummy	2	0	-502.90985	-1			1	0		
Secondary	3	141.80175	133.44387	1			0.71736	0		
IMC	4	0	(-)0	-1			1	-0.7854		
Dummy	5	0	-12.7	-1			1	-0.7854		
Stop	6	0	-98.425	-1			1	0		
Beamsplitter	7	0	-2	-4.00062			1	0.7854		
Beamsplitter	8	0	(-)0	-1			1	0		
Dummy	9	0	-54.6358	-1			1	-0.7854		
Dummy	10	0	(-)0	-1			1	0	0.25396	
Detector	11	0	(-)0	-1			1	0		
Lens/Stop	12	400	400	1		-1	1	0		5
Detector	13	0	0	1			1	0		

T1201

All lengths in millimeters, angles in radians

```
OM SUBSYSTEM, NO  OFFSETS OR TILTS
$INP
BETA0(1)=82.55,5., PZERO(1)=-1.,1., IFLG1(1)=1,IPROG(1)=1,0,2,
N(1)=-11,-2, XMUS(1)=-1.,-1.,1.,3*-1.,-4.000620,-1.,3*-1.,M(1)=6,12,
SKAPA(1)=0.,1.,.71736, BETAPX(1)=16.,
RADS(1)=-82[illegible].,0.,141.83175,8*0.,
TS(1)=0.,-[illegible]2.90989,133.4+387,0.,-12.7,-98.425,-2.,0.,-54.6358,2*0.,
TS(12)=40[illegible].,0., RADS(12)=+[illegible]0.,0., ORS(12)=-1., XMUS(12)=2*1.,
DELFS=4.141657E-3, NDET=1, IDETEC(1,1)=1,24,3*0,
THTAY(4)=2*-.78539816,
THTAY(7)=.78539816,0.,-.78539816, DLTAY(13)=.25396,
$END
```

Fig. 3-3. Input deck for OM system.

The results for the runs without alignment errors are shown in Table 3-3. The results show that the aberrations caused by off-axis operation and the astigmatism caused by the beamsplitter are both negligible. (In this table the overall efficiency to the i.f. is shown in dB degradation below the theoretical maximum antenna gain, and is also normalized to the results of the reference case.)

For the third step of this analysis, the distortions introduced into the OMSS were selected to allow comparison with the analysis conducted using ACCOS V as listed in the design report for the OMSS. Four perturbations were analyzed:

(1) The primary-secondary spacing was varied

(2) The detector was displaced from the focal plane

(3) The primary mirror was transversely displaced

(4) The primary mirror was tilted.

The results are presented graphically in Figs. 3-4 through 3-7. For the first two cases where the evaluation is conducted on-axis, the results are directly comparable to those obtained using ACCOS V. The plots show Strehl ratio, normalized heterodyne efficiency, direct detection efficiency, and local oscillator efficiency. There are several interesting results:

(1) Because the local oscillator has been spread out by the f/40 optical system, the amplitude profiles of the L.O. and received signal tend to become more closely matched as the received signal is defocused, thereby increasing the local oscillator efficiency and partially compensating the loss in signal power.

(2) Heterodyne efficiency is not as sensitive to focus as is the Strehl ratio, partially because of the above observation.

(3) The region around the focal plane of the detector would be symmetrical in the absence of aberrations. The aberrations that are present cause a slight asymmetry in the Strehl ratio, which is barely evident on the curves. However, the heterodyne efficiency shows a much greater asymmetry, implying that small aberrations affect the phase of the signal more than the amplitude.

TABLE 3-3.

Results for Nominal OMSS Configuration

	Phase Match Efficiency	Direct Detection Efficiency	L.O. Efficiency	Receiver Efficiency to I.F.		
				Decimal	dB	Relative
Reference System	1.000	0.743	0.823	0.504	-2.98	1.000
OMSS-No Beamsplitter						
On-Axis	0.996	0.742	0.820	0.496	-3.04	0.985
0.13^{o} Off-Axis	0.993	0.735	0.820	0.488	-3.12	0.967
OMSS w/beamsplitter						
On-Axis	0.990	0.741	0.821	0.495	-3.05	0.983
0.13^{o} Off-Axis	0.990	0.736	0.824	0.489	-3.11	0.970

T1202

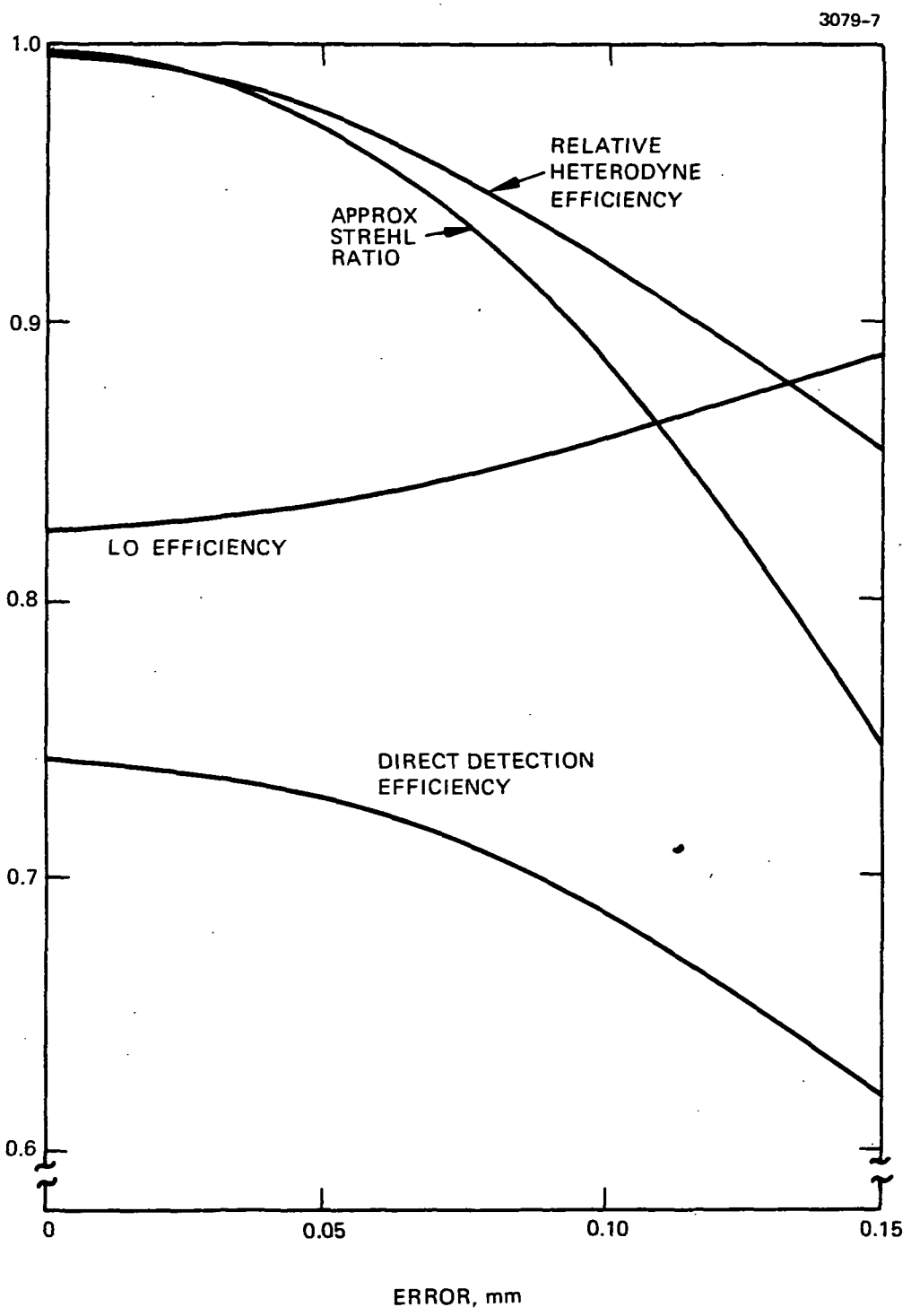

Fig. 3-4. Primary-secondary separation error.

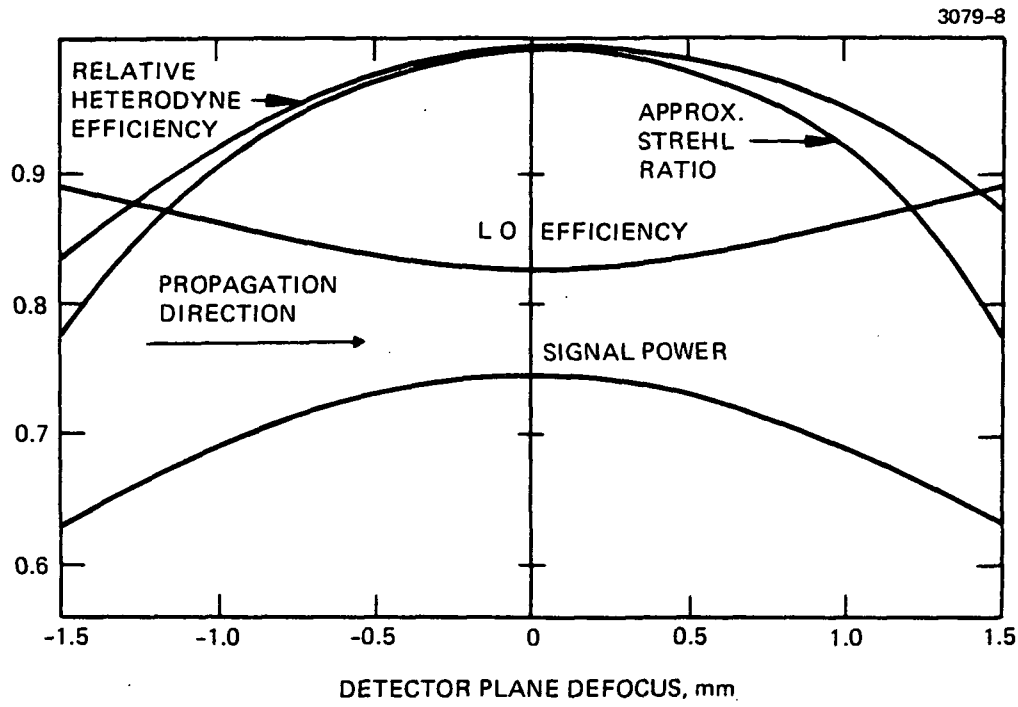

Fig. 3-5. Effects of detector position.

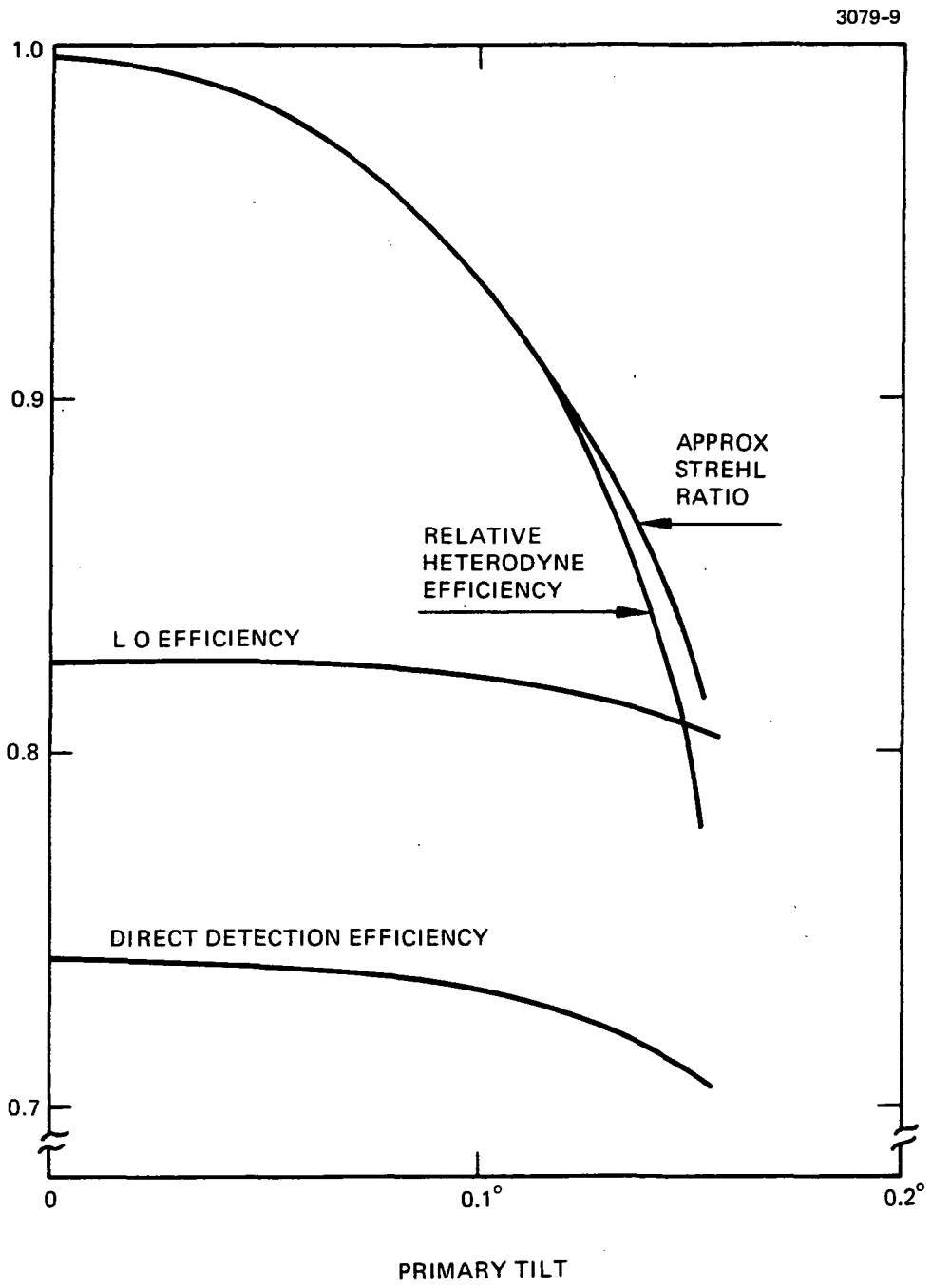

Fig. 3-6. Effects of tilted primary.

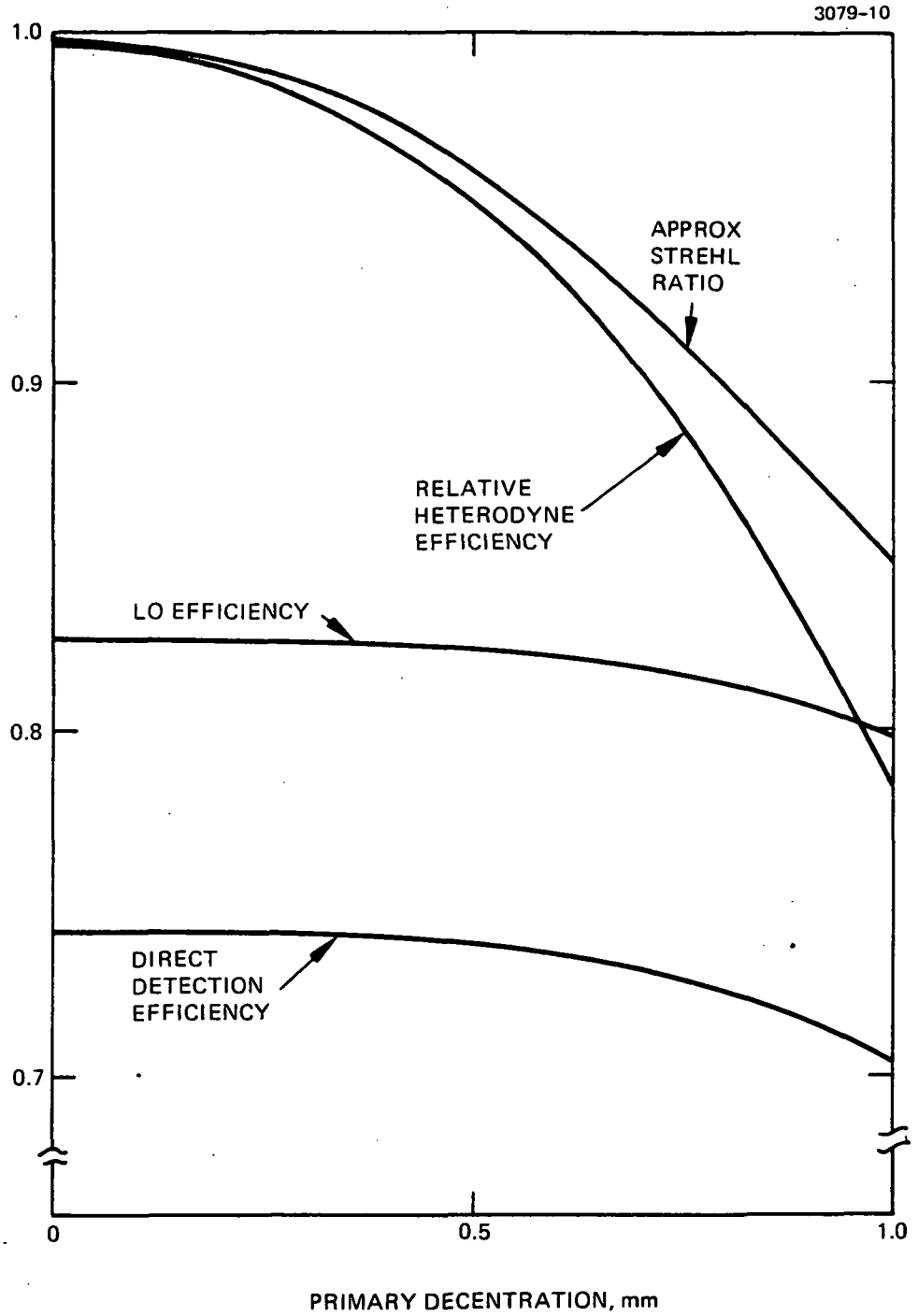

Fig. 3-7. Effects of primary offset.

For cases 3 and 4 where the primary has been tilted or displaced, the results cannot be compared directly with previous results due to differences in methods used to evaluate the system. For the LACOMA runs, the input beam was introduced along the undisturbed optical axis and the IMC was adjusted to place the chief ray of the received signal onto the detector center as would occur during the track mode in the operating system. The values for IMC correction were determined by paraxial ray trace using a desk calculator. The LACOMA option to place the peak intensities of the two beams on the center of the detector was selected to eliminate residual errors in IMC position and to compensate for peak shift due to off-axis aberrations. An alternative approach leaves the IMC centered and compensates for the angular displacement by evaluating a received signal from an off-axis location. The aberrations caused by the first approach are more severe, as is evident if the Strehl ratios in Figs. 3-6 and 3-7 are compared with corresponding figures in the OMSS design report.

For these cases, as shown in Figs. 3-6 and 3-7, the heterodyne efficiency falls off more rapidly than the Strehl ratio. This result is not unexpected, as the heterodyne signal is more sensitive to wavefront tilt, thus the phase match efficiency suffers. Also of interest is the L.O. illumination efficiency which decreases for these cases, thus adding to the degradation.

Overall, the results of this analysis tend to confirm the conclusions reached in the OMSS design report. The heterodyne signal has been shown to be more sensitive to alignments that cause angular errors than those that cause only defocusing. This result is beneficial to the OMSS, since the primary-secondary spacing is the most difficult parameter to control.

Other Analyses

The LACOMA program has been used to analyze several other problems of interest; two of these are summarized here.

Field of View — The nominal field of view of a heterodyne receiver has been generally considered to be $k\lambda/d$, where d is the receiver aperture diameter, and k is a constant dependent upon the illumination factor, detector size and definition of field of view. To evaluate k for a round detector equal in diameter to the Airy disc, LACOMA was used with a perfect system and a series of detectors spaced sequentially at varying distances from the optical axis. Figure 3-8 shows the results for a uniform L.O. illumination. From this curve, the full field of view to the 3 dB points implies that k should be 1.38 for the uniform case.

Germanium Galilean Telescope — A four-element telescope configuration meant for use in a 10.6-μm heterodyne system is shown in Figure 3-9. This telescope was designed for maximum Strehl ratio, using existing design programs. (This particular telescope has sufficient spherical aberration in this configuration to reduce the Strehl ratio to about 0.7.) Since this system was designed as an afocal system, a perfect surface was introduced into the afocal beam to provide a focal plane for evaluation, and a perfect f/40 L.O. was also selected. The lens system was evaluated, using the predicted optimum spacings, to determine the degradation caused by the spherical aberrations; also, with the spacings between the first and second elements increased by 0.25 and 0.5 mm to ascertain the effects of spacing tolerances. The results, shown in Figure 3-10, were unexpected; the overall efficiency increased from -4.55 dB to -2.58 dB, which is better than the -2.74 dB expected from a perfect system with a uniform L.O. This result can be explained by reference to the phase match efficiency and the L.O. illumination efficiency. Both of these values have increased significantly from the nominal position, even though the total signal power has dropped. This means that at a location significantly away from the best energy focus, the wavefront is nearly plane and the energy distribution is more uniform. Thus, in the presence of significant aberrations, optimum performance for a heterodyne system does not necessarily correspond to that for a direct detection system. LACOMA is the first program to put a quantitative value on this phenomena.

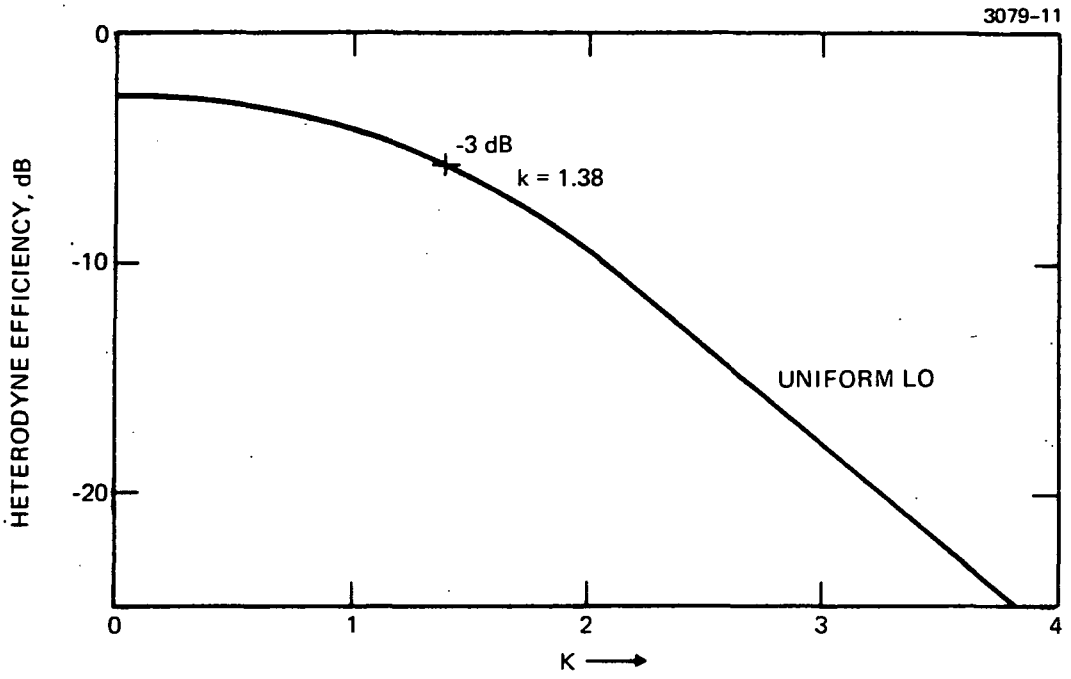

Fig. 3-8. Field of view variation.

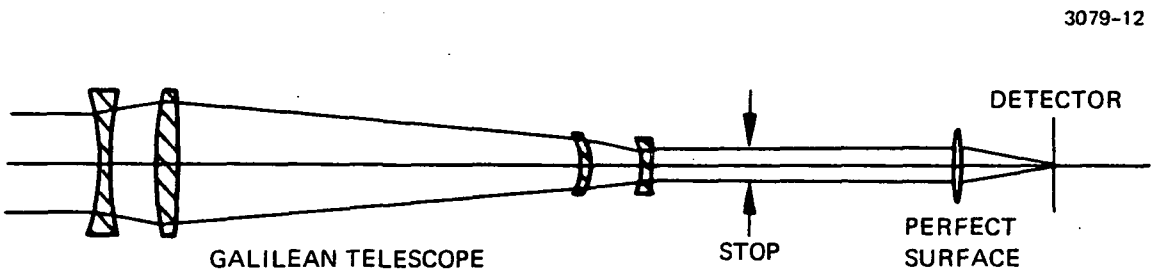

Fig. 3-9. Optical schematic for afocal evaluation.

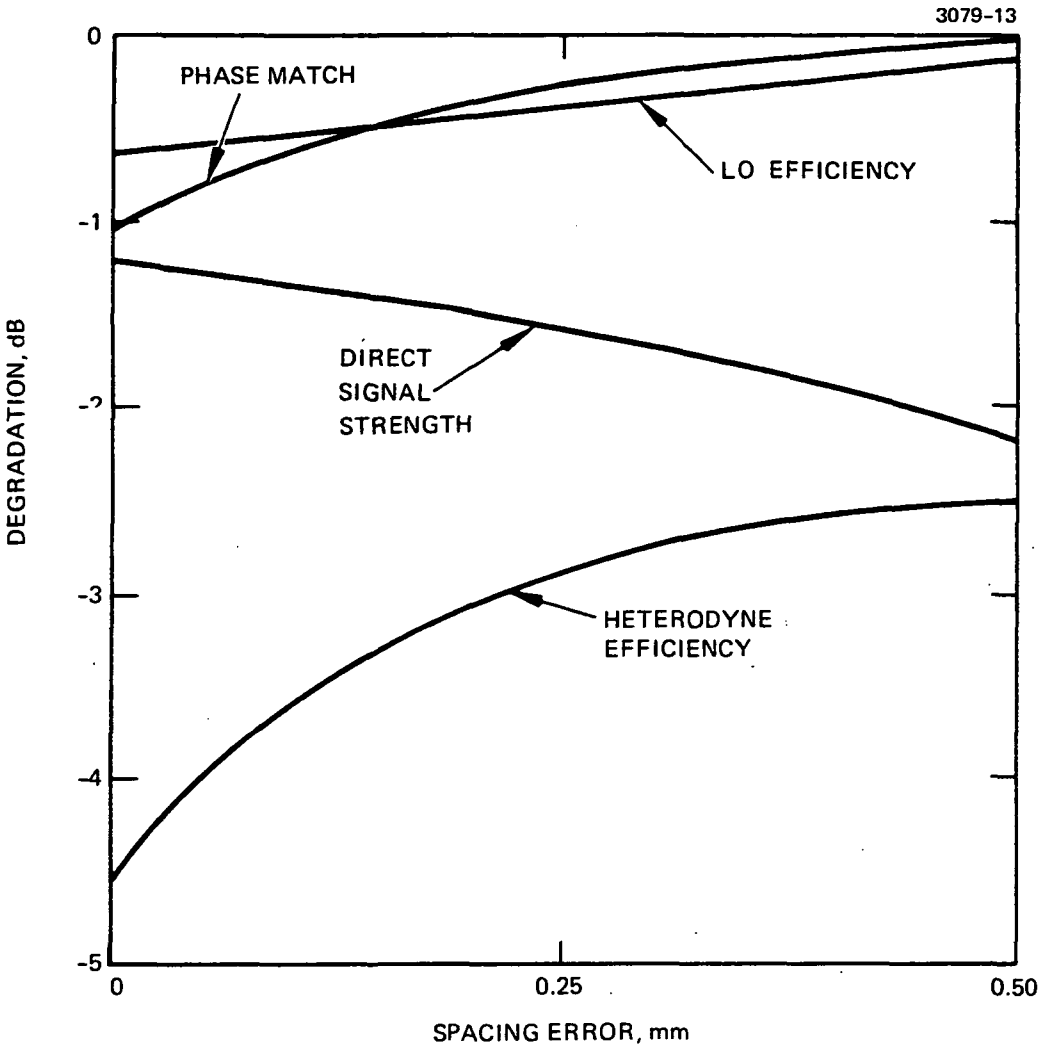

Fig. 3-10. Results on Galilean telescope.

SECTION IV

DETAILED PROGRAM DESCRIPTION

Upon reading the input data, the program determines whether it is to execute a transmitter analysis or receiver analysis based on the input of one or two sets of optical data. Specifically, it checks whether values are entered for N(1) and N(2) which identify the number of surfaces in the two sets of data for received signal optics and local oscillator optics, respectively. If N(2) = 0, then a transmitter analysis is performed. In addition to the surface number parameter, many of the other system parameters are two-element arrays; e.g., M(1) ≡ surface number of aperture stop for received signal (or transmitter) optical train while M(2) ≡ surface number of aperture stop for local oscillator optical train as is the case for H(1), H(2), FL(1), FL(2), etc. As most of the computations to be discussed are performed identically for transmitter, receiver, and local oscillator, the subscript notation will be omitted except where confusion might arise and the distinction between transmitter and receiver will be omitted except for those computations unique to a given case.

4.1 FIRST ORDER PARAMETERS

Two paraxial rays are traced through the optical trains to determine the first order parameters of the particular optical train. These parameters are:

a. Paraxial entrance pupil position T_o is the distance from the paraxial entrance pupil to the first optical surface.

b. Paraxial exit pupil position TEXIT or TR is the distance from the last optical surface (surface N-1) to the paraxial exit pupil.

c. Inverse object distance XLINV or L_o^{-1} is the inverse of the distance from the object plane to the paraxial entrance pupil.

d. Focal length

e. Back focal length, which is the distance from the (N-1) surface to the paraxial focal surface.

f. TS(N-1) is based on the input data and control parameters, and is the spacing actually used in the analysis as the back focus.

g. Paraxial Computations are where the two paraxial rays are traced with starting values at the first surface of the optical train.

β_o = input

$b_o = 0.$

$a_o = 1/\beta_o$

$\alpha_o = 0.$

With this data as input the two paraxial rays are traced using

$$\beta_s = \beta_{s-1} + b_{s-1}\, t_{s-1}/\mu_{s-1} \tag{4-1}$$

$$b_s = b_{s-1} + (\mu_{s-1} - \mu_s)\, \beta_s\, \rho_s \tag{4-2}$$

$$\alpha_s = \alpha_{s-1} + a_{s-1}\, T_{s-1}/\mu_{s-1} \tag{4-3}$$

$$a_s = a_{s-1} + (\mu_{s-1} - \mu_s)\, \alpha_s\, \rho_s \tag{4-4}$$

The parameters of these paraxial rays are illustrated in Fig. 4-1. The data for the paraxial rays at the first surface, the aperture stop, and at the rear surface are then used to compute the desired first order parameters. This data is designated as follows:

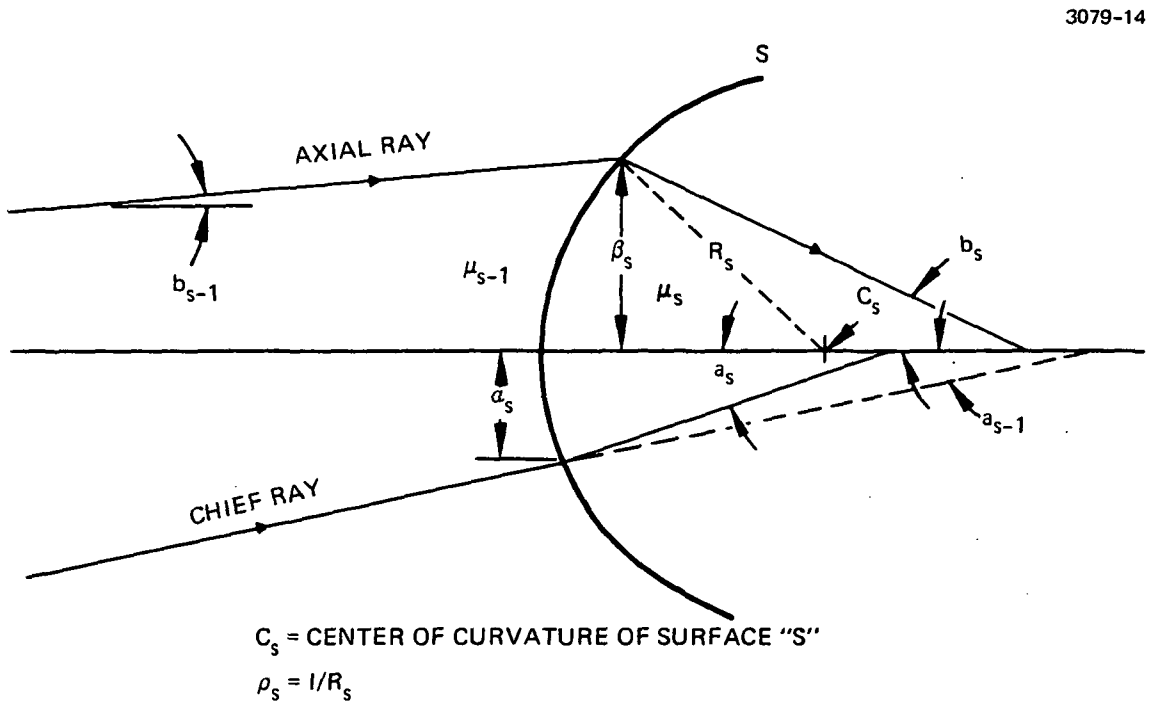

Fig. 4-1. General paraxial ray notation.

$(\beta_o, b_o, \alpha_o, a_o)$ at the first surface

$(\beta_m, b_m, \alpha_m, a_m)$ at the aperture stop

$(\beta_r, b_r, \alpha_r, a_r)$ at the rear optical surface

(The r subscript denotes the next to last or (N-1)st surface)

$$T_o = \frac{-\alpha_m \beta_o^2}{\beta_m} \tag{4-5}$$

$$T_{EXIT} = \frac{(\alpha_m \beta_r - \alpha_r \beta_m)\,\mu_r}{a_r \beta_m - \alpha_m b_r} \tag{4-6}$$

The focal length F and back focal length BF for infinite conjugates are computed:

$$F = \frac{-\beta_o}{b_r} \tag{4-7}$$

$$BF = \frac{-\beta_r \mu_r}{b_r} \tag{4-8}$$

If a finite conjugate distance is entered in the form of L_o^{-1} (XLINV) to introduce a quadratic phase component into the input beam, the focal length and back focal length are recomputed;

$$F = \frac{-\beta_o}{b_r + a_r L_o^{-1} \beta_o^2} \tag{4-9}$$

$$BF = \frac{\left[-\beta_r + \alpha_r L_o^{-1} \beta_o^2\right]\mu_r}{b_r + a_r L_o^{-1} \beta_o^2} \tag{4-10}$$

Optionally, a value may be specified for magnification as the ratio of the input beam divergence versus the output beam convergence:

$$\text{Magnification} = \text{mag} = \frac{-b_o}{b_r} \tag{4-11}$$

from which the inverse object distance is computed for use in the other calculations,

$$L_o^{-1} = \frac{-\text{mag } b_r}{\beta_o (1 + \text{mag } \beta_o a_r)} \quad . \tag{4-12}$$

Notice that for the finite conjugate case, BF is the location of the paraxial image for the given object position and the focal length FL is not the classical paraxial focal length but is

$$FL = \text{mag} \cdot LO. \tag{4-13}$$

This value is used in the computation of the input ray angles for tracing rays.

4.2 IMAGE LOCATION

The actual value used to locate the image surface of intensity plane is subject to several options. The program computes the paraxial back focus BF based on the specified object location. There is a value input as t_{N-1} for the spacing between the last ((N-1)st) surface and the image (detector or intensity) plane. The option is available for specification of which of these is to be used in the analysis. The parameter IFLG1 controls this option.

$$t'_{N-1} = \text{BF if IFLG1} = 0 \tag{4-14}$$

$$t'_{N-1} = t_{N-1} \text{ if IFLG1 } = 1 \qquad (4\text{-}15)$$

where

t'_{N-1} is the value to be used in the analysis.

Additionally, the value t_N which is usually ignored since it has no meaning, can be used to specify an incremental shift of the image location. Thus, the value of t_N is always added to the back focus or image distance.

$$t'_{N-1} = BF + t_N \text{ if IFLG1 } = 0 \qquad (4\text{-}14a)$$

$$t'_{N-1} = t_{N-1} + t_N \text{ if IFLG1 } = 1 \qquad (4\text{-}15a)$$

For example, if it is known that the best focus for a given system is 0.001 from the paraxial focus, the program can compute the paraxial back focus very accurately and then shift by 0.001 to the position of best focus. The value of t'_{N-1} thus determined is printed out as TS (N-1).

4.3 RAY TRACE – OPD

The LACOMA ray trace constitutes an optimal combination of accuracy and speed of computation. The ray trace equations are the result of many years of development, and permit the trace of both meridional and skew rays through any surface which is continuous and analytic.

Notation – (Figure 4-2). A given ray is described by the parameters X_s, Y_s, Z_s, l_s, m_s and n_s. X_s, Y_s and Z_s are the coordinates of the point of intersection of the ray with surface "s". The origin of the coordinate system is at the vertex of the surface. The Z axis is the optical axis, the Y axis the meridional axis and X the skew axis. The optical direction cosines of the ray exiting surface "s"

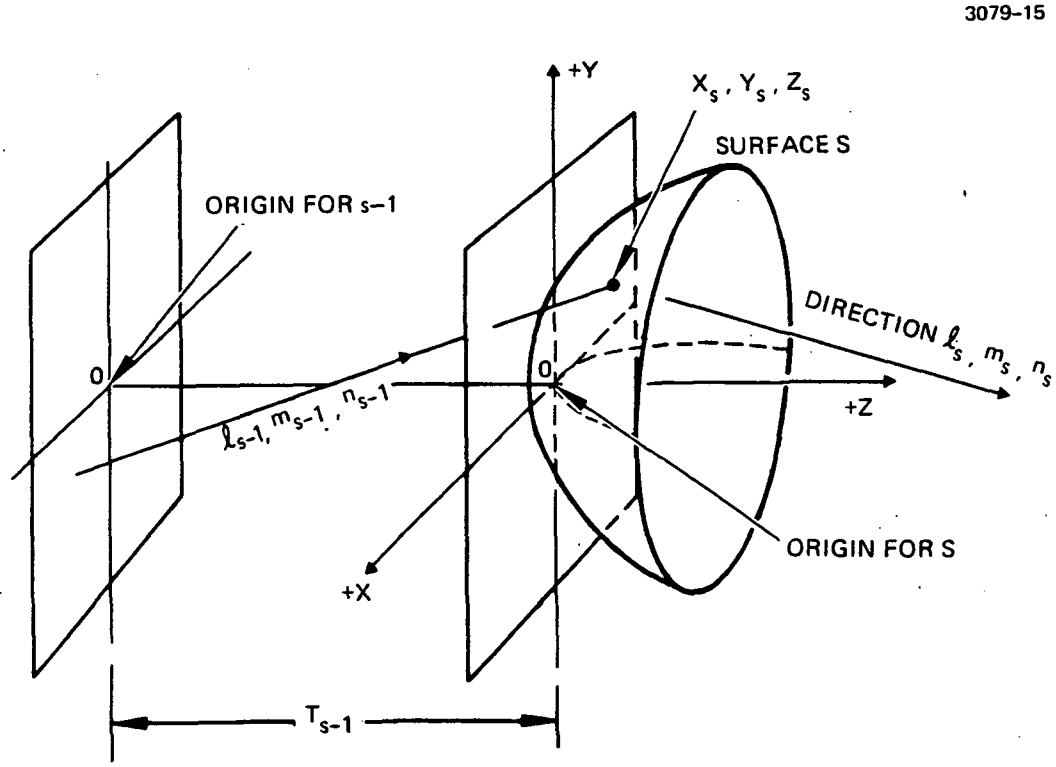

Fig. 4-2. Coordinate system and ray parameters.

are l_s, m_s and n_s. In a medium following surface "s", the refractive index is u_s and

$$l_s^2 + m_s^2 + n_s^2 = u_s^2 \tag{4-16}$$

Surface "s" itself is specified by some sagitta function $\zeta = \zeta(Q)$ and, for a general rotationally symmetrical asphere,

$$\zeta_s = \frac{\rho_{so} Q_s^2}{1 + \left(1 - K\rho_{so}^2 Q_s^2\right)^{1/2}} + \bar{\alpha}_s Q_s^4 + \bar{\beta}_s Q_s^6 + \bar{\gamma}_s Q_s^8 + \ldots \tag{4-17}$$

$$Q^2 \equiv X_s^2 + Y_s^2$$

$\rho_{so} \equiv$ vertex curvature of surface $= 1/R_{so}$

$\bar{\alpha}$, $\bar{\beta}$, $\bar{\gamma}$, etc. = general aspheric deformation coefficients (not related to α or β for paraxial ray trace)

$K_s \equiv (1 - \epsilon_s^2) =$ conic coefficient of surface

Conic sections — If the conic section surface is thought of as a mirror with two aplanatic foci F_1 and F_2 as in Figure 4-3, the conic eccentricity can be related to the distances S_1 and S_2, respectively, measured from the first focus F_1 to the mirror and from the mirror to F_2. In Fig. 4-3, S_1 is positive and S_2 is negative. The vertex curvature for the conic section is

$$\rho_{so} = \frac{1}{2}\left(\frac{1}{S_2} - \frac{1}{S_1}\right) \tag{4-18}$$

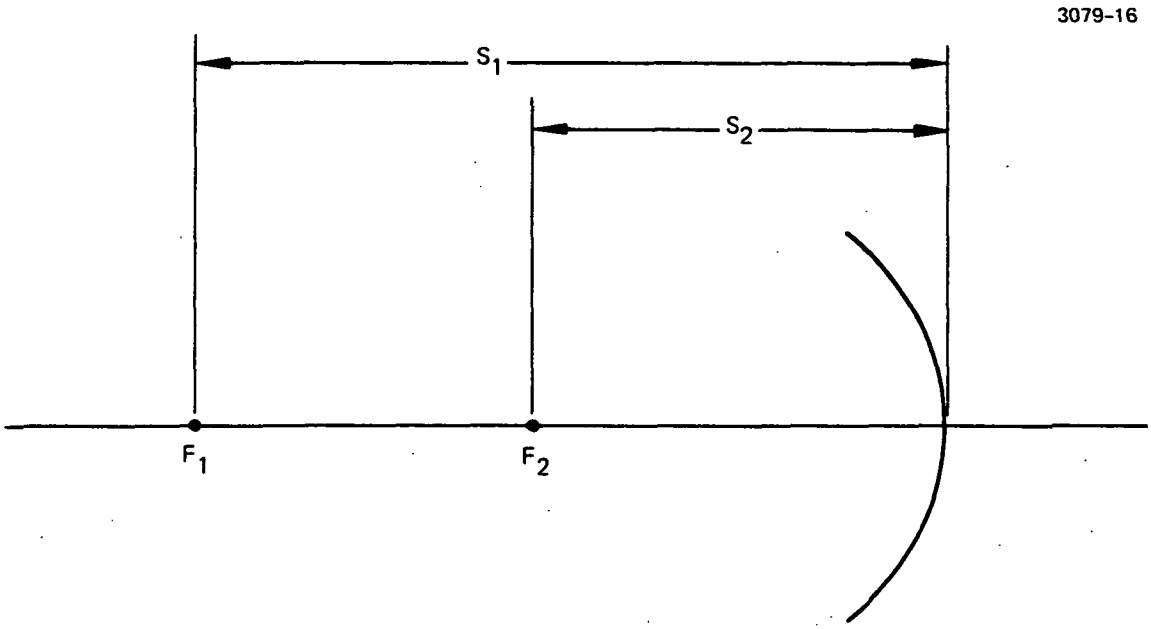

$$\rho = 1/2\,(1/S_2 - 1/S_1)$$

$$\epsilon = \frac{S_1 + S_2}{S_1 - S_2}$$

Fig. 4-3. Conic eccentricity parameters.

and the eccentricity is

$$\epsilon = \frac{S_1 + S_2}{S_1 - S_2} \tag{4-19}$$

Eccentricities for some typical surfaces are

Surface	ϵ	κ
Sphere	0.	1.
Paraboloid	1.	0.
Ellipse	$0 < \epsilon < 1.$	$0 < \kappa < 1$
Hyperboloid	$\epsilon > 1.$	$\kappa < 0.$

The sagitta expression for a sphere would be

$$\zeta = \frac{\rho_{so} Q_s^2}{1 + \left(1 - \rho_{so}^2 Q_s^2\right)^{\frac{1}{2}}} \tag{4-17a}$$

and for a paraboloid

$$\zeta = \frac{\rho_{so} Q_s^2}{2} \tag{4-17b}$$

a. Ray Trace Equations — Denoting surface "s" with the "s" subscript and the preceding surface by the "s-1" subscript. Surface-to-surface transfer equations are

$$X_s = X_{s-1} + \frac{\ell_{s-1}}{n_{s-1}} \left(t_{s-1} - Z_{s-1} + Z_s\right) \tag{4-20}$$

$$Y_s = Y_{s-1} + \frac{m_{s-1}}{n_{s-1}} \left(t_{s-1} - Z_{s-1} + Z_s\right) \tag{4-21}$$

Refraction at surface "s" converts optical direction cosines l_{s-1}, m_{s-1}, and n_{s-1} into l_s, m_s, n_s.

$$\ell_s = \ell_{s-1} + \rho_s'' X_s (n_{s-1} - n_s) \tag{4-22}$$

$$m_s = m_{s-1} + \rho_s'' Y_s (n_{s-1} - n_s) \tag{4-23}$$

or

$$\ell_s = \ell_{so} - \rho_s'' X_s n_s \tag{4-22a}$$

$$m_s = m_{so} - \rho_s'' Y_s n_s \tag{4-23a}$$

where

$$\ell_{so} = \ell_{s-1} + \rho_s'' X_s n_{s-1} \tag{4-24}$$

$$m_{so} = m_{s-1} + \rho_s'' Y_s n_{s-1} \tag{4-25}$$

and

ρ_s'' = the inverse of the subnormal

$$\rho_s'' = \frac{1}{Q}\frac{d\zeta}{dQ} = \frac{\rho_{so}}{1 - \left(K_s \rho_{so}^2 Q_s^2\right)^{1/2}\zeta} + 4\bar{\alpha}_s Q_s^2 + 6\bar{\beta}_s Q_s^4 + 8\bar{\gamma}_s Q_s^6 + \ldots \tag{4-26}$$

For the general asphere the appropriate values of Z_s and n_s are found by iteration. Dropping the "s" subscript temporarily and

substituting i and i + 1 to indicate successive iterated values, the iterations on Z and n are

$$Z_{i+1} = \frac{\zeta_i - \dfrac{Z_i \rho_i'' (\ell_{s-1} X_i + m_{s-1} Y_i)}{n_{s-1}}}{1 - \dfrac{\rho_i'' (\ell_{s-1} X_i + m_{s-1} Y_i)}{n_{s-1}}} \qquad (4\text{-}27)$$

$$n_{i+1} = \frac{\mu_s^2 + n_i^2 - \ell_i^2 - m_i^2 - 2\rho_s'' n_i (\ell_i X_s + m_i Y_s)}{2\left[n_i - \rho_s'' (X_s \ell_i + Y_s m_i)\right]} \qquad (4\text{-}28)$$

$$= \frac{\mu_s^2 - \ell_{so}^2 - m_{so}^2 + n_i^2 \left(1 + \rho_s'' Q_s^2\right)}{2\left[n_i \left(1 + \rho_s''^2 Q_s^2\right) - \rho_s'' (\ell_{so} X_s + m_{so} Y_s)\right]} \qquad (4\text{-}29)$$

using starting values of $Z_i = 0$ and $n_i = \mu_s$.

b. Spherical Surfaces — Though the above algorithms include spherical surfaces as a special case, the tracing through spherical surfaces is handled separately to expedite computing time. The transfer equations are

$$X_s = X_{so} + H_s \ell_{s-1} \qquad (4\text{-}30)$$

$$Y_s = Y_{so} + H_s m_{s-1} \qquad (4\text{-}31)$$

$$Z_s = H_s \, n_{s-1} \tag{4-32}$$

$$X_{so} = X_{s-1} + \frac{\ell_{s-1}}{n_{s-1}}\left(t_{s-1} - Z_{s-1}\right) \tag{4-33}$$

$$Y_{so} = Y_{s-1} + \frac{m_{s-1}}{n_{s-1}}\left(t_{s-1} - Z_{s-1}\right) \tag{4-34}$$

The refraction equations are

$$\ell_s = \ell_{s-1} - P_s \, \rho_s \, X_s \tag{4-35}$$

$$m_s = m_{s-1} - P_s \, \rho_s \, Y_s \tag{4-36}$$

$$n_s = n_{s-1} - P_s \left(\rho_s \, Z_s - 1\right) \tag{4-37}$$

where H_s and P_s are determined as follows:

$$(A) = \rho_s\left(X_{so}^2 + Y_{so}^2\right) \tag{4-38}$$

$$(B) = n_{s-1} - \rho_s\left(X_{so}\,\ell_{s-1} + Y_{so}\,m_{s-1}\right) \tag{4-39}$$

$$\mu_{s-1} \cos i_s = \mu_{s-1}\left[\frac{(B)^2}{\mu_{s-1}^2} - \rho_s\,(A)\right]^{\frac{1}{2}} \tag{4-40}$$

$$H_s = \frac{(A)}{(B) + \mu_{s-1} \cos i_s} \tag{4-41}$$

$$\mu_s \cos r_s = \mu_s \left[\frac{\mu_{s-1}^2 \cos^2 i_s}{\mu_s^2} - \frac{\mu_{s-1}^2}{\mu_s^2} + 1 \right]^{\frac{1}{2}} \qquad (4\text{-}42)$$

$$\rho_s = \mu_s \cos r_s - \mu_{s-1} \cos i_s \qquad (4\text{-}43)$$

These algorithms are listed here in the form they are used in the computation which is necessary to preserve proper sign conditions.

c. Special Surface Forms – Some surface forms which can be accommodated are noted below; most of them can be combined.

Cylinders

Toroids

Normal surfaces with cylindrical error

Periodic surface forms

These surface forms, mentioned above, are described by the summation

$$\zeta_s = (\zeta_1 + \zeta_2 + \zeta_e)_s \qquad (4\text{-}44)$$

ζ_1 is the expression for a cylindrical surface of curvature ρ_1 whose axis may be rotated through an angle φ, Fig. 4-4. ζ_2 can combine with ζ_1 to generate a toroidal surface where the surface (curve) generated by ζ_1 is rotated such that its vertex describes an arc of radius $1/\rho_2$. The arcs of ρ_1 and ρ_2 lie in orthogonal planes. In Fig. 4-5(a) it can be seen that the cylinder is generated by ρ_1 when $\varphi = \rho_2 = 0$. Figure 4-5(b) is the cylinder generated by ρ_2 when $\rho_1 = \varphi = 0$. The surface (curve or arc) ζ_1 may be the cross section of a sphere, any conic or higher order surface form.

The periodic surface errors ζ_e may be a radially symmetrical sinusoidal (cosine in this case) variation of sagitta, a radial sine function or a combination of the two. These radial periodic errors may be

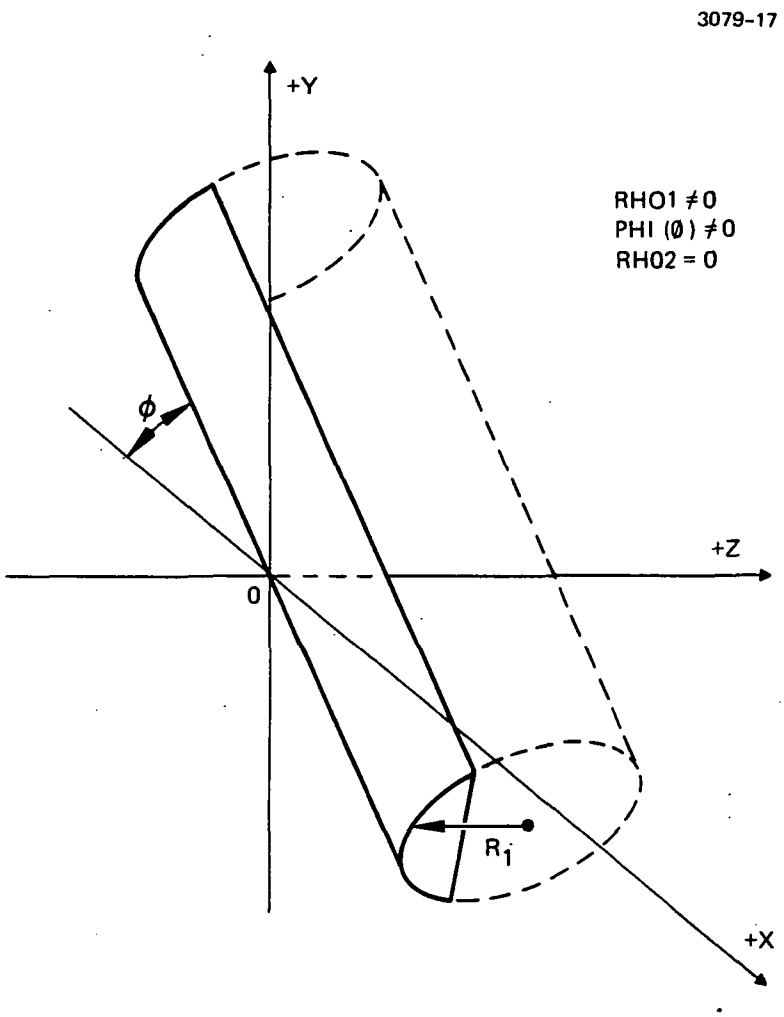

Fig. 4-4. Cylindrical surface due to RH01 but with $\phi \approx 0$.

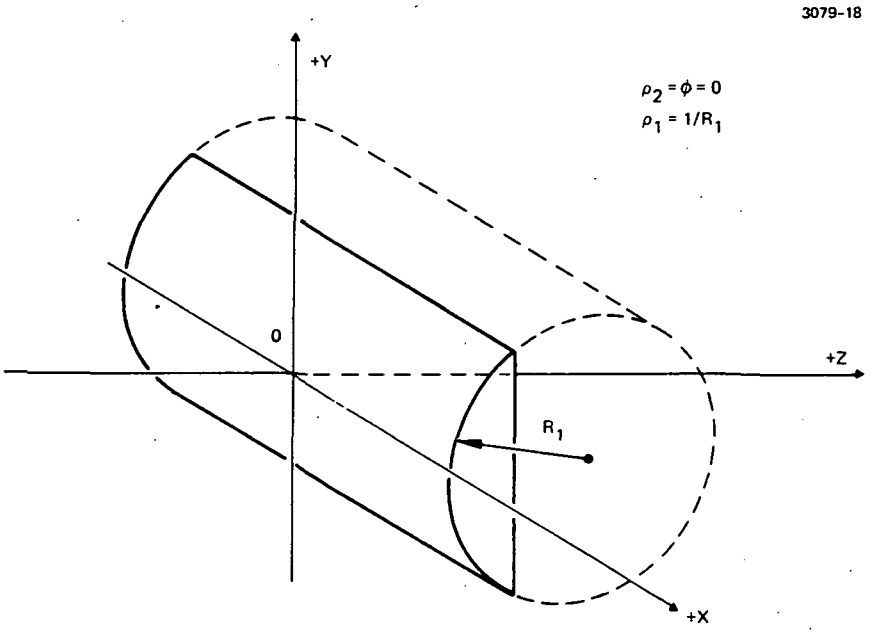

Fig. 4-5(a). Cylindrical surface due to RH01 only.

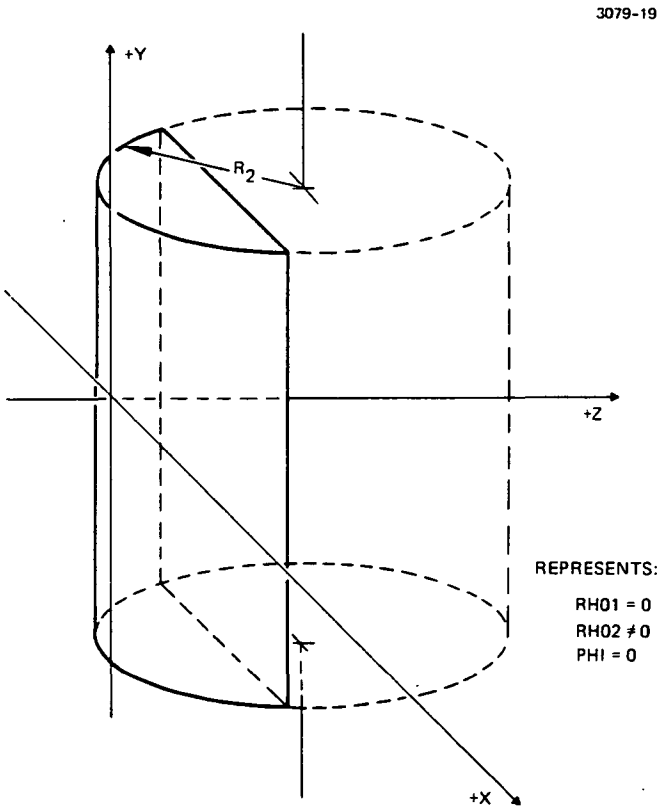

Fig. 4-5(b).
Cylindrical surface due to RH02 only.

displaced with respect to the axis by U and V in the X and Y directions, respectively, Figs. 4-6, 4-7, 4-8, 4-9, and 4-10.

In the formulation of these surface sagitta, the following definitions are used:

$\rho_1 \equiv$ curvature of cylinder ($=1/R_1$) (RH01)

$\rho_2 \equiv$ toric rotation curvature or secondary cylinder curvature ($=1/R_2$) (RH02)

$a \equiv$ constant of rotational symmetry (CRS)

$b \equiv$ cylindrical constant (CC)

$\varphi \equiv$ angular orientation of cylinder (PHI)
- = angle between cylinder axis and X axis for ρ_1
- = angle between cylinder axis and Y axis for ρ_2

$\kappa \equiv$ conic coefficient (ρ_1 surface)

$\alpha, \beta, \gamma,$ etc $\equiv$ higher order (aspheric) surface coefficients (ρ_1 surface)

$\epsilon_1, \epsilon_2, \epsilon_3 \equiv$ periodic surface error coefficients (AMP, FREQ, C3)

U and V $\equiv$ displacement in X and Y of axis of radial symmetry of periodic surface error (USI, VSI)

$$Q^2 = X_s^2 + Y_2^2 \tag{4-45}$$

$$Q_1^2 = X_s^2 (a + b \sin \varphi)^2 + Y_s^2 (a + b \cos \varphi)^2 + 2b^2 X_s Y_s \sin \varphi \cos \varphi \tag{4-46}$$

Fig. 4-6. Sinusoidal (cosine) surface error.

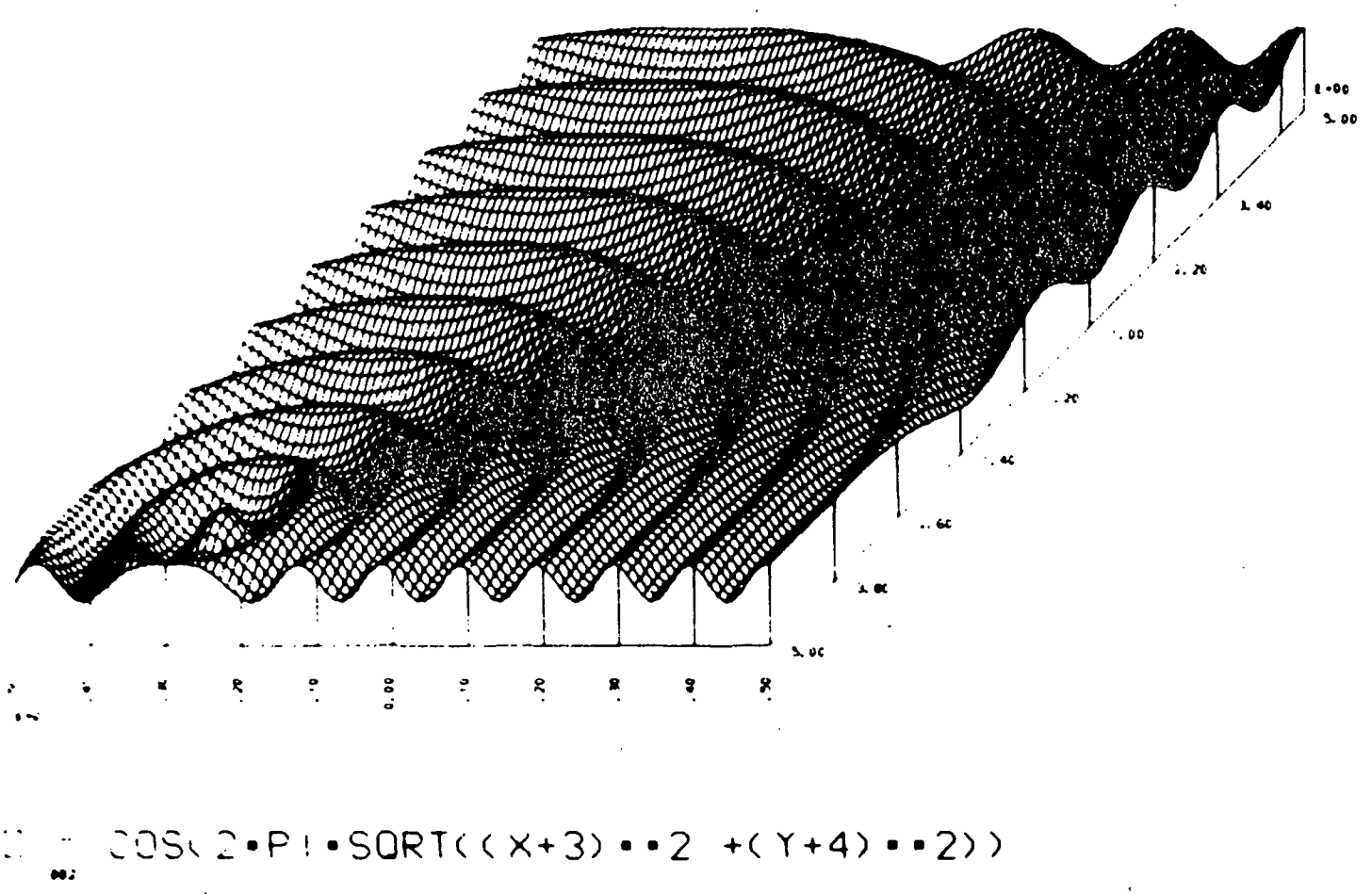

Fig. 4-7. Sinusoidal surface error with point symmetry of error decentered with respect to optical axis.

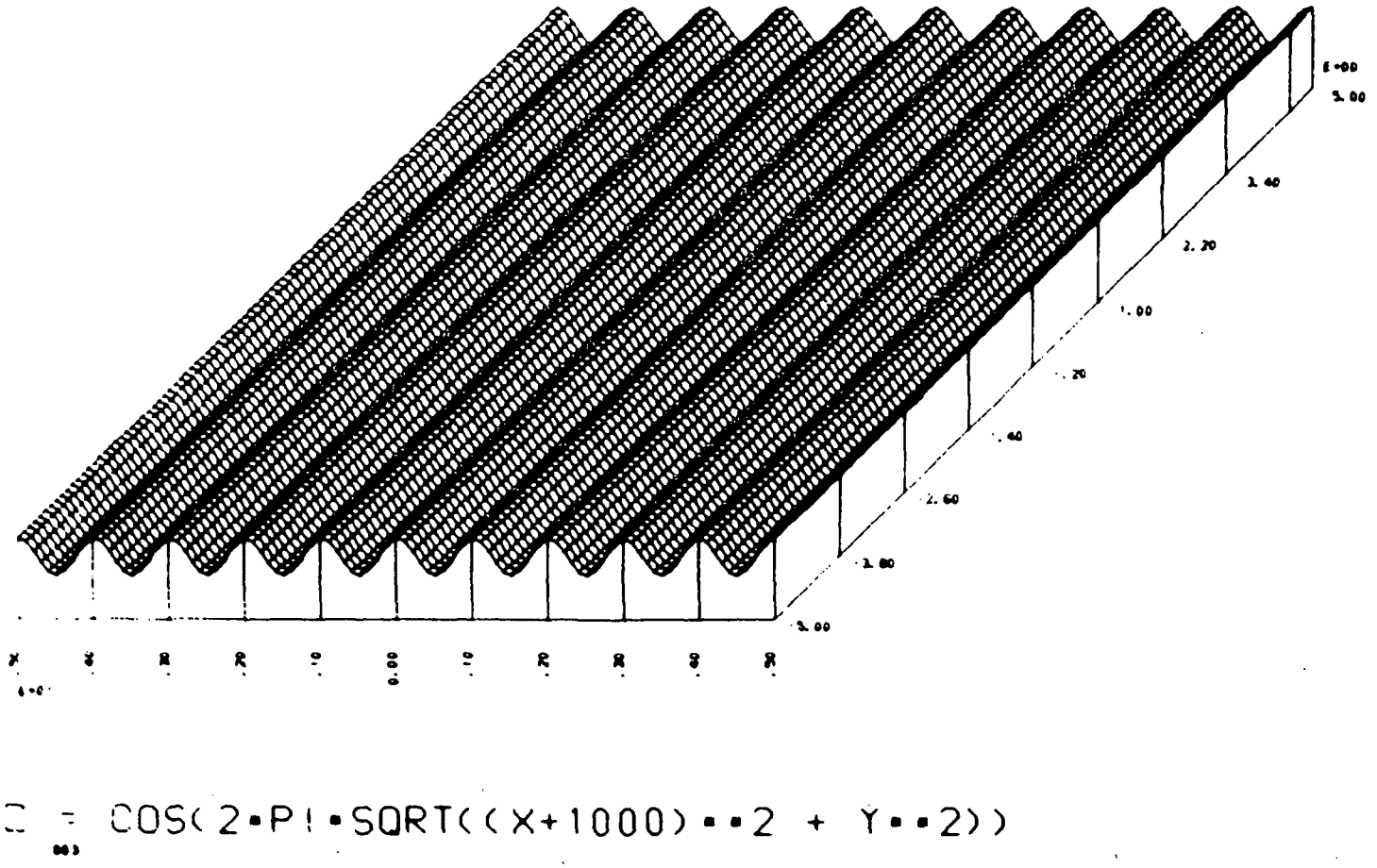

Fig. 4-8. Sinusoidal surface error with large displacement error.

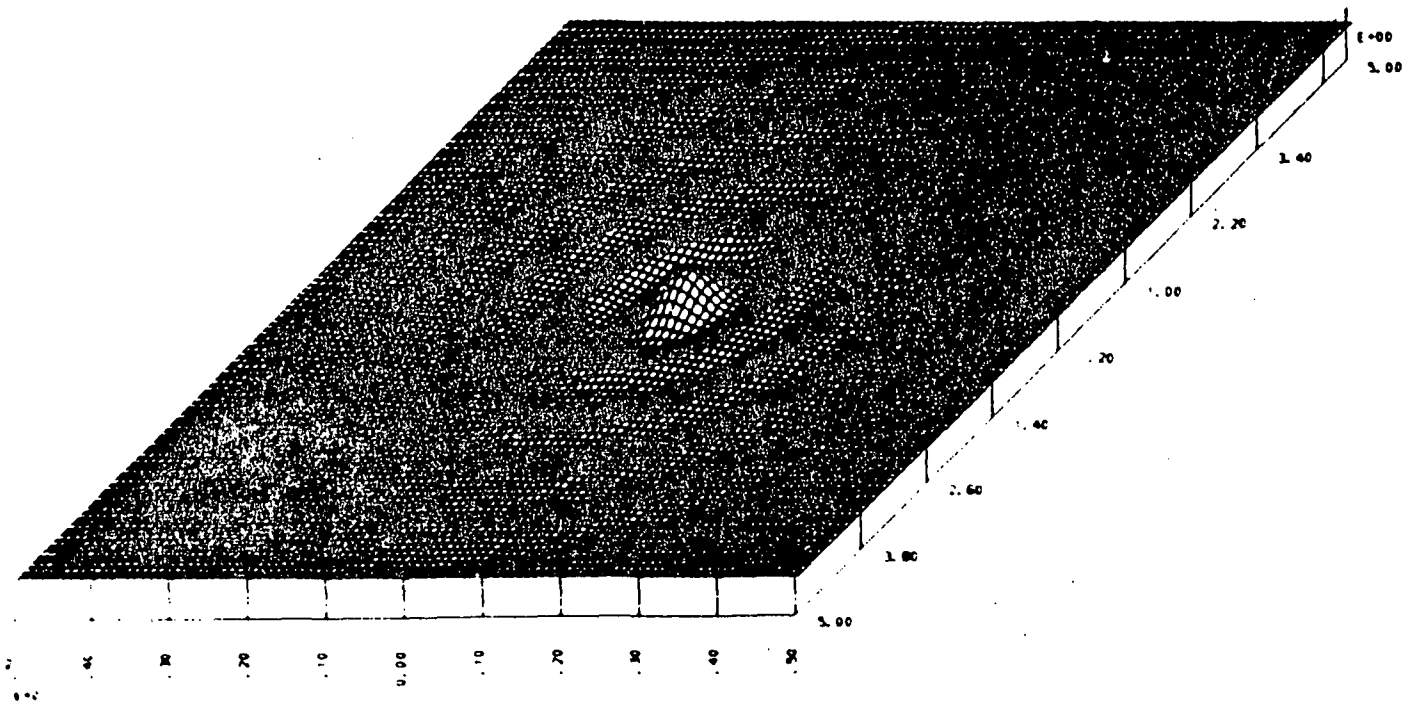

Fig. 4-9. Sinc function surface error.

Fig. 4-10. Combined sine and cosine surface error.

$$Q_2^2 = X_s^2 \cos^2\varphi + Y_s^2 \sin^2\varphi - 2X_s Y_s \sin\varphi \cos\varphi \tag{4-47}$$

$$Q_e^2 = (X_s + U_s)^2 + (Y_s + V_s)^2 \tag{4-48}$$

The sagitta expressions are:

$$\zeta_1 = \frac{\rho_1 Q_1^2}{1 + \left(1 - \kappa \rho_1^2 Q_1^2\right)^{1/2}} + \alpha Q_1^4 + \beta Q_1^6 + \gamma Q_1^8 + \ldots \tag{4-49}$$

$$\zeta_2 = \frac{\rho_2' Q_2^2}{1 + \left(1 - \rho_2'^2 Q_2^2\right)^{1/2}} \tag{4-50}$$

$$\rho_2' = \frac{\rho_2}{1 - \rho_2 \zeta_1} \tag{4-51}$$

$$\zeta_e = C_1 \left(\frac{\sin C_2 \pi Q_e}{C_2 \pi Q_e} \right) \cos C_3 \pi Q_e \tag{4-52}$$

Note that C_1 is an amplitude term while C_2 and C_3 control frequency.

The ray-tracing equations for these special surfaces are:

$$Z_{s(i+1)} = \frac{\zeta_{si} - \left[(\ell_{s-1}/n_{s-1})\, \zeta'_{si}(X) + (m_{s-1}/n_{s-1})\, \zeta'_{si}(Y) \right] Z_{si}}{1 - \left[(\ell_{s-1}/n_{s-1})\, \zeta'_{si}(X) + (m_{s-1}/n_{s-1})\, \zeta'_{si}(Y) \right]} \tag{4-53}$$

$$n_{s(i+1)} = \frac{\mu_s^2 - \ell_{s0}^2 - m_{s0}^2 + n_{si}^2 \left| 1 + [\zeta_s'(X)]^2 + [\zeta_s'(Y)]^2 \right|}{2\left[n_{si} \left| 1 + [\zeta_s'(X)]^2 + [\zeta_s'(Y)]^2 \right| - \ell_{s0}\zeta_s'(X) - m_{s0}\zeta_s'(Y) \right]} \tag{4-54}$$

where

$$\zeta_{si}'(X) = \zeta_1'(X_{si}) + \zeta_2'(X_{si}) + (X_{si}/Q_e)\left[\zeta_e'(Q_e)\right] \tag{4-55}$$

$$\zeta_{si}'(Y) = \zeta_1'(Y_{si}) + \zeta_2'(Y_{si}) + (Y_{si}/Q_e)\left[\zeta_e'(Q_e)\right] \tag{4-56}$$

and

$$\zeta_1'(X) = \rho_1'' \left[X_{si}(a + b\sin\varphi)^2 + b^2 Y_{si} \sin\varphi\cos\varphi \right] \tag{4-57}$$

$$\zeta_1'(Y) = \rho_1'' \left[Y_{si}(a + b\cos\varphi)^2 + b^2 X_{si} \sin\varphi\cos\varphi \right] \tag{4-58}$$

$$\rho_1'' = \frac{\rho_1'}{\left(1 - \rho_1^2 Q_2^2\right)^{1/2}} \tag{4-59}$$

$$\rho_1' = \frac{1}{Q_1}\frac{d\zeta_1}{dQ_1} \tag{4-60}$$

$$\zeta_2'(X) = \rho_2''\left(X_{si}\cos^2\varphi - Y_{si}\sin\varphi\cos\varphi\right) \tag{4-61}$$

$$\zeta_2'(Y) = \rho_2''\left(Y_{si}\sin^2\varphi - X_{si}\sin\varphi\cos\varphi\right) \tag{4-62}$$

$$\rho_2'' = \frac{\rho_2^1}{\left(1 - \rho_2^2 Q_2^2\right)^{1/2}} \tag{4-63}$$

$$\zeta'_e(Q_e) = d\zeta_e/dQ_e \tag{4-64}$$

The refraction equations corresponding to eqs. 4-22 and 4-23 are:

$$\ell_{si} = \ell_{s-1} + \zeta'_s(X_s)(n_{s-1} - n_{si}) \tag{4-65}$$

$$m_{si} = m_{s-1} + \zeta'_s(Y_s)(n_{s-1} - n_{si}) \tag{4-66}$$

or instead of eq 4-22a and 4-23a

$$\ell_{si} = \ell_{so} - \zeta'_s(X_s)\, n_{si} \tag{4-67}$$

$$m_{si} = m_{so} - \zeta'_s(Y_s)\, n_{si} \tag{4-68}$$

d. Perfect Surfaces — Another kind of special surface which has proved of considerable utility is the option of interspersing one or more "perfect" surfaces in a system being analyzed. The most obvious application of this is the conversion of an afocal system into an image-forming system without introducing additional aberrations. The ray trace equation for this surface utilizes the standard intercept computations for a conventional plane surface.

$$X_s = X_{s-1} + \frac{\ell_{s-1}}{n_{s-1}}(t_{s-1} - Z_{s-1}) \tag{4-69}$$

$$Y_s = Y_{s-1} + \frac{m_{s-1}}{n_{s-1}}(t_{s-1} - Z_{s-1}) \tag{4-70}$$

$$Z_s = 0$$

The refraction equations are

$$\frac{\ell_s}{n_s} = \frac{\ell_{s-1}}{n_{s-1}} - P_s X_s \tag{4-71}$$

$$\frac{m_s}{n_s} = \frac{m_{s-1}}{n_{s-1}} - P_s Y_s \tag{4-72}$$

$$n_s = \frac{\mu_s}{\left[1 + (\ell_s/n_s)^2 + (m_s/n_s)^2\right]^{1/2}} \tag{4-73}$$

where P_s is the power of the perfect surface and it is input in place of ρ_s (RHφS) or as RADS=$R_s = 1/P_s$. A perfect surface is identified by the input of the rotational symmetry constant (CRS) for that surface as CRS = -1.

e. Applications — Except for perfect surfaces, these equations can represent most, if not all, optical surfaces generated by design or inadvertence. This includes spheres, cylinders, toroids, axicons, roofs, rotationally symmetrical surfaces with small cylindrical error, and numerous combinations of these as well as the periodic errors.

The matrix in Table 4-1 illustrates some of the surface forms which may be represented by these equations.

f. Optical Path Difference or Wavefront Phase Error — The optical path length D of a ray is the product of the length d along the ray and the refractive index μ of the medium.

D = optical path length

$$D = d \cdot \mu \tag{4-74}$$

TABLE 4-1

Surface Forms

	ρ_1	ρ_2	a	b	κ	α, ρ_1, γ, etc	c_1, c_2	c_1, c_3	U, V
Sphere	X	0	1	0	1	0	0	0	0
Conic	X	0	1	0	$\kappa \pm 1$	0	0	0	0
Asphere	X	0	1	0	1	X	0	0	0
Cylinder	X	0	0	1	1	0	0	0	0
Cylinder	0	X	0	0	1	0	0	0	0
Toroid	X	X	0	1	1	0	0	0	0
Cylinder, acircular	X	0	0	1	1	X	0	0	0
Cone, axicon	$\rho_s \to \infty$	0	1	0	$\kappa < 0$	0	0	0	0
Roof	$\rho_s \to \infty$	0	0	1	$\kappa < 0$	0	0	0	0
Sphere with cylinder error	X	0	1	$b \ll 1$	1	0	0	0	0
Sphere with sinusoidal error	X	0	1	0	1	0	0	X	0
Sphere with sinc type error	X	0	1	0	1	0	X	0	0
Sphere with combined periodic errors displaced	X	0	1	0	0	0	X	X	X
Perfect Surface	P_s	0	-1 (flag only)	0	0	0	0	0	0

T1203

Defining the optical path length for a ray passing from surface s-1 to surface s to be D_s, it can be shown that

$$D_s = \frac{(t_{s-1} - Z_{s-1} + Z_s)}{n_{s-1}} \mu_{s-1}^2 \tag{4-75}$$

The total path length through the complete system is the sum of all the surface-to-surface values and is defined to be D*.

$$D^* = D_o + \sum_{s-1}^{n} D_s \tag{4-76}$$

which is in practice the summation from entrance pupil to exit pupil. D_o is the distance along the ray from the object point to the entrance pupil for a finite object, i.e. $L_o^{-1} \neq 0$.

$$D_o = \frac{\mu_o L_o^2}{n_o} \quad (L_o^{-1} \neq 0) \tag{4-77}$$

For infinite conjugates, D_o is the distance from the incident plane wave to the entrance pupil.

$$D_o = m_o y_o \quad (L_o^{-1} = 0) \tag{4-78}$$

where

$y_o \equiv$ entrance pupil ray intercept.

Note that for the infinite conjugate axial case $m_o = 0.$, hence $D_o = 0$. The difference between the total optical path length D* for an arbitrary ray and that D^*_c for a reference ray is the optical path difference or wavefront departure W for the given ray.

$$W = D^* - D_c^* \,. \tag{4-79}$$

W can be expressed as the sum of a set of W's at each surface

$$\begin{aligned} W &= D_o + \sum_1^N D_s - D_{co} - \sum_1^N D_{cs} \\ &= D_o - D_{co} + \sum_1^N (D_s - D_{cs}) \\ &= \sum_0^N (D_s - D_{cs}) \end{aligned} \tag{4-80}$$

or, defining

$$W_s = D_s - D_{cs}. \tag{4-81}$$

Then, for the ray corresponding to exit pupil coordinates (u, v) the overall optical path difference for that ray is W(u, v) and

$$W(u,v) = \sum_{s=0}^{N} W_s \,. \tag{4-80a}$$

Denoting the ray parameters for the arbitrary ray with the subscript s and those for the reference ray with the subscript cs and substituting (4-75) into (4-81),

$$\begin{aligned} W_s = \frac{\mu_{s-1}^2}{n_{s-1}\, n_{cs-1}} \Big[& n_{cs-1} (Z_s - Z_{s-1}) - n_{s-1} (Z_{cs} - Z_{cs-1}) \\ & + t_{s-1} (n_{cs-1} - n_{s-1}) \Big] \end{aligned} \tag{4-82}$$

Generalizing (4-82) to allow treatment of tilted and/or decentered surfaces

$$W_s = W_{so} - \frac{\mu_{s-1}^2}{n'_{s-1} n'_{cs-1}} \left[n'_{cs-1} (Z_s - Z_s^*) - n'_{s-1} (Z_{cs} - Z_{cs}^*) \right] \tag{4-83}$$

where

$$W_{so} = \frac{\mu_{s-1}^2}{n_{s-1} n_{cs-1}} \left[(n_{cs-1} - n_{s-1}) t_{s-1} - n_{cs-1} Z_{cs-1} Z_{s-1} + n_{s-1} Z_{cs-1} \right] \tag{4-84}$$

The primed and starred quantities of equation (4-83) are defined in Section 4.6 on tilt and decentration. W_{so} represents the path difference from surface "s-1" to the nominal tangent plane of surface "s". The remainder of eq. (4-83) represents the path difference from the nominal, untilted tangent plane of surface "s" to the tilted and/or decentered surface itself.

g. Perfect Surface OPD — When using the perfect surface option, the optical path difference for the surface is computed as follows:

$$W_s = W_{so} - P_s \mu_s \left[\frac{\left(X_s^2 + Y_s^2 \right) \cdot n_s}{\mu_s + n_s} - \frac{\left(X_{cs}^2 + Y_{cs}^2 \right) \cdot n_{cs}}{\mu_s + n_{cs}} \right] \tag{4-85}$$

4.4 VIGNETTING AND OBSCURATION

a. Vignetting – Vignetting must be accommodated and LACOMA handles it in two ways; at the entrance pupil or on a surface-by-surface basis.

If the nature of the vignetting at the entrance pupil is known, this vignetting may be described by the input of a value V_0 = VZERO or V_π = VPI representing the fractional vignetting, respectively, in the upper or lower portion of the entrance pupil. A different set (V_0, V_π) must be input for each field fraction K. The interpretation of the magnitude of the input value of V is as follows:

$$V = 0 \text{ or } 1.0 \text{ no vignetting}$$

$$0 < V < 1.0 \text{ normal vignetting}$$

The other means for handling vignetting can replace or augment the pupil vignetting. This is accomplished by the input of clear aperture data for each surface. As each ray is traced through the surface, a test determines whether the ray falls outside the clear dimensions in which case it is terminated.

b. Obscuration – As with vignetting, there are two approaches to obscuration, either in the entrance pupil or on a surface-by-surface basis. At the entrance pupil, the descriptive data are: UZERO for the radius of the obscuration; GZERO representing the distance from the center of the entrance pupil to the upper edge of the obscuration; and GPI, the distance from the center of the entrance pupil to the lower edge of the obscuration. A set (UZERO, GZERO, GPI) is required for each field angle to be traced. A circular centered obscuration would have

$$GZERO = UZERO = - GPI$$

Other cases can of course be accommodated.

In case (GZERO-GPI) > 2 · UZERO, such as in Fig. 4-11, no rays will be traced through the racetrack-shaped obscuration. If (GZERO-GPI) ≥ 2 ·(BETA0 + UZERO), the effect is that of a rectangular obscuration as per Fig. 4-12.

When UZERO > (GZERO-GPI), the effect is that of a rectangular obscuration rotated 90^{o} from that of Fig. 4-13.

The other mode of obscuration input is via obscuration at each surface.

c. Surface by Surface Vignetting and Obscuration — The parameters BETAPX, BETAPY, and BETASX and BETASY can be used to describe a circular obscuration or clear aperture, rectangular obscuration or clear aperture, annular obscuration, and segmented apertures. These are illustrated by Figures 4-14, 4-15 and 4-16. Some of the possible aperture configurations which can be described are shown in Fig. 4-17.

4.5 REFERENCE WAVEFRONT

The N^{th} surface to which the OPD values are summed is analogous to the gaussian sphere discussed in the previous literature. The relevant characteristics of this reference wavefront or gaussian sphere are obtained from the chief ray data. As with any other optical surface, the reference wavefront is defined by its radius of curvature RW, its spacing TR from the (N-1)st surface, its decentration ΔX, ΔY and tilt θX, θY.

For the axial case where there is no tilt or decentration of the reference wavefront, its location is given by TR = Texit.

Where Texit is due to eq. 4-6 and RW = T'_{n-1} - TR

Where T'_{n-1} was determined by eq. 4-14a or eq. 4-15a.

Off-Axis Wavefront — For an optical system with tilts and/or decentrations or with an off-axis input beam the full set of descriptive parameters for the reference wavefront will be required.

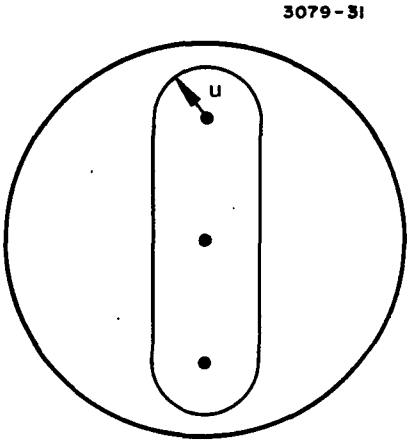

Fig. 4-11.
Racetrack obsuration (U = UZERO).

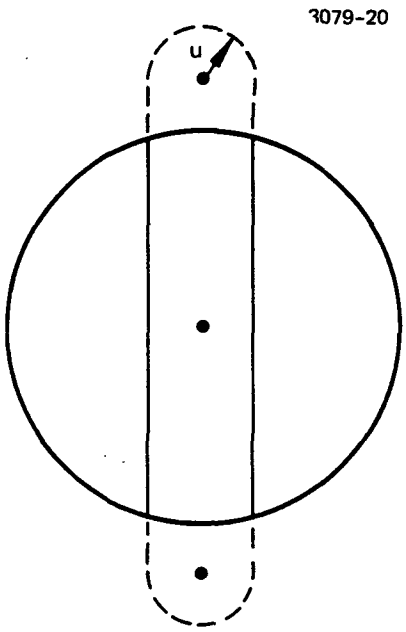

Fig. 4-12.
Rectangular obscuration.

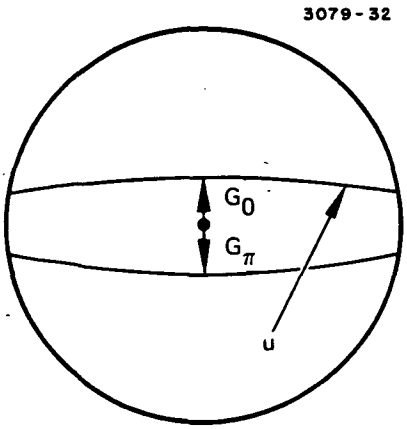

Fig. 4-13.
Rectangular or near-rectangular obscuration oriented 90^o away from Fig. 4-12. (G_0 = GZERO, G_π = ^oGPI).

3079-21

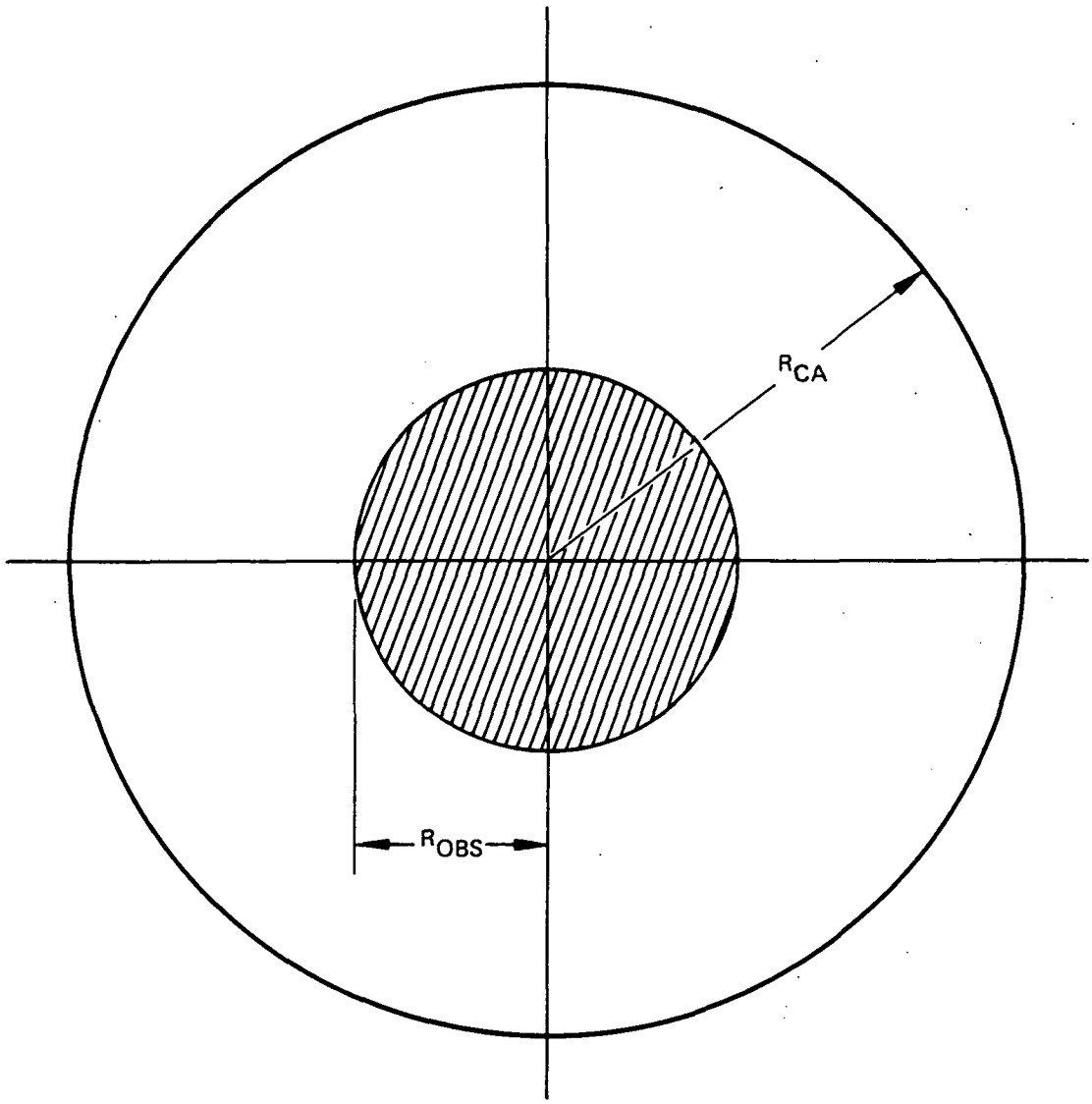

CLEAR APERTURE RADIUS = R_{CA}

OBSCURATION RADIUS = R_{OBS}

BETASX = R_{CA} AND BETASY = 0

OR BETASY = R_{CA} AND BETASX = 0

BETAPX = R_{OBS} AND BETAPY= 0

OR BETAPY = R_{OBS} AND BETAPX= 0

Fig. 4-14. Circular clear aperture and obscuration.

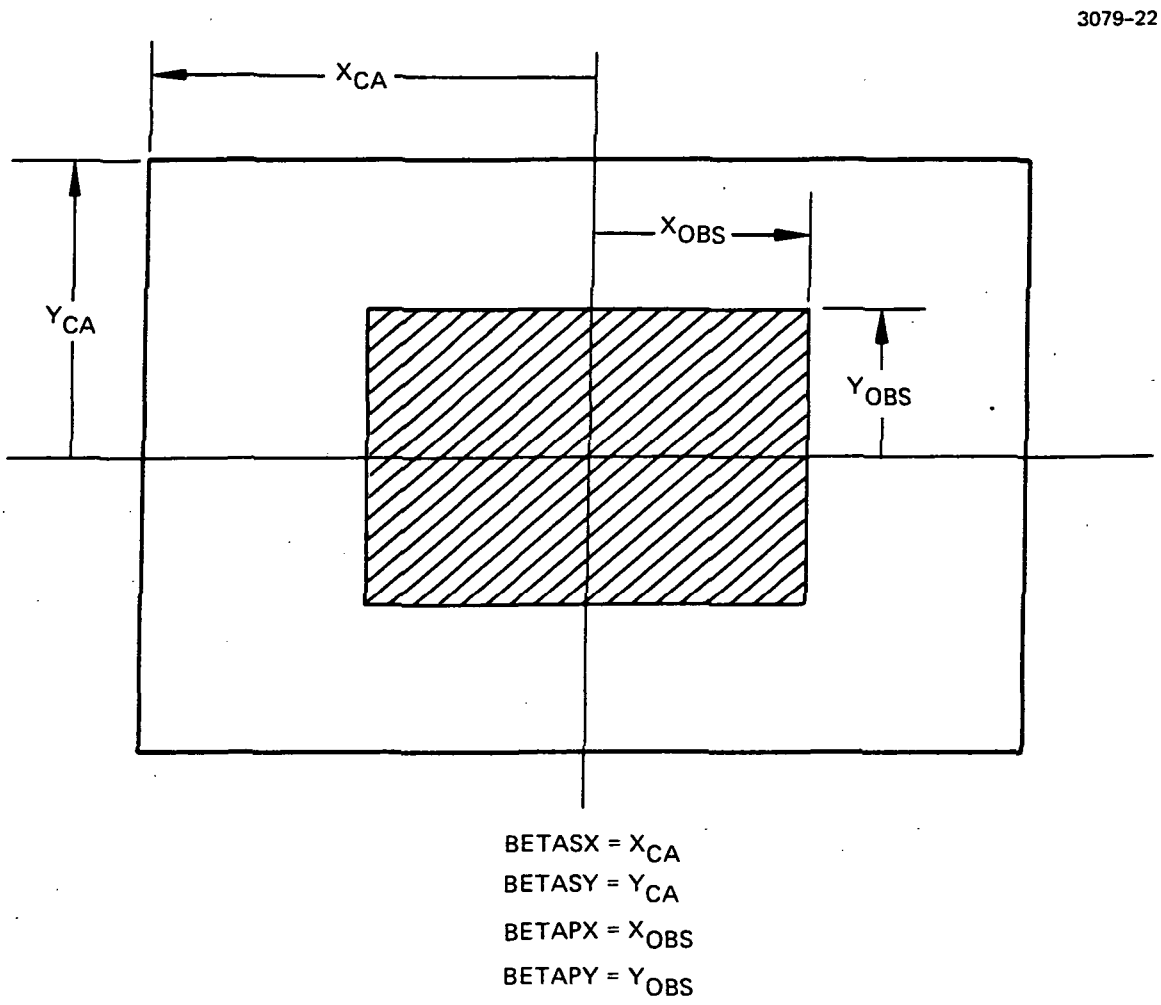

Fig. 4-15. Rectangular clear aperture and obscuration.

ANNULAR OBSCURATION

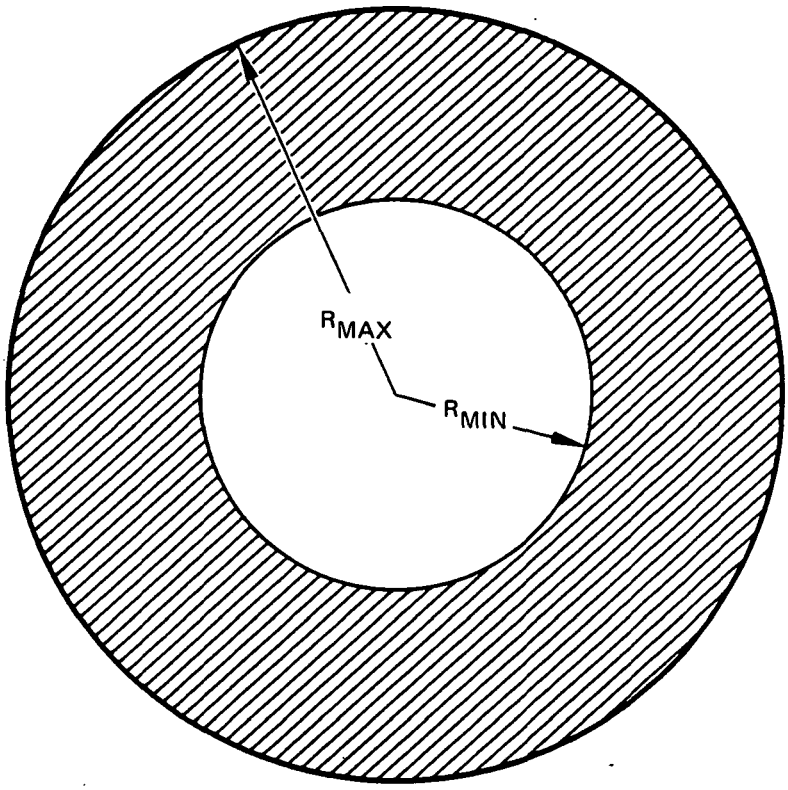

RAYS TRACED INSIDE R_{MIN} OR OUTSIDE R_{MAX}

RAYS BLOCKED BETWEEN R_{MIN} AND R_{MAX}

BETAPX = R_{MIN} AND BETAPY = 0

OR BETAPY = R_{MIN} AND BETAPX = 0

BETASX = R_{MAX} AND BETASY = 0

OR BETASY = R_{MAX} AND BETASX = 0

(ONE OF THE ABOVE VALUES MUST BE INPUT NEGATIVE)

Fig. 4-16. Annular obscuration.

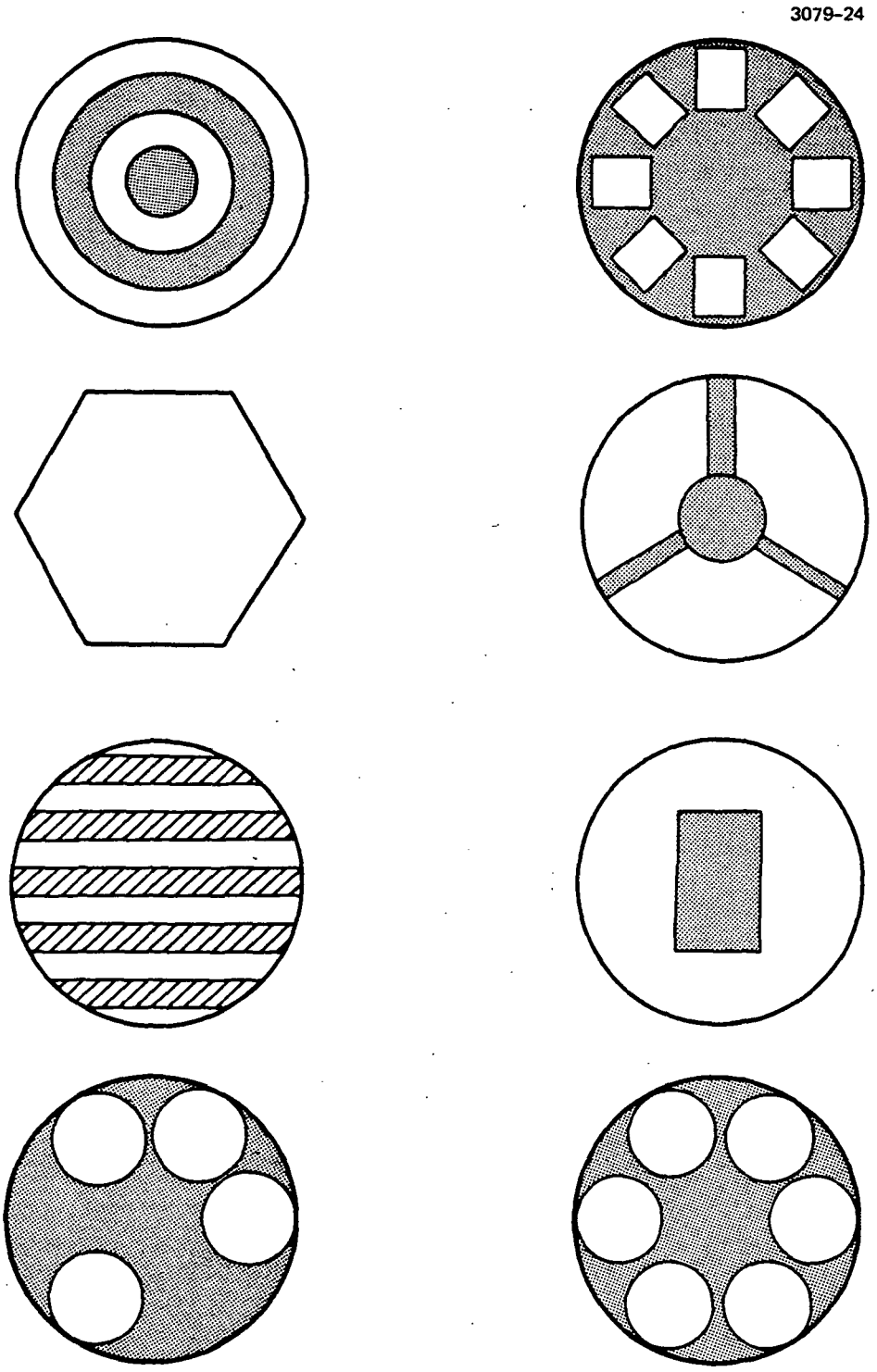

Fig. 4-17. Sample aperture configurations.

RW is the distance along the chief ray from its intersection or point of closest approach to the optical axis (exit pupil position) to its point of intersection with the image surface. The angular components of the chief ray give the tilt of the reference wavefront, etc. The computation of RW, T_r, θX, θY, ΔX and ΔY is as follows.

Given ℓ_c, m_c, n_c, for the chief ray exiting the optical train and the chief ray intercepts X_c, Y_c and Z_c at the focal surface, if $m_c \neq 0$

$$RW = \frac{Y_c \mu_{n-1}}{m_c} \tag{4-86}$$

$$TR = T'_{n-1} - \frac{Y_c n_c}{m_c} + Z_c \tag{4-87}$$

$$\Delta X = X_c - \frac{\ell_c y_c}{m_c} \tag{4-88}$$

$$\Delta Y = 0.$$

If $m_c = 0$ and $\ell_c \neq 0$

$$RW = \frac{X_c \mu_{n-1}}{\ell_c} \tag{4-89}$$

$$TR = T'_{n-1} - \frac{X_c n_c}{\ell_c} + Z_c \tag{4-90}$$

$$\Delta X = 0.$$

$$\Delta Y = Y_c - \frac{m_c RW}{\mu_{s-1}} \quad . \tag{4-91}$$

The reference wavefront tilt angles are

$$\theta X = \text{ARCTAN}\,(\ell_c / n_c) \tag{4-92}$$

$$\theta Y = \text{ARCTAN}\left[\frac{m_c}{n_c\,(1 + (\ell_c/n_c)^2)^{1/2}}\right] . \tag{4-93}$$

For a case with an IMC so that the reference wavefront is off-axis but $X_c \rightarrow Y_c \rightarrow 0$, TR is defined as that for the axial case and

$$RW = \frac{(T'_{n-1} - TR)}{n_c}\,\mu_{n-1} \tag{4-94}$$

$$\Delta X = X_c - \frac{\ell_c\,RW}{\mu_{N-1}} \tag{4-95}$$

$$\Delta Y = Y_c - \frac{m_c\,RW}{\mu_{N-1}} . \tag{4-96}$$

Equations θX and θY are defined per eqs. 4-92 and 4-93.

4.6 TILT AND DECENTRATION

The tilt and decentration procedure utilizes conventional coordinate transformation matrices.

The procedure is to trace a ray to the tangent plane for the centered surface and then locate the intersection point of the ray with the tilted-decentered tangent plane, transform the optical direction cosines of the ray into the rotated coordinate system, and then trace the ray from the new tangent plane to the surface.

The transformation matrix represents the relocation of the origin by ΔX, ΔY and ΔZ followed by rotation of this displaced coordinate system. The rotation begins with a θZ around the optical axis followed by the rotation θY around the X' axis where the X' indicates the new X axis due to the Z rotation. θX is the rotation about the Y' axis which is the result of the θZ, θY rotations.

Representing the new optical direction cosines with primes,

$$\ell'_{s-1} = \ell_{s-1} (\cos \theta X \cos \theta Z + \sin \theta X \sin \theta Y \sin \theta Z)$$

$$-m_{s-1} \cos \theta Y \sin \theta Z + n_{s-1}$$

$$(\cos \theta X \sin \theta Y \sin \theta Z - \sin \theta X \cos \theta Z) \qquad (4\text{-}97)$$

$$m'_{s-1} = m_{s-1} \cos \theta Y \cos \theta Z - n_{s-1} (\sin \theta X \sin \theta Z + \cos \theta X \sin \theta Y \cos \theta Z)$$

$$+ \ell_{s-1} (\cos \theta X \sin \theta Z - \sin \theta X \sin \theta Y \cos \theta Z) \qquad (4\text{-}98)$$

$$n'_{s-1} = n_{s-1} \cos \theta X \cos \theta Y + \ell_{s-1} \sin \theta X \cos \theta Y + m_{s-1} \sin \theta Y \, .$$

$$(4\text{-}99)$$

The values X*, Y* and Z* represent the intercept coordinates of the ray with the nominal tangent plane expressed in the transformed coordinate system relative to the new tangent plane.

$$X^* = (XS0 - \Delta X) (\cos \theta X \cos \theta Z + \sin \theta X \sin \theta Y \sin \theta Z)$$

$$-(YS0 - \Delta Y) \cdot \cos \theta Y \sin \theta Z - \Delta Z$$

$$(\cos \theta X \sin \theta Y \sin \theta Z - \sin \theta X \cos \theta Z) \qquad (4\text{-}100)$$

$$Y^* = (YS0-\Delta Y)\cos\theta Y\cos\theta Z + \Delta Z(\sin\theta X\sin\theta Z + \cos\theta X\sin\theta Y\cos\theta Z)$$

$$+ (XS0-\Delta X)(\cos\theta X\sin\theta Z = \sin\theta X\sin\theta Y\cos\theta Z) \qquad (4\text{-}101)$$

$$Z^* = (XS0-\Delta X)\sin\theta X\cos\theta Y + CYS0-\Delta Y)\sin\theta Y - \Delta Z\cos\theta X\cos\theta Y\ . \qquad (4\text{-}102)$$

Thus X'_{so} and Y'_{so} represent the intersection of the ray with the new tangent plane and

$$X'_{so} = X^* - \frac{\ell'_{s-1}}{n'_{s-1}} Z^* \qquad (4\text{-}103)$$

$$Y'_{so} = Y^* - \frac{m'_{s-1}}{n'_{s-1}} Z^* \qquad (4\text{-}104)$$

$$Z'_{so} = 0.$$

a. Sign Convention — The origin (surface vertex) of the transformed coordinate system has the coordinates ΔX, ΔY, ΔZ relative to the original origin (Fig. 4-18). Viewed along the positive direction of the optical axis, $+\theta Z$ represents a counterclockwise rotation about the optical (Z) axis. Similarly, a tilted surface has its optical axis oriented at the angles θX and θY with respect to the axis of the preceding optical surface. A surface tilted by $+\theta Y$ (or $+\theta X$) has it axis rotated such that its new direction relative to the original axis is the same as would a ray having positive direction cosines m and n. For example, a ray parallel to the original axis ($\ell = m = 0$, $n = 1$), and incident upon a surface tilted by a positive θY will have transformed incident direction cosines so that $m < 0$ (see Fig. 4-19).

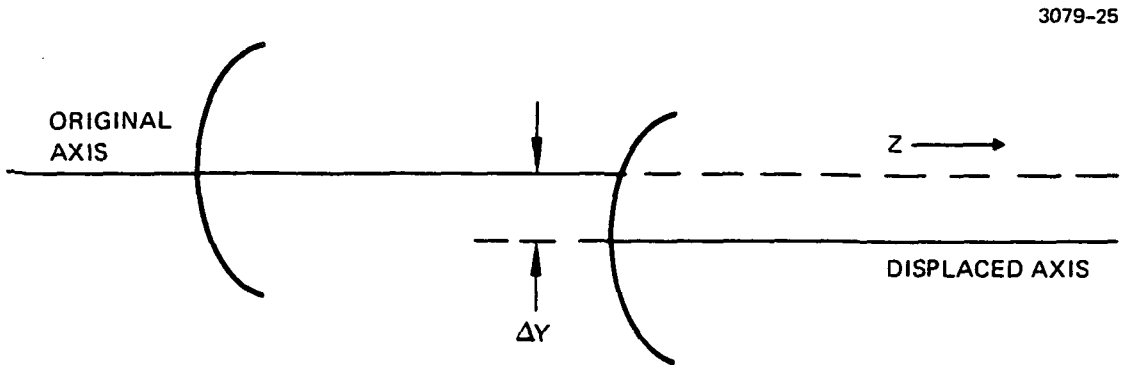

Fig. 4-18. Illustration of ΔY negative.

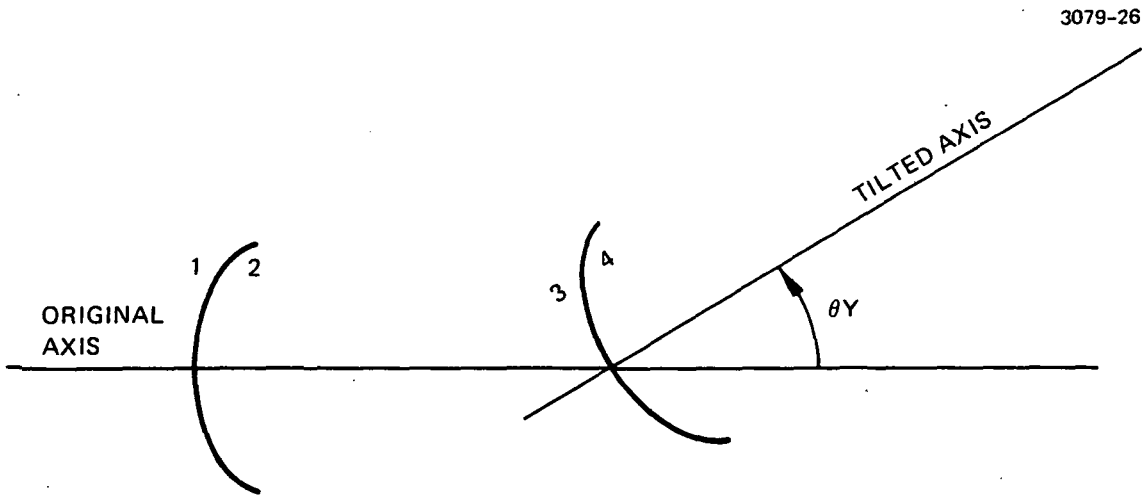

Fig. 4-19. Illustration of θ_y positive.

b. Coordinate Restoration — If a surface is tilted or decentered, all the surfaces following will be aligned with the tilted or decentered surface. Therefore, the tilt or decentration of a single surface amounts to tilting or decentering the system following the tilt with respect to the portion of the system preceding the tilt. If it is desired to misalign a given surface in the midst of a centered optical system, it is necessary to introduce a reverse tilt or decentration immediately following the misaligned surface to restore the coordinate system. If there is a combination of ΔX, ΔY, ΔZ and/or θX, θY, θZ at the surface, then because of the sequence of the operation of the decentrations and tilts the combination of $-\Delta X$, $-\Delta Y$, $-\theta X$, $-\theta Y$, etc. will not necessarily restore the proper coordinates. The following are rules to follow in the restoration of the coordinate system after traversing a misaligned surface:

1. Restoration after a single tilt θY or a single decentration ΔX is accomplished with the insertion of a dummy surface following the misaligned surface with $\rho_s = 0$, $T_{s-1} = 0$ and the refractive index μ_s the same as that following the misaligned surface. The dummy plane should have a tilt of $-\theta Y$ or a decentration of $-\Delta X$.

2. For a surface having tilts θX, θY, θZ and decentrations ΔX, ΔY, ΔZ. Four dummy planes must be inserted:

   Dummy plane No. 1 with $-\theta X$
   Dummy plane No. 2 with $-\theta Y$
   Dummy plane No. 3 with $-\theta Z$
   Dummy plane No. 4 with $-\Delta X$, $-\Delta Y$, $-\Delta Z$

3. For surfaces with more than one but less than the full six misalignment components the sequence of the operations must remain the same removing dummy planes which do not apply. For a surface with θX, θZ and ΔY three dummy planes are used:

   Dummy plane No. 1 with $-\theta X$
   Dummy plane No. 2 with $-\theta Z$
   Dummy plane No. 3 with $-\Delta Y$

4.7 PUPIL COMPUTATIONS

All the ray trace and OPD computations are initiated at the entrance pupil. Part of the input is "M" which is the surface number of the aperture stop which provides for the computation of the paraxial entrance pupil location T_o from eq. (3-5). The rays are input at the pupil in a uniform square grid as in Fig. 4-20. The input parameter NXY determines the number of grid intervals across half the pupil so that there will be (2NXY + 1) grid points across the pupil. The pupil semidiameter is divided by NXY to give

$$\epsilon x = \epsilon y = \frac{\beta_o}{NXY} \tag{4-105}$$

for the intervals between rays. The ray coordinates X_o and Y_o at the entrance pupil are then obtained by incremental steps of ϵx and ϵy. Combining these with the input values of L_o^{-1} and H for any angular obliquity of the input beam the ray input direction cosines l_o, m_o and n_o are determined

$$AA = \text{ARCTAN}\,(X_o\, L_o^{-1}) \tag{4-106}$$

$$BB = \text{ARCTAN}\,((Y_o\, L_o^{-1} + \text{Tan}\,(H))\cos\,(AA)) \tag{4-107}$$

$$l_o = \sin\,(AA)\cos\,(BB) \tag{4-108}$$

$$m_o = \sin\,(BB) \tag{4-109}$$

$$n_o = \cos\,(AA)\cos\,(BB)\ . \tag{4-110}$$

At this point W_o is determined to be used in equation (4-80a)

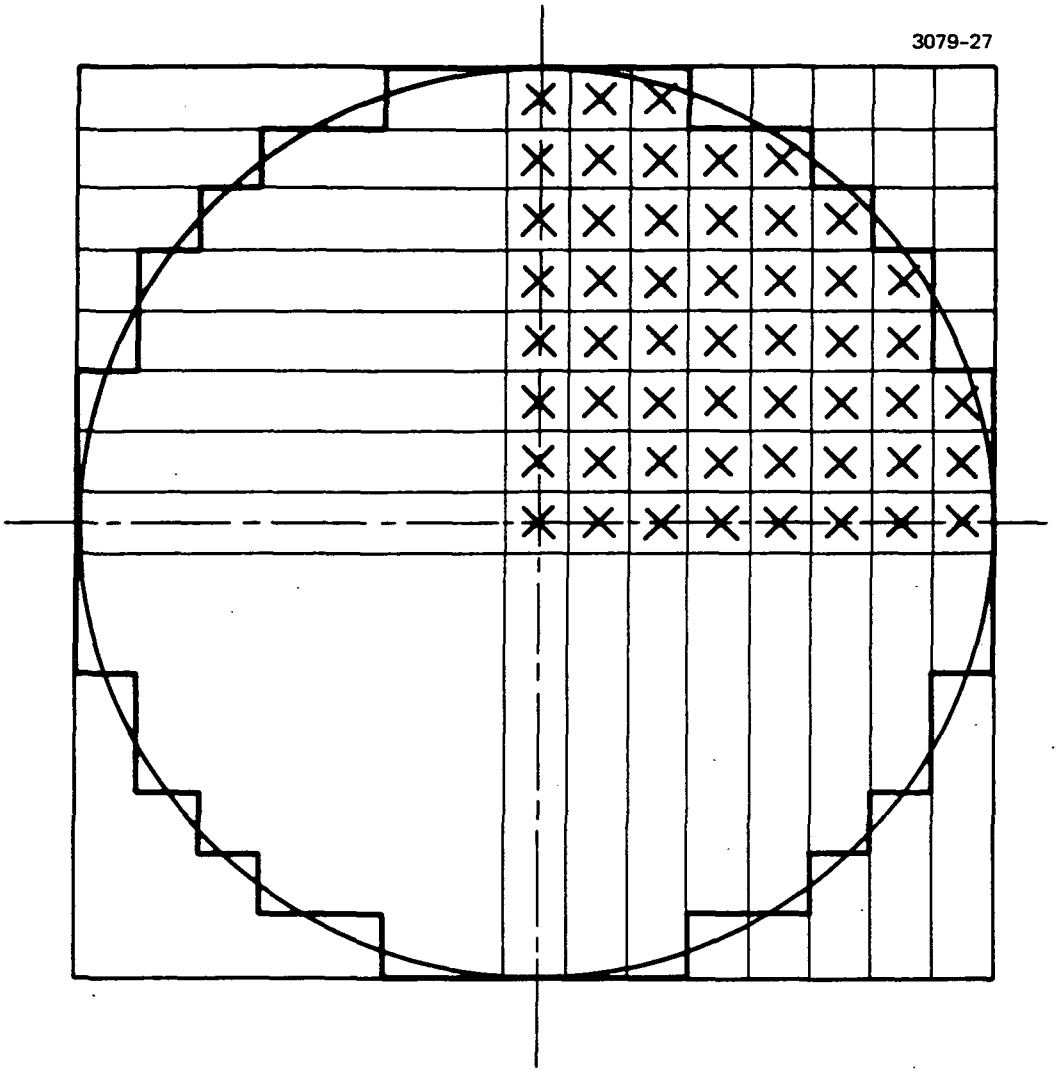

Fig. 4-20. Uniform square ray grid.

For $L_o^{-1} = 0$

$$W_o = Y_o m_o \tag{4-111}$$

For $L_o^{-1} \neq 0$

$$W_o = \left[\frac{1}{n_o} - \frac{1}{\cos (H)} \right] L_o \ . \tag{4-112}$$

Pupil Amplitude Values (B(u, v)) – The pupil coordinates are here referred to as u, v which coincides with the notation used in discussing computation of the amplitude spread function (Section 4.8) u and v apply to the exit pupil coordinates while X_o and Y_o represent the entrance pupil coordinates for the given ray.

The entrance pupil amplitude values are determined as follows:

Transmitter – Truncated gaussian amplitude distribution with total radiant power per input parameter P_o.

Receiver – (Received signal) – Uniform amplitude distribution if P_o is input positive it is the uniform intensity value I_o. If P_o is input negative it is the total radiant power, then

$$I_o = |P_o| / A_o \tag{4-113}$$

where

A_o = entrance pupil area

then

$$B(u, v) = \sqrt{I_o} \ .$$

Receiver-Local Oscillator – Truncated gaussian amplitude distribution with total radiant power per input parameter P_o.

Truncated Gaussian Intensity Function – The pupil amplitude function B(u, v) for a gaussian amplitude distribution is defined as follows:

$P_o \equiv$ Total input beam power (W)

$I_o \equiv$ peak intensity of gaussian beam

$\omega_o \equiv 1/e^2$ intensity radius

$\beta_o \equiv$ maximum input beam radius or truncation radius

$r^2 = u^2 + v^2$

$$I_o = \frac{2P_o}{\pi\omega_o^2 \left(1 - e^{-2\beta_o^2/\omega_o^2}\right)} \tag{4-115}$$

$$I(u,v) = I_o\, e^{-2r^2/\omega_o^2} \tag{4-116}$$

$$B(u,v,) = \sqrt{I\,(u,v)}\ . \tag{4-117}$$

The amplitude expressions, eq. (4-114) and (4-117), assume unit magnification between entrance and exit pupils. If the pupil magnification mP is not unity it will modify B(u, v).

$$\text{pupil magnification} \equiv mP = \frac{\text{entrance pupil diameter}}{\text{exit pupil diameter}} \tag{4-118}$$

$$B'(u,v) = mP \cdot B(u,v)\ . \tag{4-119}$$

4.8 AMPLITUDE SPREAD FUNCTION

The complex impulse response function or amplitude spread function ASF(x, y) at the Fraunhofer plane is the two dimensional Fourier transform of the pupil function F(u, v).

For the received signal

$$ASF1(x,y) = FR1(x,y) + i\ FI1(x,y) \tag{4-123}$$

$$PSF1(x,y) = |ASF1(x,y)|^2 \tag{4-124}$$

and for the local oscillator

$$ASF2(x,y) = FR2(x,y) + i\ FI2(x,y) \tag{4-123a}$$

$$PSF2(x,y) = |ASF2(x,y)|^2 \ . \tag{4-124a}$$

Signal power, local oscillator power and heterodyne power are obtained by numerical integration over the specified detector dimensions.

The computed ASF and PSF values are obtained for a uniform grid of intervals ΔX, ΔY.

$$\text{Signal Power} \equiv POWER(1) = \sum_x \sum_y PSF1\,(x,y)\,\Delta X\,\Delta Y \tag{4-125}$$

$$\text{L.O. Power} \equiv POWER\,(2) = \sum_x \sum_y PSF2\,(x,y)\,\Delta X\,\Delta Y \ . \tag{4-126}$$

Heterodyne Power — If the nominal phase difference between the receiver signal beam and the local oscillator beam is zero, heterodyne power is obtained with J12 (x, y).

$$\text{Heterodyne Power} \equiv POWER(3) = \sum_x \sum_y J12(x,y)\,\Delta X\,\Delta Y \tag{4-127}$$

where

$$J12(x,y) = FR1(x,y)\ FR2(x,y) + FI1(x,y)\ F12(x,y) \tag{4-128}$$

$$ASF(x, y) = \mathcal{F} \cdot F(u, v) \tag{4-120}$$

$\mathcal{F}$ denotes Fourier transform

$$F(u, v) = B(u, v) \cdot \exp\left[-iK \cdot W(u, v)\right] \tag{4-121}$$

$$K = 2\pi/\lambda \ .$$

With $B(u, v)$ from (4-114) or (4-117) and (4-119) with $W(u, v)$ from (4-80a).

$$ASF(x, y) = \frac{1}{\lambda \cdot RW} \iint F(u, v) \cdot \exp\left[\frac{iK}{RW}(ux + vy)\right] \, dudv. \tag{4-120a}$$

The complex amplitude function $ASF(x, y)$ is represented by the real function $FR(x, y)$ and the imaginary function $FI(x, y)$.

$$ASF(x, y) = FR(x, y) + i\, FI(x, y) \ . \tag{4-120b}$$

The intensity function or point spread function is $PSF(x, y)$

$$PSF(x, y) = \left|ASF\ (x, y)\right|^2 \tag{4-122}$$

$$= \left[FR(x, y) + i\, FI(x, y)\right] \left[FR(x, y) - iFI(x, y)\right] \ . \tag{4-122a}$$

The functions $ASF(x, y)$ and $PSF(x, y)$ provide the basis for the quality criteria for the receiver and transmitter.

4.9 RECEIVER QUALITY CRITERIA

The amplitude spread function $ASF(x, y)$ and point (intensity) spread function $PSF(x, y)$ are determined for the received signal beam and the local oscillator (L.O.) beam.

or for brevity,

$$J12 = FR1\ FR2 + FI1\ F12\ . \qquad (4\text{-}128a)$$

If there is a nominal phase difference ($\Delta\phi$) between the two beams, that phase component must be removed to obtain J12:

$$\text{Heterodyne power} \equiv \text{POWER}(3) = \sum_x \sum_y J12'(x,y)\,\Delta X\,\Delta Y \qquad (4\text{-}129)$$

$$J12' = FR1'\ FR2 + FI1'\ F12 \qquad (4\text{-}130)$$

$$J12' = (FRI \cos\Delta\phi - FI1 \sin\Delta\phi)\ FR2 + (FI1 \cos\Delta\phi + FR1 \sin\Delta\phi)\ FI2$$

$$J12' = (FR1\ FR2 + FI1\ FI2)\cos\Delta\phi + (FI2\ FR1 - FI1\ FR2)\sin\Delta\phi$$

$$J12' = J12 \cos\Delta\phi + K12 \sin\Delta\phi \qquad (4\text{-}130a)$$

where

$$K12 = FI2\ FR1 - FI1\ FR2 \qquad (4\text{-}131)$$

Phase minimization — The value of J12' will be maximized when $d(J12'/d(\Delta\phi) = 0$.

$$\frac{d(J12')}{d(\Delta\phi)} = J12 \sin\Delta\phi + K12 \cos\Delta\phi \qquad (4\text{-}132)$$

with

$$\frac{d(J12')}{d(\Delta\phi)} = 0.$$

$$J12 \sin \Delta\phi = K12 \cos \Delta\phi$$

$$\frac{\sin \Delta\phi}{\cos \Delta\phi} = \frac{K12}{J12} = \tan \Delta\phi \ .$$

The value of $\Delta\phi$ is then obtained by the summation over the specified detector as follows

$$\text{Tan} \quad = \frac{\Sigma\Sigma_{x\ y} K12\ (X\ Y)}{\Sigma\Sigma_{x\ y} J12\ (X\ Y)} \ . \qquad (4\text{-}133)$$

The remaining received signal quality criteria are determined as follows:

$$\text{Phase Match Efficiency} = \frac{\text{POWER (3)}}{\text{POWER (5)}} \qquad (4\text{-}134)$$

$$\text{POWER (3)} \equiv \text{Heterodyne power}$$

$$\text{POWER (5)} = \Sigma\Sigma_{x\ y} \left[\text{PSF1}(X, Y)\ \text{PSF2}(X, Y)\right]^{1/2} \Delta X \Delta Y \qquad (4\text{-}135)$$

$$\text{Optical transmission} \equiv \frac{\text{POWER(6)}}{\text{PZERO}} \qquad (4\text{-}136)$$

$$\text{POWER(6)} \equiv \text{Exit pupil power}$$

$$\text{PZERO} = \text{Total received power}$$

$$\text{Focusing Efficiency} = \frac{\text{POWER(1)}}{\text{POWER(6)}} \qquad (4\text{-}137)$$

$$\text{Nonheterodyne detection efficiency} \equiv \frac{\text{POWER(1)}}{\text{PZERO}} \qquad (4\text{-}138)$$

$$\text{L.O. illumination efficiency} = \frac{\text{POWER(5)}}{(\text{POWER(1)}\ \text{POWER(2)})^{1/2}} \qquad (4\text{-}139)$$

$$\text{Maximum Antenna Gain} = \frac{4\pi A_o}{\lambda^2} \qquad (4\text{-}140)$$

$A_o \equiv$ entrance pupil area

λ = spectral wavelength

$$\text{Receiver efficiency to I. F.} = \frac{(\text{POWER (3)})^2}{\text{PZERO} \cdot \text{POWER(2)}} . \qquad (4\text{-}141)$$

4.10 TRANSMITTER QUALITY CRITERIA

The point (intensity) spread function PSF(X, Y) is determined for the transmitter at the specified range. The quality criteria for the transmitter are:

$$\text{Peak intensity} \equiv \text{IP} = \text{maximum value of PSF (X, Y)} \qquad (4\text{-}142)$$

$$\text{Optical transmission} = \frac{\text{POWER(6)}}{\text{PZERO}} \qquad (4\text{-}143)$$

$$\text{Maximum antenna gain} = \frac{4\pi \ \text{POWER(7)}}{\lambda^2} \qquad (4\text{-}144)$$

POWER(7) $\equiv$ Effective exit pupil area

$\lambda \equiv$ Spectral wavelength

$$\text{Overall transmitter efficiency} \equiv \frac{\text{IP (RW } \lambda)^2}{\text{PZERO POWER(7)}} \qquad (4\text{-}145)$$

where RW = Range.

4.11 ERROR ANALYSES

The errors associated with these computations come from numerous sources. The major error sources are discussed here with some indication of guidelines to be followed to keep them to a minimum.

a. Aberrations – The conventional Fraunhofer diffraction integrals used in these computations are derived based on certain approximations. The fundamental integral involves the exponential

$$\frac{\exp\,[iK(W + S)]}{S} \qquad (4\text{-}146)$$

where W = OPD error for a given point on the wavefront and S is defined to be the distance from the gaussian sphere to a given observation point in the intensity (or amplitude) plane as illustrated in Fig. 4-21.

The assumption is that $S \approx R$ in the denominator of eq. (4-146) where R = radius of gaussian sphere. It is also assumed that in the numerator of eq. (4-146)

$$S \approx R - \frac{(x\,u + y\,v)}{R}$$

where u, v represent the coordinates of a given wavefront point and x, y are the coordinates of the observation point in the intensity plane. As the aberrations become large, these approximate representations begin to break down and the computed results lose accuracy. There is no well defined threshold of aberrations where the diffraction integrals become inaccurate; but, in general, it can be said that results are best when $W/\lambda \ll 1$.

b. Aperture Description – The pupil amplitude B(u, v) and OPD W(u, v) data are obtained for a rectangular array of points uniformly distributed over the pupil. For a circular aperture the process of fitting

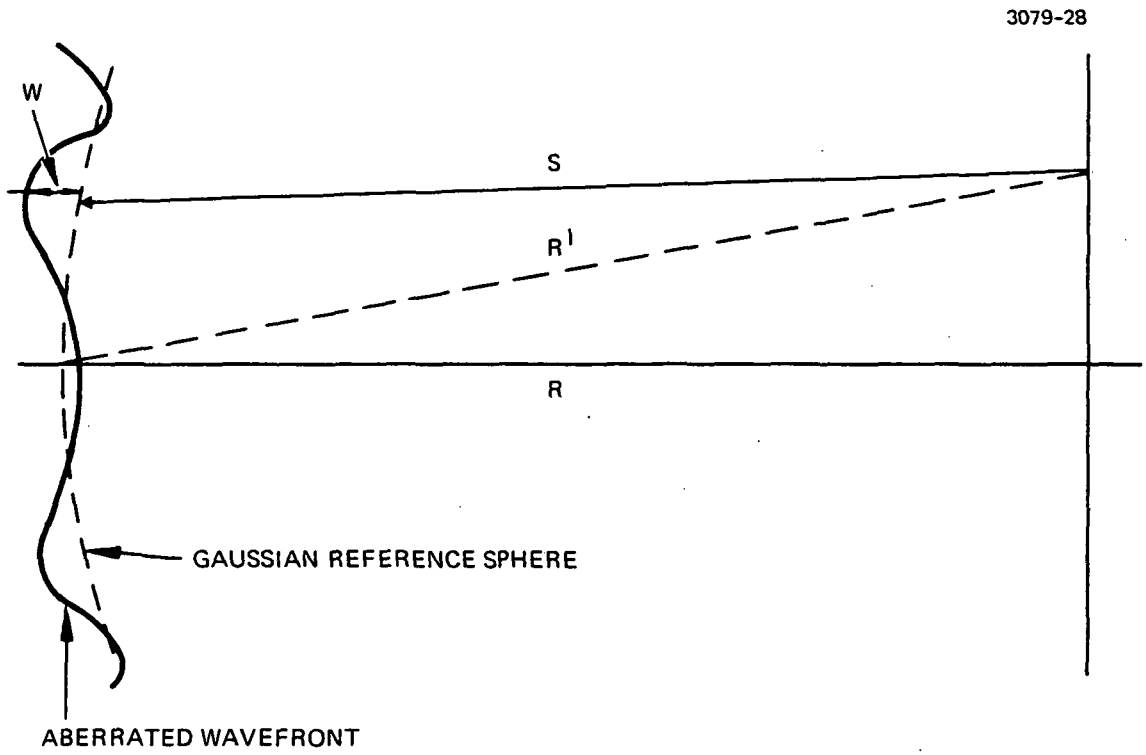

Fig. 4-21. Deviations from the gaussian sphere.

square pegs in the round aperture hole can only represent the aperture boundary accurately if there are a large number of small square pegs. This effect is further compounded by circular obscuring apertures, or even rectilinear blockages such as spiders or support struts which do not line up with the u, v coordinate system. Figure 4-22 illustrates how the rectangular u, v array describes a circular aperture boundary. The uncertainty of determination of the area of the pupil, hence signal power, etc. will be ± dA where

$$dA = \epsilon X \; \epsilon Y \qquad (4\text{-}147)$$

There are techniques for weighting the amplitude values of array elements lying on the boundary for which there is an accuracy improvement. The tradeoff of accuracy gain versus increased computational complexity of these weighting techniques must be compared against a simple increase in grid size (number of array points).

In terms of some representative values of NXY, the normalized uncertainty dA/A would vary per following tabulation.

NXY	dA/A
10	0.0032
15	0.0014
20	0.0008
25	0.0005
30	0.0004
40	0.0002
50	0.0001

c. Circular Detector – The errors associated with a circular detector sampled via the square spread function grid will follow the same rules as the aperture description. The uncertainties in the computed results associated with the detector would follow Table 4-2

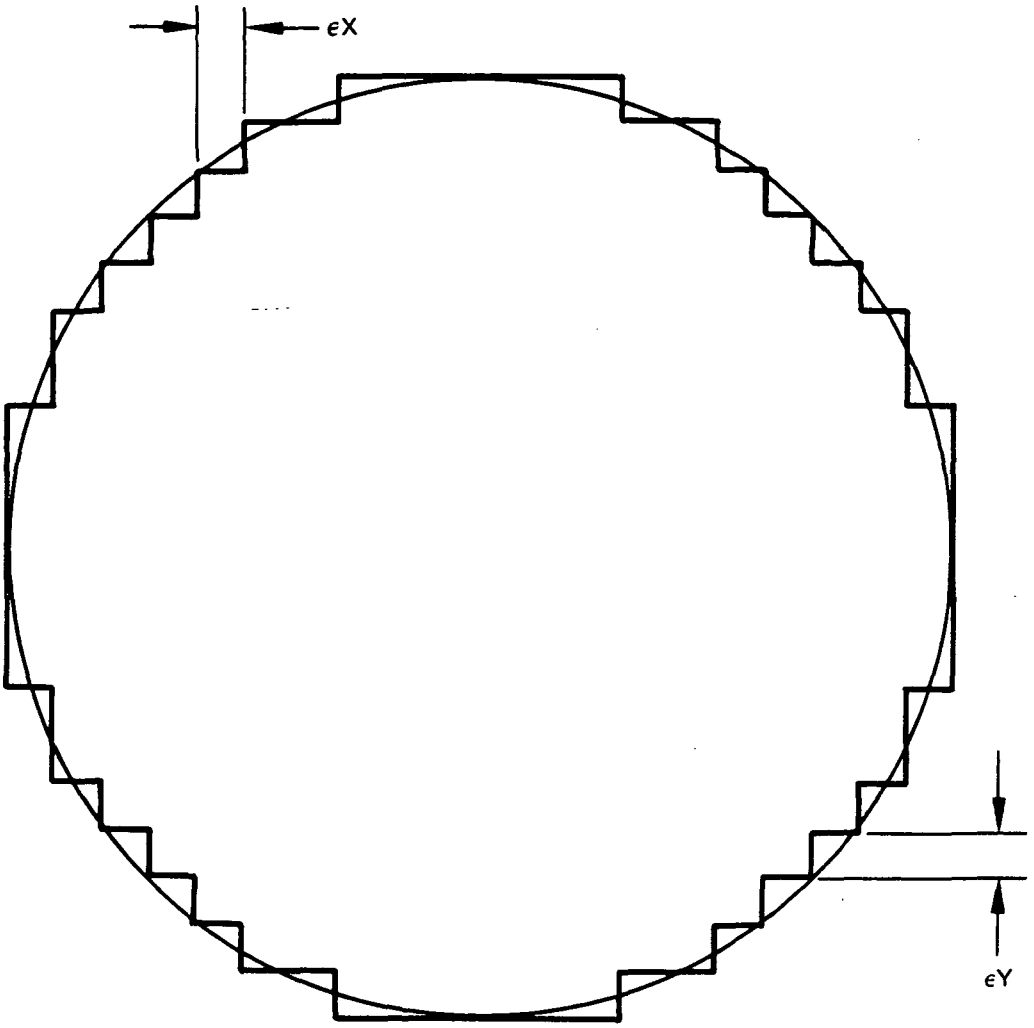

Fig. 4-22. Description of circular aperture boundary by array of square elements.

with NXY replaced by IDIM. IDIM is the array size for the detector.

$$\text{IDIM} = \frac{\text{Circular Detector Diameter}}{2\ \text{DELFS}}$$

$$\text{IDIM} = \text{IDETEC}(2, J)$$

$$= 10 \text{ (Default)}$$

d. Aliasing — The computed Fraunhofer diffraction function is based on a discrete complex amplitude array (pupil function). This discreteness results in a series of replicated, overlapping far-field patterns as illustrated in Fig. 4-23 which constitute an infinite periodic function. The spacing between these replicated patterns is directly proportional to the array size or number of points across the pupil. These patterns overlap so that each computed ASF or PSF value represents the superposition of all the replicated spread functions at a given point in the image plane. Thus, a point midway between two replicated spread function peaks will have a value twice that of either spread function plus a contribution from all the other surrounding spread functions. The larger the number of sample points across the beam, the greater the separation between these replicated spread functions, hence, the lower the errors in the spread function due to aliasing or overlapping.

Aliasing errors increase with aberration since the effect of aberrations is to increase the spread function values away from the center while reducing the central spread function values.

e. Effect of Defocusing on Aliasing — As indicated in Fig. 4-23, the distance between peaks of the replicated overlapping spread functions is Δxrep and

$$\Delta\text{xrep} = 2\lambda\ \text{NXY}\ f\#$$

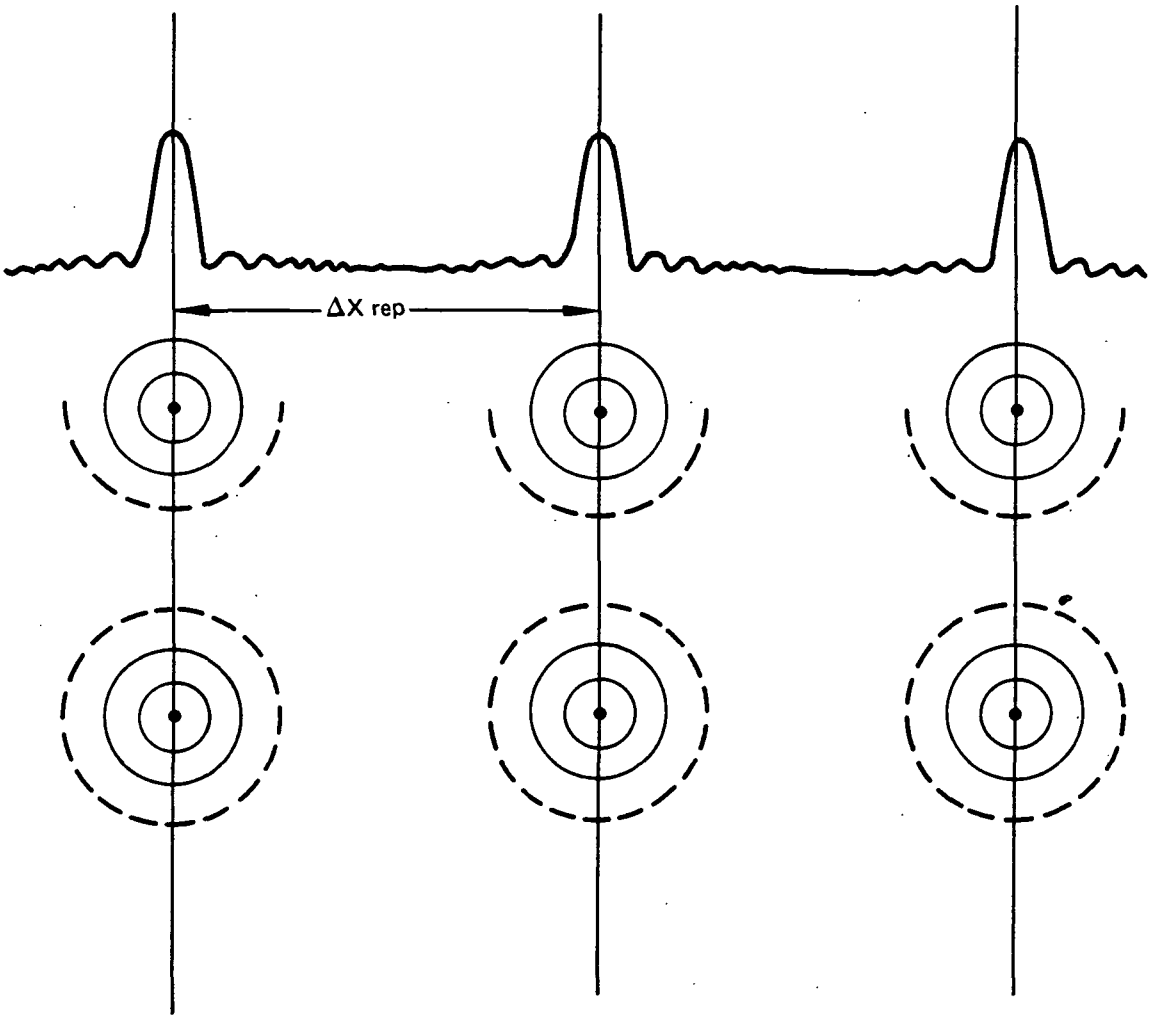

Fig. 4-23. Replicated (aliased) spread functions due to discrete sampling of pupil.

where

$\lambda \equiv$ spectral wavelength

NXY $\equiv$ number of grid points over entrance pupil semidiameter

f# $\equiv$ relative aperture

Aberrations and/or defocusing which cause geometrical spread approaching Δxrep will destroy the accuracy of these computations. A defocusing ΔF resulting in a geometrical spread of Δxrep would be

$$\Delta F = 2 \text{ f\#} \Delta \text{xrep}$$
$$= 4\lambda \text{ NXY } (\text{f\#})^2$$

which is obviously excessive as would be a defocusing of half or one-fourth that amount. It can be said, therefore, that to minimize aliasing error due to defocusing

$$\Delta F \ll \lambda \text{ NXY}(\text{f\#})^2$$

and preferably

$$\Delta F \rightarrow 0.$$

f. LACOMA Test Case – Numerical Results – A test case was devised to check accuracy. It consists of diffraction limited received signal and L.O. optics. The relative aperture of the received signal optics is 10, and for the L.O. is 100. The matrix of optical path differences indicates zero (10^{-16}) over the pupil. The (complex amplitude) pupil function indicates a uniform 100%. A peak value of 1.0013013 rather than 1.0 indicates a slight demagnification of the exit pupil as used for the analysis. The ASF for the received signal is real with a peak value of 73.74928 compared to a predicted value of 74.0147

$$a_o = \left(\frac{A_c P_o}{F^2 \, 2} \right)^{1/2} = 74.0147$$

$A_c \equiv$ entrance pupil area

$P_o \equiv$ total input power

F = focal length

representing an error of 0.3%. Signal power is computed to be 65.6453 which compares with a predicted diffraction limited value of 65.82 for an error of 0.3%. Both these errors are to be expected from the value of IDIM = 10 and the predicted uncertainty of 0.0032 for NXY = 10 per Table 4-2.

The local oscillator results were examined in terms of the peak ASF value a_o. The computed value is 0.8018 while the predicted value is a_o = 0.8352. The 4% error here is due to the gaussian pupil function changing rapidly at the edge of the aperture where the aperture sampling errors are thereby enhanced. The further the $1/e^2$ point is from the aperture edge or truncation point (in either direction) the lower this error will be.

Review of numerical results for the various sample cases indicates that the above accuracy values represent a realistic range to be encountered in the analysis of typical systems.

APPENDIX A


```
*** TRANSMITTER TEST CASE ***
$INP
BETAD(1) =5., .5, N(1) = 3,., H(1) =0., 0., XLINV(1) =0.,3.,
MAG(1) =0.,0., IFLG1(1) = 0,0,
RHOS(1) =0.,.01,0., 0.,.01,3.,
TS(1) =0., 100.,0.,0.,100.,0.,
XMUS(1) = 0*1.,
CRS(2) =-1., CRS(5) = -1.,
 NFRS = 10, DELFS = .01,
NXY = 25,
$END
```

* * * * * LACOMA - LASER COMMUNICATOR ANALYSIS PROGRAM * * * * *

* * * * * PAGOS CORPORATION * * * * *

*** TRANSMITTER TEST CASE ***

N 3 BETA0 5.0000000E+00 M 0. PZERO 0.

M 0 XLINV 0. MAG 0. IFLG1 0

SURFACE PARAMETERS

SURF. NO.	CURVATURE RHOS	SEPARATION TS	INDEX XMUS	OBSCURATION DATA BETAPX	BETAPY	VIGNETTING DATA BETASX	BETASY
1	0.	0.	1.000000	0.	0.	0.	0.
2	1.0000000E-02	1.0000000E+02	1.000000	0.	0.	0.	0.
3	0.	0.	1.000000	0.	0.	0.	0.

SPECIAL SURFACES

SURFACE	RHO1	RHO2	CRS	CC	PHI	AMP	FREQ
2	0.	0.	-1.0000000	0.0000000	0.0000000	0.0000000	0.0000000

(ANGLES INPUT GREATER THAN 6.283 ARE ASSUMED TO BE IN DEGREES)

FIELD ANGLE = 0.

NXY = 25 NDET = 1 NFRS = 10

DELFS = 1.0000000E-02 ZOMEGA = 0. VLAMDA = 1.0611385E-02

DETECTOR NO. 1 IDETEC = 1 0 0 0 0

PARAXIAL RAY TRACE

BETA	B	ALPHA	A
5.[illegible]E+0[illegible]	0.	0.	2.0J000J0CE-J1
5.[illegible]E+0[illegible]	-5.0[illegible]E-02	0.	2.00000J00E-01
0.	-5.00J[illegible]E-02	2.0000JJ0JE+01	2.0J000J00E-01

PARAXIAL ENTRANCE PUPIL POSITION T(0) = -0. TEXIT= 0.

INVERSE OBJECT DISTANCE XLINV = 0.

FOCAL LENGTH = 1.[illegible]E+02 BACK FOCAL LENGTH = 1.000J0[illegible]E+02

TS(N-1) = 1.[illegible]E+02 FL = 1.00000J0JE+02

*** TRANSMITTER TEST CASE ***

CHIEF RAY DATA FOR TRANSMITTER.

FIELD ANGLE (RADIANS) = 0.000000000

CHIEF RAY COORDINATES ON SURFACE N

X	Y	Z
0.	0.	0.

DIRECTION COSINES ON SURFACE N-1

L	M	N
0.	0.	1.000000000E+00

RADIUS RW AND POSITION TR OF EXIT PUPIL

RW	TR
1.000000000E+02	0.

TILT AND DISPLACEMENT OF EXIT PUPIL IN X- AND Y-DIRECTIONS

XTILT	YTILT	XDISP	YDISP
0.	0.	0.	0.

WAVEFRONT ERROR INFORMATION

VARIANCE = 4.500023327E-14
RMS = 4.3037b957E-14
WAVELENGTH = 1.0611385DE-02
MAXIMUM UNNORMALIZED ERROR= 1.33226763E-15
MINIMUM UNNORMALIZED ERROR=-1.33226763E-15
MAXIMUM NORMALIZED ERROR= 1.25553777E-13
MINIMUM NORMALIZED ERROR=-1.25553777E-13
APPROXIMATE STREHL RATIO = 1.000000000E+00

```
*** TRANSMITTER TEST CASE ***

TRANSMITTER DATA.

 PEAK INTENSITY =  8.4122819E+01
OPTICAL TRANSMISSION =  9.9956826E-01 (    -.002 DB )
MAXIMUM ANTENNA GAIN =  8.7311969E+06 (   69.411 DB )
OVERALL TRANSMITTER EFFICIENCY =  9.2286733E-01 (    -.349 DB )
```

APPENDIX B

```
TRANSMITTER TEST CASE *1
$INP  BETAL(1) = 2.25, H(1) = J., IFLG1(1) = 0, N(1) = -7,
RADS(1) = L., 43.14952, 67.65544, 0.,-1028.,8.0E+6, J.,
TS(1) = 414., 2.,36.11, 514., -514., J., J.,
ZOMEGA = 0.925,
XMUS(1) = 1., 4.00162, 1.,  1., -1., -1., -1.,
SKAPA(5) = J.,
CRS(6) = -1.,
NFRS = 51, DELFS = 50,
$END
```

* * * * * LACOMA - LASER COMMUNICATOR ANALYSIS PROGRAM * * * * *

* * * * * PACOS CORPORATION * * * * *

TRANSMITTER TEST CASE *1

N -7 BETAO 2.2500000E+00 M 0. PZERO 0.

M 0 XLINV 0. MAG 0. IFLG1 0

SURFACE PARAMETERS

SURF. NO.	CURVATURE RMCS	SEPARATION TS	INDEX XMUS	OBSCURATION DATA BETAPX	BETAPY	VIGNETTING DATA BETASX	BETASY
1	0.	4.1400000E+02	1.000000	0.	0.	0.	0.
2	2.4175229E-02	2.0000000E+00	4.000621	0.	0.	0.	0.
3	1.4780777E-02	3.6111000E+01	1.000000	0.	0.	0.	0.
4	0.	5.1400000E+02	1.000000	0.	0.	0.	0.
5	-9.7276265E-04	-5.1400000E+02	-1.000000	0.	0.	0.	0.
6	1.2500000E-07	0.	-1.000000	0.	0.	0.	0.
7	0.	0.	-1.000000	0.	0.	0.	0.

SPECIAL SURFACES

SURFACE	PHO1	R402	CRS	CC	PHI	AMP	FREQ
6	0.	0.	-1.0000000	0.0000000	0.0000000	0.0000000	0.0000000

(ANGLES INPUT GREATER THAN 6.283 ARE ASSUMED TO BE IN DEGREES)

SURFACE	SKAPA	ASPHERIC COEFFICIENTS ALPHA	BETA	GAMMA	DELTA	EPSILON
5	0.	0.	0.	0.	0.	0.

FIELD ANGLE = 0.

NXY = 25 NDET = 1 NFRS = 51

DELFS = 5.0000000E+01 ZOMEGA = 9.2500000E-01 VLAMDA = 1.0611850E-02

PARAXIAL RAY TRACE

BETA	B	ALPHA	A
2.25[illegible]E+01	0.	0.	4.44444444E-01
2.25[illegible]E+00	-1.56465124E-01	1.84[illegible]E+02	-1.23509257E+01
2.17177956E+00	-6.01434507E-02	1.77825494E+02	-4.46409894E+00
-4.44282776E-07	-6.01434507E-02	1.66268813E+01	-4.46409894E+00
-3.09137341E+01	8.64362814E-10	-2.27791998E+03	-3.23480181E-02
-3.09137337E+01	-3.86335235E-06	-2.29454686E+03	-3.26348365E-02
-3.09137337E+01	-3.86335235E-06	-2.29454686E+03	-3.26348365E-02

PARAXIAL ENTRANCE PUPIL POSITION T(0) = -0. TEXIT= 7.[illegible]97397E+04

INVERSE OBJECT DISTANCE XLINV = 0.

FOCAL LENGTH = 5.82395753E+05 BACK FOCAL LENGTH = 8.00178987E+06

TS(N-1) = 8.00178987E+06 FL = 5.82395753E+05

TRANSMITTER TEST CASE #1

CHIEF RAY DATA FOR TRANSMITTER.

FIELD ANGLE (RADIANS) = 0.00000000

CHIEF RAY COORDINATES ON SURFACE N

X	Y	Z
0.	0.	0.

DIRECTION COSINES ON SURFACE N-1

L	M	N
0.	0.	-1.00000000E+00

RADIUS RW AND POSITION TR OF EXIT PUPIL

RW	TR
7.93146013E+06	7.03097397E+04

TILT AND DISPLACEMENT OF EXIT PUPIL IN X- AND Y-DIRECTIONS

XTILT	YTILT	XDISP	YDISP
0.	0.	0.	0.

WAVEFRONT ERROR INFORMATION

VARIANCE = 4.97536274E-04
RMS = 7.48377005E-04
WAVELENGTH = 1.06113850E-02
MAXIMUM UNNORMALIZED ERROR= 1.38112276E-10
MINIMUM UNNORMALIZED ERROR=-1.77046895E-05
MAXIMUM NORMALIZED ERROR= 1.30154805E-08
MINIMUM NORMALIZED ERROR=-1.66846171E-03
APPROXIMATE STREHL RATIO = 9.99377889E-01

```
 TRANSMITTER TEST CASE *1

TRANSMITTER DATA.

 PEAK INTENSITY =  1.4187304E-07
OPTICAL TRANSMISSION =  9.9999984E-01 (     -.000 DB )
MAXIMUM ANTENNA GAIN =  3.3319166E+08 (    85.227 DB )
OVERALL TRANSMITTER EFFICIENCY =  3.3667774E-01 (    -4.729 DB )
```

APPENDIX C

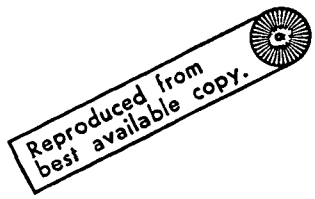


```
RECEIVER TEST CASE #1
$INP  BETAL(1) = 82.5,1.39, M(1) = 0.,0., XLINV(1) = 0.,0., MAG(1) = 1.,0.,
N(1) = -9,-3, M(1) = 5,6,  IFLG1(1) = 1,0,
RADS(1) = 0., -820.,0., 141.80175, 6*0., 111.2, 0.,
TS(1) = 366.725, 0., -502.90983, 146.14387,98.425, 2., -2.,
TS(8) = 56.775, 0., 0., 111.2, 0.,
XMUS(1) = 1., -1.,-1., 1., 1., 4.00062, 6*1.,
SKAPA(2) = 0., 1., .71736,
CRS(11) = -1.,
THTAY(6) = .78539816, 0., -.78539816,
BETAPX(1) = 12.45,
M(1) = 5,10,
IPROG(1) = 1,1,1,0,
$END
```

Preceding page blank

* * * * * LACOMA - LASER COMMUNICATOR ANALYSIS PROGRAM * * * * *

* * * * * PAGOS CORPORATION * * * * *

RECEIVER TEST CASE *1

RECEIVED SIGNAL OPTICAL DATA.

N -9 BETA0 8.250000000E+01 M 0. PZERO 0.

M 5 XLINV 0. MAG 0. IFLG1 1

SURFACE PARAMETERS

SURF. NO.	CURVATURE RHOS	SEPARATION TS	INDEX XMUS	OBSCURATION DATA BETAPX	BETAPY	VIGNETTING DATA BETASX	BETASY
1	0.	3.6872500E+02	1.000000	1.2450E+01	0.	0.	0.
2	-1.2195122E-03	0.	-1.000000	0.	0.	0.	0.
3	0.	-5.0290985E+02	-1.000000	0.	0.	0.	0.
4	7.0526991E-03	1.4614387E+02	1.000000	0.	0.	0.	0.
5	0.	9.8425000E+01	1.000000	0.	0.	0.	0.
6	0.	2.0000000E+00	4.000620	0.	0.	0.	0.
7	0.	-2.0000000E+00	1.000000	0.	0.	0.	0.
8	0.	5.6775000E+01	1.000000	0.	0.	0.	0.
9	0.	0.	1.000000	0.	0.	0.	0.

TILT AND DISPLACEMENT DATA

SURF.	THTAX	THTAY	THTAZ	DLTAX	DLTAY	DLTAZ
6	0.	7.8539816E-01	0.	0.	0.	0.
8	0.	-7.8539816E-01	0.	0.	0.	0.

(ANGLES INPUT GREATER THAN 6.283 ARE ASSUMED TO BE IN DEGREES)

SURFACE	SKAPA	ASPHERIC COEFFICIENTS ALPHA	BETA	GAMMA	DELTA	EPSILON
2	0.	0.	0.	0.	0.	0.
4	7.1736300E-01	0.	0.	0.	0.	0.

FIELD ANGLE = 0.

LOCAL OSCILLATOR OPTICAL DATA.

N -3 BETAJ 1.390000JJE+JC H 0. PZERO 0.

M 10 XLINV 0. MAG 0. IFLG1 0

SURFACE PARAMETERS

SURF. NO.	CURVATURE RHOS	SEPARATION TS	INDEX XMUS	OBSCURATION DATA BETAPX	BETAPY	VIGNETTING DATA BETASX	BETASY
10	0.	0.	1.C00000	0.	0.	0.	0.
11	8.99280565E-03	1.112000J0E+02	1.C00000	0.	0.	0.	0.
12	0.	0.	1.C00000	0.	0.	0.	0.

SPECIAL SURFACES

SURFACE	RHO1	RHO2	CRS	CC	PHI	AMP	FREQ
11	0.	0.	-1.C000000	0.0000000	0.00000.	0.0000000	0.0000000

(ANGLES INPUT GREATER THAN 6.283 ARE ASSUMED TO BE IN DEGREES)

FIELD ANGLE = 0.

NXY = 25 NDET = 1 NFRS = 26
DELFS = 0. ZOMEGA = 0. VLAMDA = 1.0611385JE-02

DETECTOR DATA.

DETECTOR NO. 1 IDETEC = 1 J 0 0 0

PARAXIAL RAY TRACE - RECEIVED SIGNAL OPTICS.

BETA	B	ALPHA	A
8.25[illegible]E+01	1.	0.	1.21212121E-02
8.25[illegible]E+01	-2.01219512E-01	4.46939394E+00	1.22025129E-03
8.25[illegible]E+01	-2.01219512E-01	4.46933394E+00	1.22025129E-03
-1.06952747E+01	6.24623492E-02	5.08307033E+00	-7.04723806E-02
-9.56678525E+00	6.24623492E-02	-5.21603610E+00	-7.04723806E-02
-3.41892853E+00	6.24623492E-02	-1.21522802E+01	-7.04723806E-02
-3.38772220E+00	6.24623492E-02	-1.21875109E+01	-7.04723806E-02
-3.51282769E+00	6.24623492E-02	-1.20465661E+01	-7.04723806E-02
3.36729607E-02	6.24623492E-02	-1.60476355E+01	-7.04723806E-02

PARAXIAL ENTRANCE PUPIL POSITION T(0) = -3.71692742E+03 TEXIT= -9.59249225E+01

INVERSE OBJECT DISTANCE X_INV = 0.

FOCAL LENGTH = -1.32079555E+03 BACK FOCAL LENGTH = 5.62359076E+01

TS(N-1) = 9.67750000E+01 FL = -1.32079566E+03

PARAXIAL RAY TRACE - LOCAL OSCILLATOR OPTICS.

BETA	9	ALPHA	A
1.390[illegible]E+01	0.	0.	7.19424460E-01
1.390[illegible]E+01	-1.25[illegible]E-02	0.	7.19424460E-01
1.421[illegible]E-14	-1.25[illegible]E-02	9.0000000[illegible]E+01	7.19424460E-01

PARAXIAL ENTRANCE PUPIL POSITION T(0) = -0. TEXIT= 0.

INVERSE OBJECT DISTANCE XLINV = 0.

FOCAL LENGTH = 1.112[illegible]E+02 BACK FOCAL LENGTH = 1.112[illegible]E+02

TS(N-1) = 1.112[illegible]E+02 FL = 1.112[illegible]E+02

RECEIVER TEST CASE #1

CHIEF RAY DATA FOR RECEIVED SIGNAL.

FIELD ANGLE (RADIANS) = 0.000.0000

CHIEF RAY COORDINATES ON SURFACE N

X	Y	Z
0.	1.1602539+E+00	0.

DIRECTION COSINES ON SURFACE N-1

L	M	N
0.	-7.10542736E-14	1.00000000E+00

RADIUS RW AND POSITION TR OF EXIT PUPIL

RW	TR
1.53699923E+02	-9.69243225E+01

TILT AND DISPLACEMENT OF EXIT PUPIL IN X- AND Y-DIRECTIONS

XTILT	YTILT	XDISP	YDISP
0.	-7.10542736E-14	0.	1.16025394E+00

WAVEFRONT ERROR INFORMATION

VARIANCE = 3.84398649E-02
RMS = 7.87468726E-02
WAVELENGTH = 1.06113850E-02
MAXIMUM UNNORMALIZED ERROR= 0.
MINIMUM UNNORMALIZED ERROR=-1.64269496E-03
MAXIMUM NORMALIZED ERROR= 0.
MINIMUM NORMALIZED ERROR=-1.54804011E-01
APPROXIMATE STREHL RATIO = 7.55191571E-01

RECEIVER TEST CASE #1

ASF (REAL), FOR RECEIVED SIGNAL.
QUADRANT 1, 100 CORRESPONDS TO 1.3644915E+03

```
 1  1  1  1  1  1  1  0 -0 -1 -1 -2 -3 -3 -4 -4 -5 -5 -5 -5 -4 -4 -3 -2 -2 -1
 2  2  2  2  2  2  2  1  1  1  0 -1 -1 -2 -3 -3 -4 -4 -5 -5 -5 -4 -4 -3 -2 -2
 3  3  3  3  3  3  3  2  2  2  1  1 -0 -1 -2 -2 -3 -4 -4 -5 -5 -5 -4 -4 -3 -2
 2  2  2  3  3  3  3  3  3  3  2  2  1  0 -0 -1 -2 -3 -4 -4 -4 -5 -5 -4 -4 -3
 1  1  1  2  2  2  2  3  3  3  3  2  2  1  1 -0 -1 -2 -3 -3 -4 -4 -5 -5 -4 -4
-1 -1 -1 -0  1  1  1  2  2  3  3  3  3  2  2  1  1 -1 -2 -3 -3 -4 -5 -5 -5 -4
-3 -3 -3 -2 -2 -1 -1  0  1  2  2  3  3  3  2  2  1  1 -1 -2 -3 -4 -4 -5 -5 -5
-5 -5 -5 -4 -3 -4 -3 -2 -1  0  1  2  2  3  3  3  2  1  0 -1 -2 -3 -4 -4 -5 -5
-9 -9 -9 -8 -8 -7 -6 -5 -5 -2 -1  0  1  2  3  3  3  2  1  0 -1 -2 -3 -4 -5 -5
-12-12-11-11-10 -9 -8 -7 -6 -4 -3 -1  0  1  2  3  3  3  2  1  0 -1 -2 -3 -4 -5
-14-13-13-13-13-12-11-10 -9 -7 -6 -3 -2 -0  1  2  3  3  3  2  1 -0 -1 -3 -4 -5
-14-14-14-14-14-13-13-12-11 -9 -8 -5 -4 -2 -1  1  2  3  3  3  2  1 -1 -2 -3 -4
-13-13-13-13-14-14-14-13-13-11-10 -8 -6 -4 -2  0  2  3  3  3  3  2  0 -1 -2 -4
-10-10-11-11-12-13-13-14-14-13-12-10 -8 -6 -4 -1  0  2  3  3  3  2  1 -0 -2 -3
 -4 -4 -5 -7 -8-10-12-13-14-14-13-12-10 -9 -6 -3 -1  1  2  3  3  3  2  1 -1 -2
  4  3  2 -1 -3 -5 -8-11-12-14-14-13-12-10 -7 -5 -2  0  2  3  3  3  3  1 -0 -2
 13 13 11  8  5  1 -3 -7-10-12-14-14-13-12 -9 -7 -4 -1  1  3  3  4  3  2  0 -1
 25 24 22 18 13  8  3 -2 -7-11-13-14-14-13-11 -8 -5 -2  0  2  3  4  3  2  1 -.
 37 36 34 29 23 17 11  3 -3 -8-12-14-15-14-12-10 -7 -4 -1  1  3  4  4  3  2  0
 51 49 46 41 34 26 18  9  2 -5-10-13-15-15-13-11 -8 -5 -2  1  3  4  4  3  2  0
 63 62 59 52 44 35 25 16  7 -1 -7-12-14-15-14-12 -9 -6 -3  0  2  3  4  3  2  1
 76 74 70 63 54 44 33 22 11  2 -5-11-14-15-15-13-11 -7 -3 -0  2  3  4  4  3  1
 86 84 79 72 62 51 39 27 15  5 -3 -9-13-15-15-14-11 -7 -4 -1  2  3  4  4  3  1
 93 92 87 79 69 57 44 31 19  8 -1 -8-13-15-15-14-11 -8 -5 -1  1  3  4  4  3  2
 98 97 92 83 73 60 47 33 21  3 -0 -8-13-15-16-14-12 -8 -5 -2  1  3  4  4  3  2
```

QUADRANT 2, 100 CORRESPONDS TO 1.3044915GE+03

```
-1 -2 -2 -3 -4 -4 -5 -5 -5 -5 -4 -4 -3 -3 -2 -1 -1 -0  0  1  1  1  1  1  1
-2 -2 -3 -4 -4 -5 -5 -5 -4 -4 -3 -3 -2 -1 -1 -0  1  1  1  2  2  2  2  2  2
-2 -3 -4 -4 -5 -5 -5 -4 -4 -3 -2 -2 -1 -0  1  1  2  2  2  3  3  3  3  3  3
-3 -4 -4 -5 -5 -5 -4 -4 -3 -2 -1 -0  0  1  2  2  2  3  3  3  3  3  2  2
-4 -4 -5 -5 -4 -4 -4 -3 -2 -1 -0  1  1  2  2  3  3  3  3  2  2  2  1  1
-4 -5 -5 -5 -4 -3 -3 -2 -1  0  1  2  2  3  3  3  3  2  2  1  1  0 -0 -0 -1
-5 -5 -5 -4 -4 -3 -2 -1  0  1  2  2  3  3  3  2  2  1  0 -1 -1 -2 -2 -3 -3
-5 -5 -4 -4 -3 -2 -1  0  1  2  3  3  3  2  2  1  0 -1 -2 -3 -4 -5 -5 -6 -6
-5 -5 -4 -3 -2 -1  0  1  2  3  3  3  2  1  1 -1 -2 -3 -4 -6 -7 -7 -8 -9 -9
-5 -4 -3 -2 -1  0  1  2  3  3  3  2  1  0 -1 -3 -4 -6 -7 -8 -9-10-11-11-12
-5 -4 -3 -2 -0  1  2  3  3  3  2  1 -0 -2 -3 -5 -7 -8-10-11-12-12-13-13-13
-4 -3 -2 -1  1  2  3  3  3  2  1 -0 -2 -4 -6 -8 -9-11-12-13-13-14-14-14-14
-4 -3 -1  0  1  2  3  3  3  2  0 -2 -4 -6 -8-10-11-12-13-14-14-14-13-13-13
-3 -2 -0  1  2  3  3  3  2  1 -1 -3 -6 -8-10-12-13-13-14-13-13-12-11-10-10
-2 -1  0  2  3  3  3  3  1 -1 -3 -5 -8-10-12-13-14-13-13-12-10 -8 -7 -5 -4
-2 -0  1  2  3  3  3  2  0 -2 -5 -7-10-12-13-14-13-12-11 -8 -6 -3 -0  2  3
-1  0  2  3  3  3  3  1 -1 -4 -6 -9-11-13-14-14-12-10 -7 -3  1  4  8 11 13
-1  1  2  3  4  3  2  0 -2 -5 -8-11-13-14-14-13-11 -7 -3  3  8 13 18 22 24
-0  1  3  4  4  3  2 -1 -3 -6 -9-12-14-14-14-12 -8 -3  3 10 17 23 29 33 36
 0  2  3  4  4  3  1 -2 -5 -8-11-13-14-14-13-10 -5  2  9 17 26 34 40 46 49
 1  2  3  4  4  2  0 -2 -5 -9-12-14-15-14-12 -8 -1  6 15 25 35 44 52 58 62
 1  2  4  4  3  2 -0 -3 -5-10-13-14-15-14-11 -5  2 11 21 32 43 53 62 69 74
 1  3  4  4  3  2 -1 -4 -7-10-13-15-15-13 -9 -3  5 15 26 38 50 62 72 79 84
 1  3  4  4  3  1 -1 -4 -8-11-14-15-15-13 -9 -2  7 18 30 43 56 69 79 87 92
 1  3  4  4  3  1 -1 -5 -8-11-14-15-15-13 -8 -1  9 20 33 46 60 72 83 91 96
```

QUADRANT 3, 100 CORRESPONDS TO 1.3E44915CE+03

```
 1  3  4  4  3  1 -1 -5 -8-11-14-15-15-12 -9 -0  9 21 34 47 61 73 84 93 98
 1  3  4  4  3  1 -1 -5 -8-11-14-15-15-13 -9 -1  9 20 33 46 60 72 83 91 96
 1  3  4  4  3  1 -1 -4 -8-11-14-15-15-13 -9 -2  7 18 30 43 56 68 79 87 92
 1  3  4  4  3  2 -1 -4 -7-10-13-15-15-13 -9 -3  5 15 26 38 50 62 72 79 84
 1  2  4  4  3  2 -0 -3 -6-10-13-14-15-14-11 -5  2 11 21 32 43 53 62 69 74
 1  2  3  4  4  2  0 -2 -6 -9-12-14-15-14-12 -8 -1  6 15 25 35 44 52 58 62
 1  2  3  4  4  3  1 -2 -5 -8-11-13-14-14-13-10 -5  2  9 17 26 34 40 46 49
-0  1  3  4  4  3  2 -1 -3 -6 -9-12-14-14-14-12 -8 -3  3 10 17 23 29 33 36
-1  1  2  3  4  3  2  0 -2 -5 -8-11-13-14-14-13-11 -7 -3  3  8 13 18 22 24
-1  0  2  3  3  3  3  1 -1 -4 -6 -9-11-13-14-14-12-10 -7 -3  1  4  8 11 13
-2 -0  1  2  3  3  3  2  0 -2 -5 -7-10-12-13-14-13-12-11 -8 -6 -3 -0  2  3
-2 -1  0  2  3  3  3  3  1 -1 -3 -5 -8-10-12-13-14-13-13-12-10 -8 -7 -5 -4
-3 -2 -1  1  2  3  3  3  2  1 -1 -3 -6 -8-10-12-13-13-14-13-13-12-11-10-10
-4 -3 -1  0  1  2  3  3  3  2  0 -2 -4 -6 -9-10-11-12-13-14-14-14-13-13-13
-4 -3 -2 -1  1  2  3  3  3  2  1 -0 -2 -4 -6 -8 -9-11-12-13-13-14-14-14-14
-5 -4 -3 -2 -0  1  2  3  3  3  2  1 -0 -2 -3 -5 -7 -8-10-11-12-12-13-13-13
-5 -4 -3 -2 -1  0  1  2  3  3  3  2  1  0 -1 -3 -4 -6 -7 -8 -9-10-11-11-12
-5 -5 -4 -3 -2 -1 -0  1  2  3  3  3  2  1  1 -1 -2 -3 -4 -6 -7 -7 -8 -9 -9
-5 -5 -4 -4 -3 -2 -1 -0  1  2  3  3  3  2  2  1  0 -1 -2 -3 -4 -5 -5 -6 -6
-5 -5 -5 -4 -4 -3 -2 -1 -0  1  2  2  3  3  3  2  2  1  0 -1 -1 -2 -2 -3 -3
-4 -5 -5 -5 -4 -4 -3 -3 -2 -1 -0  1  2  2  3  3  3  3  2  2  1  1  0 -0 -0 -1
-4 -4 -5 -5 -4 -4 -4 -3 -2 -1 -0  1  1  2  2  3  3  3  3  2  2  2  2  1  1
-3 -4 -4 -5 -5 -5 -4 -4 -3 -2 -1 -0  0  1  2  2  2  3  3  3  3  3  3  2  2
-2 -3 -4 -4 -5 -5 -5 -4 -4 -3 -2 -2 -1 -0  1  1  2  2  2  3  3  3  3  3  3
-2 -2 -3 -4 -4 -5 -5 -5 -4 -4 -3 -3 -2 -1 -1 -0  1  1  1  2  2  2  2  2  2
-1 -2 -2 -3 -4 -4 -5 -5 -5 -5 -4 -4 -3 -3 -2 -1 -1 -0  0  1  1  1  1  1  1
```

QUADRANT 4, 100 CORRESPONDS TO 1.3644915GE+03

```
100  98  93  85  74  62  48  34  21  10  -0  -7-12-15-16-14-12  -8  -5  -2   1   3   4   4   3   2
 98  97  92  83  73  60  47  33  21   9  -0  -8-13-15-16-14-12  -8  -5  -2   1   3   4   4   3   2
 93  92  87  79  69  57  44  31  19   8  -1  -8-13-15-15-14-11  -8  -5  -1   1   3   4   4   3   2
 86  84  79  72  62  51  39  27  15   5  -3  -9-13-15-15-14-11  -7  -4  -1   2   3   4   4   3   1
 75  74  70  63  54  44  33  22  11   2  -5-11-14-15-15-13-10  -7  -3  -0   2   3   4   4   3   1
 63  62  58  52  44  35  25  16   7  -1  -7-12-14-15-14-12  -9  -6  -3   0   2   3   4   3   2   1
 50  49  46  41  34  26  18   9   2  -5-10-13-15-15-13-11  -8  -5  -2   1   3   4   4   3   2   0
 37  36  34  29  23  17  10   3  -3  -8-12-14-15-14-12-10  -7  -4  -1   1   3   4   4   3   2   0
 25  24  22  18  13   8   3  -2  -7-11-13-14-14-13-11  -8  -5  -2   0   2   3   4   3   2   1  -1
 13  13  11   8   5   1  -3  -7-10-12-14-14-13-12  -9  -7  -4  -1   1   3   3   4   3   2   0  -1
  4   3   2  -0  -3  -5  -8-11-12-14-14-13-12-10  -7  -5  -2   0   2   3   3   3   3   1  -0  -2
 -4  -4  -5  -7  -8-10-12-13-14-14-13-12-10  -8  -6  -3  -1   1   2   3   3   3   2   1  -1  -2
-10-10-10-11-12-13-13-14-14-13-12-10  -8  -6  -4  -1   0   2   3   3   3   2   1  -0  -2  -3
-13-13-13-13-14-14-14-13-13-11-10  -8  -6  -4  -2   0   2   3   3   3   2   0  -1  -2  -4
-14-14-14-14-14-13-13-12-11  -9  -8  -6  -4  -2  -0   1   2   3   3   3   2   1  -1  -2  -3  -4
-14-13-13-13-13-12-11-10  -8  -7  -5  -3  -2  -0   1   2   3   3   3   2   1  -0  -1  -3  -4  -5
-12-12-11-11-10  -9  -8  -7  -6  -4  -3  -1   0   1   2   3   3   3   2   1   0  -1  -2  -3  -4  -5
 -9  -9  -9  -8  -8  -7  -6  -5  -3  -2  -1   0   1   2   3   3   3   2   1   0  -1  -2  -3  -4  -5  -5
 -6  -6  -6  -6  -5  -4  -3  -2  -1   0   1   2   2   3   3   3   2   1   0  -1  -2  -3  -4  -4  -5  -5
 -3  -3  -3  -2  -2  -1  -1   0   1   2   2   3   3   3   2   2   1   0  -1  -2  -3  -4  -4  -5  -5  -5
 -1  -1  -0  -0   0   1   1   2   2   3   3   3   3   2   2   1   0  -1  -2  -3  -3  -4  -5  -5  -5  -4
  1   1   1   2   2   2   2   3   3   3   3   2   2   1   1  -0  -1  -2  -3  -3  -4  -4  -5  -5  -4  -4
  2   2   2   3   3   3   3   3   3   3   2   2   1   0  -0  -1  -2  -3  -4  -4  -4  -5  -5  -4  -4  -3
  3   3   3   3   3   3   3   2   2   2   1   1  -0  -1  -2  -2  -3  -4  -4  -5  -5  -5  -4  -4  -3  -2
  2   2   2   2   2   2   2   1   1   1   0  -1  -1  -2  -3  -3  -4  -4  -5  -5  -5  -4  -4  -3  -2  -2
  1   1   1   1   1   1   1   0  -0  -1  -1  -2  -3  -3  -4  -4  -5  -5  -5  -5  -4  -4  -3  -2  -2  -1
 INTERVAL =   1.03629545E-02 NUMBER INTERVALS = 51 SUM =   0.
```

RECEIVER TEST CASE *1

ASF (IMAGINARY),FOR RECEIVED SIGNAL.
QUADRANT 1, 100 CORRESPONDS TO 6.0C983078E+02

```
 -6 -6 -6 -5 -5 -4 -3 -2 -1  1  2  4  5  6  7  8  8  8  8  7  6  4  2  1 -1 -3
-10-10-10 -9 -9 -8 -7 -6 -4 -3 -1  0  2  4  5  6  7  8  8  8  7  7  5  4  2  1 -1
-13-13-13-12-12-11-11 -9 -8 -7 -5 -3 -1  1  3  4  6  7  7  8  7  7  5  4  2  1
-15-15-15-14-14-14-13-12-11-10 -8 -7 -5 -3 -0  2  3  5  6  7  7  7  6  5  4  2
-14-14-15-15-15-15-14-14-13-12-11-10 -8 -6 -4 -1  1  3  5  6  7  7  7  6  5  4
-12-12-12-12-13-13-14-14-14-14-14-13-12-11 -9 -7 -4 -2  0  2  4  5  7  7  7  7  6  5
 -8 -8 -8 -9-10-11-11-12-12-13-14-14-14-13-12-11 -9 -7 -5 -3 -1  2  4  6  7  7  7  6
 -2 -2 -2 -3 -5 -6 -8 -9-11-12-13-13-13-13-12-11-10 -8 -5 -3 -0  2  4  6  7  7  7
  6  6  5  4  2  0 -2 -4 -5 -9-10-12-13-13-13-12-11-10 -8 -5 -2  0  3  5  6  7  8
 14 14 13 12 10  7  5  2 -1 -4 -7 -9-11-12-13-12-11-10 -7 -5 -2  1  3  5  7  7
 22 22 21 20 17 15 12  9  5  1 -2 -5 -8-10-12-12-12-11 -9 -7 -4 -1  1  4  6  7
 29 29 28 26 24 22 19 15 12  7  3 -1 -4 -7-10-11-12-12-11 -9 -6 -3 -0  2  5  6
 34 33 33 32 30 28 25 21 18 13  9  4  0 -4 -7-10-11-12-11-10 -8 -5 -2  1  3  5
 36 35 35 34 33 31 29 26 23 19 14 10  5  0 -4 -7-10-11-12-11 -9 -7 -4 -1  2  4
 33 33 33 33 33 32 31 29 27 23 19 14  9  4 -0 -5 -8-10-12-11-10 -8 -6 -3  0  3
 28 28 28 29 30 31 31 30 29 26 23 19 14  8  3 -2 -6 -9-11-12-11-10 -7 -4 -1  2
 18 18 20 21 23 26 27 29 29 28 25 22 17 12  7  2 -3 -7-10-11-11-10 -8 -6 -3  0
  9  6  7 10 14 18 22 25 27 27 26 24 20 16 10  5 -0 -5 -8-11-11-11 -9 -7 -4 -1
-11-10 -7 -3  2  8 14 19 23 26 26 25 23 18 13  8  2 -3 -7-10-11-11-10 -8 -5 -2
-28-27-24-18-11 -4  4 12 18 23 25 25 24 21 16 10  5 -1 -5 -9-11-11-11 -9 -6 -3
-46-45-41-34-26-16 -6  4 12 19 23 25 25 22 18 13  7  1 -4 -8-10-11-11 -9 -7 -3
-63-62-57-49-39-28-16 -4  5 15 21 24 25 23 20 14  9  3 -3 -7-10-11-11 -9 -7 -4
-78-77-71-62-51-38-25-11  1 11 18 23 25 24 21 16 10  4 -1 -6 -9-11-11-10 -7 -4
-90-88-82-73-61-47-32-17 -4  8 16 22 25 24 21 17 11  5 -1 -5 -9-11-11-10 -8 -5
-97-95-89-79-67-52-36-21 -5  6 15 21 24 24 22 17 12  6 -0 -5 -9-11-11-10 -8 -5
```

QUADRANT 2, 100 CORRESPONDS TO 6.00063078E+02

```
-3 -1  0  2  4  5  7  8  8  8  8  7  6  5  4  2  1 -1 -2 -3 -4 -5 -5 -6 -6
-1  0  2  4  5  7  7  8  8  7  6  5  4  2  1 -1 -3 -4 -6 -7 -8 -9 -9-10-10
 0  2  4  5  6  7  7  7  7  6  4  3  1 -1 -3 -5 -7 -8 -9-10-11-12-12-13-13
 2  4  5  6  7  7  7  6  5  4  2 -0 -2 -4 -6 -8-10-11-12-13-14-14-14-15-15
 4  5  6  7  7  7  6  5  3  1 -1 -3 -6 -8-10-11-12-13-14-14-15-15-15-15-14
 5  6  7  7  7  6  4  3  0 -2 -4 -7 -9-10-12-13-14-14-14-14-14-13-13-12-12
 6  7  7  7  6  4  2  0 -2 -5 -7 -9-11-12-13-14-14-13-13-12-11-10 -9 -8 -8
 7  7  7  6  5  2  0 -2 -5 -7 -9-11-12-13-13-13-12-11 -9 -8 -6 -5 -3 -2 -2
 7  7  6  5  3  0 -2 -5 -7 -9-11-12-13-13-12-10 -9 -7 -4 -2  0  2  4  5  6
 7  7  5  3  1 -2 -4 -7 -9-11-12-12-12-11 -9 -7 -4 -1  2  5  7 10 12 13 14
 7  6  4  2 -1 -4 -7 -9-11-12-12-12-10 -8 -5 -2  1  5  8 12 15 17 19 21 22
 6  5  2 -0 -3 -6 -8-10-12-12-11-10 -8 -5 -1  3  7 11 15 19 22 24 26 28 29
 5  3  1 -2 -5 -8-10-11-12-11-10 -7 -4 -0  4  9 13 17 21 25 27 30 31 33 33
 4  2 -1 -4 -7 -9-11-12-11-10 -8 -4 -0  4  9 14 18 23 26 29 31 33 34 35 35
 3  0 -3 -6 -8-10-11-11-10 -8 -5 -1  4  9 14 19 23 26 29 31 32 33 33 33 33
 2 -1 -4 -7 -9-11-11-11 -9 -6 -2  3  8 13 18 22 26 28 30 31 30 30 29 28 28
 0 -2 -5 -8-10-11-11-10 -7 -3  1  7 12 17 21 25 27 29 29 27 26 24 21 20 18
-1 -4 -7 -9-11-11-11 -9 -5 -1  4 10 15 20 24 26 27 27 25 22 18 14 11  8  6
-2 -5 -8-10-11-11-10 -7 -3  2  7 13 18 22 25 26 26 23 19 14  9  2 -3 -7-10
-2 -6 -8-10-11-11 -9 -6 -1  4 10 15 20 24 25 25 23 18 12  5 -3-11-18-24-27
-3 -6 -9-11-11-10 -8 -4  1  6 12 18 22 25 25 23 19 13  4 -5-15-25-34-40-45
-4 -7 -9-11-11-10 -7 -3  2  8 14 19 23 25 24 21 15  7 -3-15-27-38-49-57-62
-4 -7 -9-11-11 -9 -6 -2  4 10 15 20 24 25 23 19 11  2-10-24-37-50-62-71-76
-4 -7-10-11-11 -9 -6 -1  5 11 16 21 24 25 22 17  8 -3-16-31-46-60-72-82-88
-4 -7-10-11-11 -9 -5 -0  5 11 17 22 24 24 22 16  6 -6-20-35-51-66-79-89-95
```

QUADRANT 3, 100 CORRESPONDS TO 6.JC683078E+02

```
-4 -7-10-11-10 -9 -5 -0  3 12 17 22 24 24 21 15  6 -7-21-37-53-69-81-91-98
-4 -7-10-11-11 -9 -5 -0  3 11 17 22 24 24 22 16  6 -6-20-35-51-66-79-89-95
-4 -7-10-11-11 -9 -6 -1  3 11 16 21 24 25 22 17  8 -3-16-31-46-60-72-82-88
-4 -7 -9-11-11 -9 -6 -2  4 10 15 20 24 25 23 19 11  2-10-24-37-50-62-71-76
-4 -7 -9-11-11-10 -7 -3  2  8 14 19 23 25 24 21 15  7 -3-15-27-38-49-57-62
-3 -6 -9-11-11-10 -8 -4  1  6 12 18 22 25 25 23 19 13  4 -5-15-25-34-40-45
-2 -6 -8-10-11-11 -9 -6 -1  4 10 15 20 24 25 25 23 18 12  5 -3-11-18-24-27
-2 -5 -8-10-11-11-10 -7 -3  2  7 13 18 22 25 26 26 23 19 14  8  2 -3 -7-10
-1 -4 -7 -9-11-11-11 -9 -5 -1  4 10 15 20 24 26 27 27 25 22 18 14 11  8  6
 0 -2 -5 -8-10-11-11-10 -7 -3  1  7 12 17 21 25 27 29 29 27 26 24 21 20 18
 2 -1 -4 -7 -9-11-11-11 -9 -6 -2  3  8 13 18 22 26 28 30 31 30 30 29 28 28
 3  0 -3 -6 -8-10-11-11-10 -8 -5 -1  4  9 14 19 23 26 29 31 32 33 33 33 33
 4  2 -1 -4 -7 -9-11-12-11-10 -8 -4 -0  4  9 14 18 23 26 29 31 33 34 35 35
 5  3  1 -2 -5 -8-10-11-12-11-10 -7 -4 -0  4  9 13 17 21 25 27 30 31 33 33
 6  5  2 -0 -3 -6 -8-10-12-12-11-10 -8 -5 -1  3  7 11 15 19 22 24 26 28 29
 7  6  4  2 -1 -4 -7 -9-11-12-12-12-10 -8 -5 -2  1  5  8 12 15 17 19 21 22
 7  7  5  3  1 -2 -4 -7 -9-11-12-12-12-11 -9 -7 -4 -1  2  5  7 10 12 13 14
 7  7  6  5  3  0 -2 -5 -7 -9-11-12-13-13-12-10 -9 -7 -4 -2  0  2  4  5  6
 7  7  7  6  5  2  0 -2 -5 -7 -9-11-12-13-13-13-12-11 -9 -8 -6 -5 -3 -2 -2
 6  7  7  7  6  4  2  0 -2 -5 -7 -9-11-12-13-14-14-13-13-12-11-10 -9 -8 -8
 5  6  7  7  7  6  4  3  1 -2 -4 -7 -9-10-12-13-14-14-14-14-14-13-13-12-12
 4  5  6  7  7  7  6  5  3  1 -1 -3 -6 -8-10-11-12-13-14-14-15-15-15-15-14
 2  4  5  6  7  7  7  6  5  4  2 -0 -2 -4 -6 -8-10-11-12-13-14-14-14-15-15
 0  2  4  5  6  7  7  7  7  6  4  3  1 -1 -3 -5 -7 -8 -9-10-11-12-12-13-13
-1  0  2  4  5  7  7  8  8  7  6  5  4  2  1 -1 -3 -4 -6 -7 -8 -9 -9-10-10
-3 -1  0  2  4  5  7  8  8  8  8  7  6  5  4  2  1 -1 -2 -3 -4 -5 -5 -6 -6
```

QUADRANT 4, 100 CORRESPONDS TO 6.0C083078E+02

```
*00-98-92-82-69-54-38-22 -7  5 15 21 24 24 22 18 12  6  0 -5 -8-10-11-10 -8 -5
-97-95-89-79-67-52-35-21 -6  6 15 21 24 24 22 17 12  6 -0 -5 -9-11-11-10 -8 -5
-90-88-82-73-61-47-32-17 -4  8 16 22 25 24 21 17 11  5 -1 -5 -9-11-11-10 -8 -5
-78-77-71-62-51-38-25-11  1 11 18 23 25 24 21 16 10  4 -1 -6 -9-11-11-10 -7 -4
-63-62-57-49-39-28-16 -4  5 15 21 24 25 23 20 14  9  3 -3 -7-10-11-11 -9 -7 -4
-46-45-41-34-26-16 -6  4 12 19 23 25 25 22 18 13  7  1 -4 -8-10-11-11 -9 -7 -3
-28-27-24-18-11 -4  4 12 18 23 25 25 24 21 16 10  5 -1 -5 -9-11-11-11 -9 -6 -3
-11-10 -7 -3  2  8 14 19 23 26 26 25 23 18 13  8  2 -3 -7-10-11-11-10 -8 -5 -2
  5  6  7 11 14 18 22 25 27 27 26 24 20 16 10  5 -0 -5 -8-11-11-11 -9 -7 -4 -1
 18 18 20 21 23 26 27 29 29 28 25 22 17 12  7  2 -3 -7-10-11-11-10 -8 -6 -3  0
 28 28 26 29 30 31 31 30 29 26 23 19 14  8  3 -2 -6 -9-11-12-11-10 -7 -4 -1  2
 33 33 33 33 33 32 31 29 27 23 19 14  9  4 -0 -5 -8-10-12-11-10 -8 -6 -3  0  3
 35 35 35 34 33 31 29 26 23 19 14 10  5  0 -4 -7-10-11-12-11 -9 -7 -4 -1  2  4
 34 33 33 32 30 28 25 21 18 13  9  4  0 -4 -7-10-11-12-11-10 -8 -5 -2  1  3  5
 29 29 28 26 24 22 19 15 12  7  3 -1 -4 -7-10-11-12-12-11 -9 -6 -3 -0  2  5  6
 22 22 21 20 17 15 12  9  5  1 -2 -5 -8-10-12-12-12-11 -9 -7 -4 -1  1  4  6  7
 14 14 13 12 10  7  5  2 -1 -4 -7 -9-11-12-13-12-12-11 -9 -7 -5 -2  1  3  5  7  7
  6  6  5  4  2  0 -2 -4 -5 -9-10-12-13-13-12-11-10 -8 -5 -2  0  3  5  6  7  8
 -2 -2 -2 -3 -5 -6 -8 -9-11-12-13-13-13-12-11-10 -8 -5 -3 -0  2  4  6  7  7  7
 -8 -8 -8 -9-10-11-12-12-13-14-14-13-12-11 -9 -7 -5 -3 -0  2  4  6  7  7  7  6
-12-12-12-13-13-14-14-14-14-14-13-12-11 -9 -7 -4 -2  0  2  4  6  7  7  7  6  5
-14-14-15-15-15-15-14-14-13-12-11-10 -8 -6 -4 -1  1  3  5  6  7  7  7  6  5  4
-15-15-15-14-14-14-13-12-11-10 -8 -7 -5 -3 -0  2  3  5  6  7  7  7  6  5  4  2
-13-13-13-12-12-11-11 -9 -8 -7 -5 -3 -1  1  3  4  6  7  7  8  7  7  5  4  2  1
-10-10-10 -9 -9 -8 -7 -6 -4 -3 -1  0  2  4  5  6  7  8  8  8  8  7  7  5  4  2  1 -1
 -6 -6 -6 -5 -5 -4 -3 -2 -1  1  2  4  5  6  7  8  8  8  8  7  6  4  2  1 -1 -3
 INTERVAL =   1.0362945E-02 NUMBER INTERVALS = 51 SUM =   0.
```

PHASE

QUADRANT 1, 100 CORRESPONDS TO TWO PI

```
-16-16-16-16-16-17-17-19-32 43 39 39 38 38 39 39 39 39 40 41 41 43 45 48-45-35
-16-16-16-16-16-16-16-16-15-17-23 45 40 39 39 39 39 39 40 40 41 42 43 45 48-45
-17-17-17-17-17-16-16-16-15-16-16-18-26 44 40 39 39 39 39 40 40 41 42 43 45 48
-19-19-19-18-18-17-17-17-15-16-16-16-16-19-42 42 40 39 39 39 40 40 41 42 43 45
-21-21-21-21-20-19-18-18-17-17-16-16-16-16-16-17-26 44 40 40 39 40 40 40 41 42 43
-26-26-25-24-23-22-21-20-19-18-17-17-16-16-16-16-17-21 48 41 40 40 40 40 40 41 42
-36-35-34-33-32-28-26-23-22-20-19-18-17-16-16-16-16-16-19-48 41 40 40 40 40 41 41
-47-47-46-45-42-39-35-31-27-24-21-19-18-17-16-16-15-16-16-19-48 41 40 40 40 40 41
 45 45 46 47 48 50-47-43-37-31-26-23-20-18-17-16-15-15-16-16-19 48 41 40 40 40 40
 42 42 42 43 43 44 46 48-48-43-36-29-24-20-18-17-16-15-15-15-15-20 45 41 40 40 40
 40 40 40 41 41 42 43 44 45 48-46-39-31-25-21-18-17-15-15-15-15-16-26 43 41 40 40
 38 38 38 39 39 40 41 42 43 44 47-48-41-32-25-20-18-16-15-15-15-15-16-43 42 41 40
 36 36 36 37 37 38 39 40 41 42 44 46 50-42-32-24-19-17-15-15-14-15-19 46 41 41
 33 34 34 35 36 36 37 38 40 41 42 44 46 50-42-30-22-18-16-15-14-14-15-30 43 41
 29 29 30 31 33 34 36 37 38 39 41 42 44 46-48-39-27-20-17-15-14-14-14-17 49 42
 21 21 23 25 28 31 33 35 37 38 40 41 42 44 47-47-35-24-18-16-15-14-14-15-28 44
  9  9 11 14 19 24 29 33 35 37 39 40 41 43 45 48-43-29-20-17-15-14-14-14-18 48
  1  2  2  4  7 13 21 28 33 36 38 39 41 42 43 46-48-37-24-18-15-14-13-14-15-38
 -1 -1 -1 -1  1  3  9 19 29 34 37 39 40 41 43 44 48-43-28-19-16-14-13-13-14-23
 -3 -3 -3 -2 -1 -0  2  8 22 32 36 38 40 41 42 43 46-48-34-21-16-14-13-13-14-18
 -4 -4 -4 -4 -3 -2 -1  2 11 27 35 38 39 40 42 43 45 49-40-23-17-15-13-13-13-16
 -5 -5 -5 -5 -4 -4 -2 -0  4 20 33 37 39 40 41 42 44 47-44-26-18-15-13-13-13-15
 -5 -5 -5 -5 -5 -4 -3 -2  1 12 31 36 39 40 41 42 44 46-46-29-18-15-14-13-13-14
 -6 -6 -6 -5 -5 -5 -4 -3 -3  7 28 36 39 40 41 42 43 45-48-32-19-15-14-13-13-14
 -6 -6 -6 -6 -5 -5 -4 -3 -1  4 26 36 38 40 41 42 43 45-49-34-20-15-14-13-13-14
```

QUADRANT 4, 100 CORRESPONDS TO TWO PI

```
-6 -6 -6 -6 -5 -5 -5 -4 -2  4 25 35 38 40 41 42 43 45 50-34-20-15-14-13-13-14
-6 -6 -6 -6 -5 -5 -4 -3 -1  4 26 35 38 40 41 42 43 45-49-34-20-15-14-13-13-14
-6 -6 -6 -6 -5 -5 -4 -3 -0  7 28 36 39 40 41 42 43 45-48-32-19-15-14-13-13-14
-5 -5 -5 -5 -5 -4 -3 -2  1 12 31 35 39 40 41 42 44 46-46-29-19-15-14-13-13-14
-5 -5 -5 -4 -4 -4 -2 -0  4 20 33 37 39 40 41 42 44 47-44-26-18-15-13-13-13-15
-4 -4 -4 -4 -3 -2 -1  2 11 27 35 38 39 40 42 43 45 49-40-23-17-15-13-13-13-16
-3 -3 -3 -2 -1 -0  2  8 22 32 36 38 40 41 42 43 46-48-34-21-16-14-13-13-14-18
-1 -1 -1 -1  1  3  9 19 29 34 37 39 40 41 43 44 48-43-28-19-16-14-13-13-14-23
 1  2  2  4  7 13 21 28 33 36 38 39 41 42 43 46-48-37-24-18-15-14-13-14-15-38
 9  9 11 14 19 24 29 33 35 37 39 40 41 43 45 48-43-29-20-17-15-14-14-14-18 48
21 21 23 25 28 31 33 35 37 38 40 41 42 44 47-47-35-24-18-16-15-14-14-15-28 44
29 29 30 31 33 34 36 37 38 39 41 42 44 46-48-39-27-20-17-15-14-14-14-17 49 42
33 34 34 35 36 36 37 38 40 41 42 44 46 50-42-30-22-18-16-15-14-14-15-30 43 41
36 36 36 37 37 38 39 40 41 42 44 46 50-42-32-24-19-17-15-15-14-15-19 46 41 41
38 38 38 39 39 40 41 42 43 44 47-48-41-32-25-20-18-16-15-15-15-16-43 42 41 40
40 40 40 41 41 42 43 44 45 48-46-39-31-25-21-18-17-15-15-15-16-26 43 41 40 40
42 42 42 43 43 44 46 48-48-43-36-29-24-20-18-17-16-15-15-15-20 45 41 40 40 40
45 45 46 47 48 50-47-43-37-31-26-23-20-18-17-16-15-15-16-19 48 41 40 40 40 40
-47-47-46-45-42-39-35-31-27-24-21-19-18-17-16-16-15-16-19-48 41 40 40 40 40 41
-36-35-34-33-30-28-26-23-22-20-19-18-17-16-16-16-16-16-19-48 41 40 40 40 40 41 41
-26-26-25-24-23-22-21-20-19-18-17-17-16-16-16-17-21 48 41 40 40 40 40 40 41 42
-21-21-21-20-20-19-18-18-17-17-16-16-16-16-16-17-26 44 40 40 39 40 40 40 41 42 43
-19-19-18-18-18-17-17-17-16-16-16-16-16-19-42 42 40 39 39 39 40 40 41 42 43 45
-17-17-17-17-17-16-16-16-16-16-16-16-18-26 44 40 39 39 39 39 40 40 41 42 43 45 48
-16-16-16-16-16-16-16-16-16-17-23 45 40 39 39 39 39 39 40 40 41 42 43 45 48-45
-16-16-16-16-16-17-17-19-32 43 39 39 38 38 39 39 39 39 40 41 41 43 45 48-45-35
```

FOR THIS FIELD ANGLE AND WAVELENGTH 26 RAYS WERE VIGNETTED OR OBSCURED,
0 RAYS FAILED TO CONVERGE IN SSRT.

RECEIVER TEST CASE *1

CHIEF RAY DATA FOR LOCAL OSCILLATOR.

FIELD ANGLE (RADIANS) = 0.0000000

CHIEF RAY COORDINATES ON SURFACE N

X	Y	Z
0.	0.	0.

DIRECTION COSINES ON SURFACE N-1

L	M	N
0.	0.	1.00000000E+00

RADIUS RW AND POSITION TR OF EXIT PUPIL

RW	TR
1.11200000E+02	0.

TILT AND DISPLACEMENT OF EXIT PUPIL IN X- AND Y-DIRECTIONS

XTILT	YTILT	XOISP	YOISP
0.	0.	0.	0.

WAVEFRONT ERROR INFORMATION

VARIANCE = 3.63318706E-15
RMS = 4.71549876E-15
WAVELENGTH = 1.06113850E-02
MAXIMUM UNNORMALIZED ERROR= 5.55111512E-17
MINIMUM UNNORMALIZED ERROR=-2.22044605E-16
MAXIMUM NORMALIZED ERROR= 5.23128237E-15
MINIMUM NORMALIZED ERROR=-2.09251295E-14
APPROXIMATE STREHL RATIO = 1.00000000E+00

RECEIVER TEST CASE *1

ASF (REAL), FOR LOCAL OSCILLATOR.
  QUADRANT 1, 100 CORRESPONDS TO 2.00436003E+00

```
 67 67 66 66 66 65 65 64 64 63 62 61 60 59 58 57 56 54 53 51 50 48 47 45 44 42
 69 69 69 68 68 68 67 67 66 65 64 63 62 61 60 59 58 56 55 53 52 50 49 47 45 44
 71 71 71 71 70 70 69 69 68 67 66 65 64 63 62 61 60 58 57 55 54 52 50 49 47 45
 73 73 73 73 73 72 72 71 70 69 69 68 66 65 64 63 62 60 59 57 55 54 52 50 49 47
 75 75 75 75 75 74 74 73 72 71 71 70 68 67 66 65 63 62 60 59 57 56 54 52 50 48
 78 77 77 77 77 76 76 75 74 73 73 72 70 69 68 67 65 64 62 61 59 57 55 54 52 50
 80 80 79 79 79 78 78 77 75 75 74 73 72 71 70 68 67 66 64 62 61 59 57 55 53 51
 81 81 81 81 81 80 80 79 78 77 76 75 74 73 72 70 69 67 66 64 62 60 59 57 55 53
 83 83 83 83 83 82 81 81 80 79 78 77 76 75 73 72 70 69 67 66 64 62 60 58 56 54
 85 85 85 85 84 84 83 83 82 81 80 79 78 76 75 73 72 70 69 67 65 63 62 60 58 56
 87 87 87 86 86 85 85 84 83 82 81 80 79 78 76 75 73 72 70 68 67 65 63 61 59 57
 88 88 88 88 88 87 86 86 85 84 83 82 81 79 78 76 75 73 72 70 68 66 64 62 60 58
 90 90 90 90 89 89 88 87 86 85 84 83 82 81 79 78 76 75 73 71 69 67 65 63 61 59
 91 91 91 91 91 90 89 89 88 87 86 85 83 82 81 79 78 76 74 72 70 68 66 64 62 60
 93 93 93 92 92 91 91 90 89 88 87 86 85 83 82 80 79 77 75 73 72 70 68 65 63 61
 94 94 94 93 93 93 92 91 90 89 88 87 86 84 83 81 80 78 76 74 73 71 69 66 64 62
 95 95 95 95 94 94 93 92 91 90 89 88 87 85 84 82 81 79 77 75 73 71 69 67 65 63
 96 96 96 96 95 95 94 93 92 91 90 89 88 86 85 83 82 80 78 76 74 72 70 68 66 64
 97 97 97 96 96 96 95 94 93 92 91 90 89 87 86 84 83 81 79 77 75 73 71 69 67 64
 98 98 98 97 97 96 96 95 94 93 92 91 89 88 86 85 83 81 80 78 76 74 72 69 67 65
 98 98 98 98 98 97 96 96 95 94 93 91 90 89 87 85 84 82 80 78 76 74 72 70 68 65
 99 99 99 98 98 98 97 96 95 94 93 92 91 89 88 86 84 83 81 79 77 75 73 70 68 66
 99 99 99 99 98 98 97 96 95 95 93 92 91 90 88 86 85 83 81 79 77 75 73 71 68 66
100100100 99 99 98 98 97 95 95 94 93 91 90 88 87 85 83 81 79 77 75 73 71 69 66
100100100 99 99 98 98 97 95 95 94 93 91 90 88 87 85 83 81 80 77 75 73 71 69 67
```

QUADRANT 2, 100 CORRESPONDS TO 2.0E436003E+00

```
42 44 45 47 48 50 51 53 54 56 57 58 59 60 61 62 63 64 64 65 65 66 66 66 67
44 45 47 49 50 52 53 55 55 58 59 60 61 62 63 64 65 66 67 67 68 68 68 69 69
45 47 49 50 52 54 55 57 58 60 61 62 63 64 65 66 67 68 69 69 70 70 71 71 71
47 49 50 52 54 55 57 59 60 62 63 64 65 66 68 69 69 70 71 72 72 73 73 73 73
48 50 52 54 56 57 59 60 62 63 65 66 67 68 70 71 71 72 73 74 74 75 75 75 75
50 52 54 55 57 59 61 62 64 65 67 68 69 70 72 73 73 74 75 76 76 77 77 77 77
51 53 55 57 59 61 62 64 66 67 68 70 71 72 73 74 75 76 77 78 78 79 79 79 80
53 55 57 59 60 62 64 66 67 69 70 72 73 74 75 76 77 78 79 80 80 81 81 81 81
54 56 58 60 62 64 66 67 69 70 72 73 75 76 77 78 79 80 81 81 82 83 83 83 83
56 58 60 62 63 65 67 69 70 72 73 75 76 78 79 80 81 82 83 83 84 84 85 85 85
57 59 61 63 65 67 68 70 72 73 75 75 78 79 80 81 82 83 84 85 85 86 86 87 87
58 60 62 64 66 68 70 72 73 75 76 78 79 81 82 83 84 85 86 86 87 88 88 88 88
59 61 63 65 67 69 71 73 75 76 78 79 81 82 83 84 85 86 87 88 89 89 90 90 90
60 62 64 66 68 70 72 74 75 78 79 81 82 83 85 86 87 88 89 89 90 91 91 91 91
61 63 65 68 70 72 73 75 77 79 80 82 83 85 86 87 88 89 90 91 91 92 92 93 93
62 64 66 69 71 73 74 76 78 80 81 83 84 86 87 88 89 90 91 92 93 93 93 94 94
63 65 67 69 71 73 75 77 79 81 82 84 85 87 88 89 90 91 92 93 94 94 95 95 95
64 66 68 70 72 74 76 78 80 82 83 85 86 88 89 90 91 92 93 94 95 95 96 96 96
64 67 69 71 73 75 77 79 81 83 84 86 87 89 90 91 92 93 94 95 96 96 96 97 97
65 67 69 72 74 76 78 80 81 83 85 86 88 89 91 92 93 94 95 96 96 97 97 98 98
65 68 70 72 74 76 78 80 82 84 85 87 89 90 91 93 94 95 96 96 97 98 98 98 98
66 68 70 73 75 77 79 81 83 84 86 88 89 91 92 93 94 95 96 97 98 98 98 99 99
66 68 71 73 75 77 79 81 83 85 86 88 90 91 92 93 95 96 96 97 98 98 99 99 99
66 69 71 73 75 77 79 81 83 85 87 88 90 91 93 94 95 96 97 98 98 99 9910 0100
67 69 71 73 75 77 80 81 83 85 87 88 90 91 93 94 95 96 97 98 98 99 9910 0100
```

QUADRANT 3, 100 CORRESPONDS TO 2.00436003E+00

```
67 69 71 73 75 78 80 81 83 85 87 88 90 91 93 94 95 96 97 98 99 99 1000100
67 69 71 73 75 77 80 81 83 85 87 88 90 91 93 94 95 96 97 98 98 99 1000100
66 69 71 73 75 77 79 81 83 85 87 88 90 91 93 94 95 96 97 98 98 99 1000100
66 68 71 73 75 77 79 81 83 85 86 88 90 91 92 93 95 96 96 97 98 98 99 99 99
66 68 70 73 75 77 79 81 83 84 86 88 89 91 92 93 94 95 96 97 98 98 98 99 99
65 68 70 72 74 76 78 80 82 84 85 87 89 90 91 93 94 95 96 96 97 98 98 98 98
65 67 69 72 74 76 78 80 81 83 85 85 88 89 91 92 93 94 95 96 96 97 97 98 98
64 67 69 71 73 75 77 79 81 83 84 85 87 89 90 91 92 93 94 95 96 96 96 97 97
64 66 68 70 72 74 76 78 80 82 83 85 86 88 89 90 91 92 93 94 95 95 96 96 96
63 65 67 69 71 73 75 77 79 81 82 84 85 87 88 89 90 91 92 93 94 94 95 95 95
62 64 66 69 71 73 74 76 78 80 81 83 84 86 87 88 89 90 91 92 93 93 93 94 94
61 63 65 68 70 72 73 75 77 79 80 82 83 85 86 87 88 89 90 91 91 92 92 93 93
60 62 64 66 68 70 72 74 76 78 79 81 82 83 85 86 87 88 89 89 90 91 91 91 91
59 61 63 65 67 69 71 73 75 76 78 79 81 82 83 84 85 86 87 88 89 89 90 90 90
58 60 62 64 66 68 70 72 73 75 76 78 79 81 82 83 84 85 86 86 87 88 88 88 88
57 59 61 63 65 67 69 70 72 73 75 75 78 79 80 81 82 83 84 85 85 86 86 87 87
56 58 60 62 63 65 67 69 70 72 73 75 76 78 79 80 81 82 83 83 84 84 85 85 85
54 56 58 60 62 64 66 67 69 70 72 73 75 76 77 78 79 80 81 81 82 83 83 83 83
53 55 57 59 60 62 64 66 67 69 70 72 73 74 75 76 77 78 79 80 80 81 81 81 81
51 53 55 57 59 61 62 64 65 67 68 70 71 72 73 74 75 76 77 78 78 79 79 79 80
50 52 54 55 57 59 61 62 64 65 67 68 69 70 72 73 73 74 75 76 76 77 77 77 77
48 50 52 54 56 57 59 60 62 63 65 66 67 68 70 71 71 72 73 74 74 75 75 75 75
47 49 51 52 54 55 57 59 60 62 63 64 65 66 68 69 69 70 71 72 72 73 73 73 73
45 47 49 51 52 54 55 57 58 60 61 62 63 64 65 66 67 68 69 69 70 70 71 71 71
44 45 47 49 50 52 53 55 56 58 59 60 61 62 63 64 65 66 67 67 68 68 68 69 69
42 44 45 47 48 50 51 53 54 56 57 58 59 60 61 62 63 64 64 65 65 66 66 66 67
```

QUADRANT 4, 100 CORRESPONDS TO 2.0643600J3E+06

```
100100100 99 99 98 98 97 95 95 94 93 91 90 88 87 85 83 81 80 79 75 73 71 69 67
100100100 99 99 98 98 97 95 95 94 93 91 90 88 87 85 83 81 80 77 75 73 71 69 67
100100100 99 99 98 98 97 96 95 94 93 91 90 88 87 85 83 81 79 77 75 73 71 69 66
 99 99 99 99 98 98 97 96 95 95 93 92 91 90 88 86 85 83 81 79 77 75 73 71 68 66
 99 99 99 98 98 98 97 96 95 94 93 92 91 89 88 86 84 83 81 79 77 75 73 70 68 66
 98 98 98 98 98 97 96 96 95 94 93 91 90 89 87 85 84 82 80 78 76 74 72 70 68 65
 98 98 98 97 97 96 96 95 94 93 92 91 89 88 86 85 83 81 80 78 76 74 72 69 67 65
 97 97 97 96 96 96 95 94 93 92 91 90 89 87 86 84 83 81 79 77 75 73 71 69 67 64
 96 96 96 96 95 95 94 93 92 91 90 89 88 86 85 83 82 80 78 76 74 72 70 68 66 64
 95 95 95 95 94 94 93 92 91 90 89 88 87 85 84 82 81 79 77 75 73 71 69 67 65 63
 94 94 94 93 93 93 92 91 90 89 88 87 86 84 83 81 80 78 76 74 73 71 69 66 64 62
 93 93 93 92 92 91 91 90 89 88 87 86 85 83 82 80 79 77 75 73 72 70 68 65 63 61
 91 91 91 91 91 90 89 89 88 87 96 95 83 82 81 79 78 76 74 72 70 68 66 64 62 60
 90 90 90 90 89 89 88 87 86 85 84 83 82 81 79 78 76 75 73 71 69 67 65 63 61 59
 88 88 88 88 88 87 86 86 85 84 93 82 81 79 78 76 75 73 72 70 68 66 64 62 60 58
 87 87 87 86 86 85 85 84 83 82 91 80 79 78 76 75 73 72 70 68 67 65 63 61 59 57
 85 85 85 85 84 84 83 83 82 81 80 79 78 76 75 73 72 70 69 67 65 63 62 60 58 56
 83 83 83 83 83 82 81 81 80 79 78 77 76 75 73 72 7C 69 67 66 64 62 60 58 56 54
 81 81 81 81 81 80 80 79 78 77 76 75 74 73 72 70 69 67 66 64 62 60 59 57 55 53
 80 80 79 79 79 78 78 77 75 75 74 73 72 71 70 68 67 66 64 62 61 59 57 55 53 51
 78 77 77 77 77 76 76 75 74 73 73 72 70 69 68 67 65 64 62 61 59 57 55 54 52 50
 75 75 75 75 75 74 74 73 72 71 71 70 68 67 66 65 63 62 60 59 57 56 54 52 50 48
 73 73 73 73 73 72 72 71 70 69 69 68 66 65 64 63 62 60 59 57 55 54 52 50 49 47
 71 71 71 71 70 70 69 69 68 67 66 65 64 63 62 61 60 58 57 55 54 52 50 49 47 45
 69 69 69 68 68 68 67 67 66 65 64 63 62 61 61 59 58 56 55 53 52 50 49 47 45 44
 67 67 66 66 66 65 65 64 64 63 62 61 60 59 59 57 56 54 53 51 50 48 47 45 44 42
 INTERVAL =   1.03629545E-02 NUMBER INTERVALS = 51 SUM =   0.
```

RECEIVER TEST CASE *1

ASF (IMAGINARY),FOR LOCAL OSCILLATOR.
QUADRANT 1, 100 CORRESPONDS TO 2.42048796E-09

```
-71-71-7[-7[-69-68-67-65-63-61-57-53-50-45-42-38-35-30-22-18-14 -9 -5 -3 -1  0
-71-71-71-7[-7]-69-67-66-64-61-57-53-49-45-41-38-34-29-21-17-13 -8 -4 -2 -0  1
-71-71-71-7[-70-69-67-65-63-61-57-53-49-44-41-37-33-28-20-16-11 -6 -2 -0  2  3
-70-70-7[-7[-69-68-67-65-63-60-56-52-48-43-39-36-32-27-19-14 -9 -4 -0  2  4  5
-67-67-66-66-65-64-63-61-53-56-52-48-44-39-36-32-28-23-15-10 -5  0  4  6  8  9
-61-61-61-6[-60-59-57-55-53-51-47-43-39-34-30-27-23-17 -9 -5 -0  5  9 11 13 14
-57-57-56-56-55-54-53-51-49-46-42-38-34-29-26-22-18-13 -5  0  5 10 14 16 17 18
-52-52-52-52-51-50-49-47-45-42-38-34-30-25-21-18-14 -8 -0  5  9 15 19 20 21 22
-43-43-43-42-42-41-40-38-35-33-29-25-21-16-13 -9 -5 -0  8 13 17 23 27 28 29 30
-37-37-37-37-36-36-34-32-30-28-24-20-16-11 -7 -4  0  5 14 18 23 28 32 33 34 35
-34-34-34-33-33-32-31-29-27-24-20-16-12 -7 -3 -0  4  9 18 22 27 32 36 37 38 38
-30-30-3[-3[-29-29-27-25-23-21-17-12 -8 -4 -0  3  7 13 21 26 30 36 39 41 41 42
-27-27-27-26-26-25-24-22-20-17-13 -9 -5  0  4  7 11 16 25 29 34 39 43 44 45 45
-22-22-22-21-21-20-19-17-15-12 -8 -4 -0  5  8 12 16 21 30 34 39 44 48 49 49 50
-18-18-18-17-17-16-15-13-11 -8 -4  0  4  9 12 16 20 25 34 38 43 48 52 53 53 53
-14-14-13-13-13-12-11 -9 -7 -4  [  4  8 13 17 20 24 29 38 42 47 52 56 57 57 57
 -9 -9 -9 -9 -8 -8 -6 -4 -3 -0  4  8 12 17 21 24 28 33 42 46 51 56 60 61 61 61
 -7 -7 -6 -6 -6 -5 -4 -2 -0  3  7 11 15 20 23 27 30 36 45 49 53 59 63 63 64 63
 -5 -5 -5 -4 -4 -3 -2 -0  2  4  9 13 17 22 25 29 32 38 47 51 55 61 65 65 66 65
 -3 -3 -3 -2 -2 -1 -0  2  4  6 11 15 19 24 27 31 34 40 49 53 57 63 67 67 67 67
 -2 -2 -1 -1 -1 -0  1  3  5  8 12 16 20 25 29 32 36 41 50 54 59 64 68 69 69 68
 -1 -1 -1 -0 -0  1  2  4  6  8 13 17 21 26 29 33 36 42 51 55 60 65 69 70 70 69
 -0 -0 -0 -0  0  1  2  4  6  9 13 17 21 26 30 33 37 42 52 56 60 66 70 70 70 70
 -0 -0 -0  0  1  1  3  5  6  9 13 18 22 27 30 34 37 43 52 56 61 66 70 71 71 70
 -0 -0  0  0  1  2  3  5  7  9 14 18 22 27 30 34 37 43 52 57 61 67 70 71 71 71
```

QUADRANT 2, 100 CORRESPONDS TO 2.42048798E-09

```
-89-91-93-95-94-92-91-90-88-87-86-82-80-78-77-75-73-72-72-71-71-70-71-71-71
-91-94-95-97-96-94-93-92-87-85-84-83-81-79-78-76-74-73-72-71-71-71-71-71-71
-93-95-97-99-98-96-94-93-88-86-84-83-82-80-78-76-74-73-72-71-71-71-71-71-71
-95-97-99-00-99-97-95-94-89-86-85-84-82-80-78-76-73-72-72-71-70-70-70-70-70
-94-96-98-99-98-96-94-92-87-84-82-81-79-77-75-73-70-69-68-67-67-67-66-67-67
-92-94-96-97-96-93-91-89-83-80-78-77-75-72-70-68-65-64-63-62-61-61-61-61-61
-91-93-94-95-94-91-89-87-80-77-75-74-72-69-66-64-61-60-59-58-57-57-57-57-57
-90-92-93-94-92-89-87-84-78-74-72-71-68-65-63-60-57-55-54-53-53-52-52-52-52
-86-87-88-89-87-83-80-78-71-67-65-63-61-57-54-52-48-47-46-44-44-43-43-43-43
-83-85-86-86-84-80-77-74-67-63-61-59-56-53-50-47-43-42-40-39-38-38-38-37-37
-82-84-84-85-82-78-75-72-65-61-58-56-53-50-47-43-40-38-37-35-35-34-34-34-34
-82-83-83-84-81-77-74-70-63-59-56-54-51-47-44-41-37-35-34-32-31-31-31-30-30
-80-82-82-82-79-75-72-68-61-56-53-51-48-44-41-37-34-32-30-29-28-27-27-27-27
-78-79-80-80-77-72-69-65-57-53-50-47-44-40-36-33-29-27-26-24-23-22-22-22-22
-77-78-78-78-75-70-66-63-54-50-47-44-41-37-33-29-25-23-22-20-19-18-18-18-18
-75-76-76-76-73-68-64-60-52-47-43-41-37-33-29-26-22-19-18-16-15-14-14-14-14
-73-74-74-73-70-65-61-57-48-43-40-37-34-29-25-22-17-15-13-12-11-10 -9 -9 -9
-72-73-73-72-69-64-60-55-47-42-38-35-32-27-23-19-15-13-11 -9 -8 -7 -7 -7 -7
-72-72-72-72-68-63-59-54-45-40-37-34-30-26-22-18-13-11 -9 -7 -6 -6 -5 -5 -5
-71-71-71-71-67-62-58-53-44-39-35-32-29-24-20-16-12 -9 -7 -6 -4 -4 -3 -3 -3
-71-71-71-70-67-61-57-53-44-38-35-31-28-23-19-15-11 -8 -6 -4 -3 -2 -2 -2 -2
-71-71-71-70-67-61-57-52-43-38-34-31-27-22-18-14-10 -7 -6 -4 -2 -2 -1 -1 -1
-71-71-71-70-66-61-57-52-43-38-34-31-27-22-18-14 -9 -7 -5 -3 -2 -1 -1 -0 -0
-71-71-71-70-67-61-57-52-43-37-34-30-27-22-18-14 -9 -7 -5 -3 -2 -1 -0 -0 -0
-71-71-71-70-67-61-57-52-43-37-34-30-27-22-18-14 -9 -7 -5 -3 -2 -1 -0 -0 -0
```

QUADRANT 3, 100 CORRESPONDS TO 2.42048798E-09

```
-71-71-71-7L-67-61-57-52-43-37-34-30-27-22-18-14 -9 -7 -5 -3 -2 -1 -0 -0 -0
-71-71-71-7L-67-61-57-52-43-37-34-30-27-22-18-14 -9 -7 -5 -3 -2 -1 -0 -0 -0
-70-71-71-7C-66-61-56-52-43-37-34-30-27-22-18-13 -9 -6 -5 -3 -1 -1 -0 -0  0
-70-70-70-7L-66-60-56-52-42-37-33-30-26-21-17-13 -9 -6 -4 -2 -1 -0  0  0  0
-69-70-70-69-65-60-55-51-42-36-33-29-26-21-17-13 -8 -6 -4 -2 -1  0  0  1  1
-68-69-69-68-64-59-55-50-41-36-32-29-25-20-16-12 -8 -5 -3 -1  0  1  1  1  2
-67-67-67-67-63-57-53-49-40-34-31-27-24-19-15-11 -6 -4 -2  0  1  2  2  3  3
-65-66-65-65-61-55-51-47-38-32-29-25-22-17-13 -9 -4 -2  0  2  3  4  4  5  5
-63-64-63-63-59-53-49-45-36-30-27-23-20-15-11 -7 -3  0  2  4  5  6  6  6  7
-61-61-61-60-56-51-46-42-33-28-24-21-17-12 -8 -4  0  3  4  6  8  8  9  9  9
-57-57-57-56-52-47-42-38-29-24-20-17-13 -8 -4 -0  4  7  9 11 12 13 13 13 14
-53-53-53-52-48-43-38-34-25-20-16-12 -9 -4 -0  4  8 11 13 15 16 17 17 18 18
-50-49-49-48-44-39-34-30-21-16-12 -8 -5 -0  4  8 12 15 17 19 20 21 21 22 22
-45-45-44-43-39-34-29-25-16-11 -7 -4 -0  5  9 13 17 20 22 24 25 26 26 27 27
-42-41-41-39-36-30-26-21-13 -7 -3  0  4  8 12 17 21 23 25 27 29 29 30 30 30
-38-38-37-36-32-27-22-18 -9 -4  0  3  7 12 16 20 24 27 29 31 32 33 33 34 34
-35-34-33-32-28-23-18-14 -5 -0  4  7 11 16 20 24 28 30 32 34 36 36 37 37 37
-30-29-28-27-23-17-13 -8  0  5  9 13 16 21 25 29 33 36 38 40 41 42 42 43 43
-22-21-20-19-15 -9 -5  0  8 14 18 21 25 30 34 38 42 45 47 49 50 51 52 52 52
-18-17-16-14-10 -5 -0  5 13 18 22 25 29 34 38 42 46 49 51 53 54 55 56 56 57
-14-13-11 -9 -5  0  5  9 17 23 27 30 34 39 43 47 51 53 55 57 59 60 60 61 61
 -9 -8 -6 -4 -0  5 10 15 23 28 32 36 39 44 48 52 56 59 61 63 64 65 66 66 67
 -5 -4 -2  L  4  9 14 19 27 32 36 39 43 48 52 56 60 63 65 67 68 69 70 70 70
 -3 -2  0  2  6 11 16 20 28 33 37 41 44 49 53 57 61 63 65 67 69 70 70 71 71
 -1  0  2  4  8 13 17 21 29 34 38 41 45 49 53 57 61 64 65 67 69 70 70 71 71
 -0  1  3  5  9 14 18 22 30 35 38 42 45 50 53 57 61 63 65 67 68 69 70 70 71
```

QUADRANT 4, 100 CORRESPONDS TO 2.42048798E-09

```
-0   0   0       1   2   3   5   7   9  14  18  22  27  30  34  37  43  52  57  61  67  70  71  71  71
 0   0   0   .   1   2   3   5   7   9  14  18  22  27  30  34  37  43  52  57  61  67  70  71  71  71
 0   0   0   .   1   2   3   5   7   9  14  18  22  27  30  34  37  43  52  57  61  67  70  71  71  71
 0   0   0   1   1   2   3   5   7   9  14  18  22  27  31  34  38  43  52  57  61  66  70  71  71  71
 1   1   1   1   2   2   4   6   7  10  14  18  22  27  31  34  38  43  52  57  61  67  70  71  71  71
 2   2   2   2   2   3   4   6   8  11  15  19  23  28  31  35  39  44  53  57  61  67  70  71  71  71
 3   3   3   3   4   4   6   7   9  12  16  20  24  29  32  35  39  44  53  58  62  67  71  71  71  71
 5   5   5   5   6   6   7   9  11  13  18  22  26  30  34  37  40  46  54  59  63  68  72  72  72  72
 7   7   7   7   7   8   9  11  13  15  19  23  27  32  35  38  42  47  55  60  64  69  72  73  73  72
 9   9   9   9  10  11  12  13  15  17  22  25  29  34  37  40  43  48  57  61  65  70  73  74  74  73
14  14  14  14  14  15  15  16  19  22  26  29  33  37  41  43  47  52  60  64  68  73  76  76  76  75
18  18  18  18  18  19  20  22  23  25  29  33  37  41  44  47  50  54  63  66  70  75  78  78  78  77
22  22  22  22  22  23  24  26  27  29  33  36  40  44  47  50  53  57  65  69  72  77  80  80  79  78
27  27  27  27  27  28  29  30  32  34  37  41  44  48  51  53  56  61  68  72  75  79  82  82  82  80
30  30  30  31  31  31  32  34  35  37  41  44  47  51  54  56  59  63  70  74  77  81  84  83  83  82
34  34  34  34  34  35  35  37  38  40  43  47  50  53  56  58  61  65  72  75  78  82  85  84  84  82
37  37  37  36  36  38  39  40  42  43  47  50  53  56  59  61  63  67  74  77  80  84  86  86  85  83
43  43  43  43  43  44  44  46  47  48  52  54  57  61  63  65  67  71  78  80  83  87  89  88  87  86
52  52  52  52  52  53  53  54  55  57  60  63  65  68  71  72  74  78  84  86  89  92  94  93  92  90
57  57  57  57  57  57  58  59  60  61  64  66  69  72  74  75  77  80  87  89  91  94  95  94  93  91
61  61  61  61  61  61  62  63  64  65  68  70  72  75  77  78  80  83  89  91  93  96  97  96  94  92
67  67  67  66  67  67  67  68  69  70  73  75  77  79  81  82  84  87  92  94  96  98  99  98  96  94
70  70  70  70  70  70  71  72  72  73  76  78  80  82  84  85  86  89  94  95  97  99100  99  97  95
71  71  71  71  71  71  71  72  73  74  76  78  80  82  83  84  86  88  93  94  96  98  99  97  95  93
71  71  71  71  71  71  71  72  73  74  76  78  79  81  83  84  85  87  92  93  94  96  97  95  94  91
71  71  71  71  70  71  71  72  72  73  75  77  78  80  82  82  83  86  90  91  92  94  95  93  91  89
INTERVAL =    1.13629545E-02 NUMBER INTERVALS = 51 SUM =    0.
```

PHASE

QUADRANT 1, 100 CORRESPONDS TO TWO PI

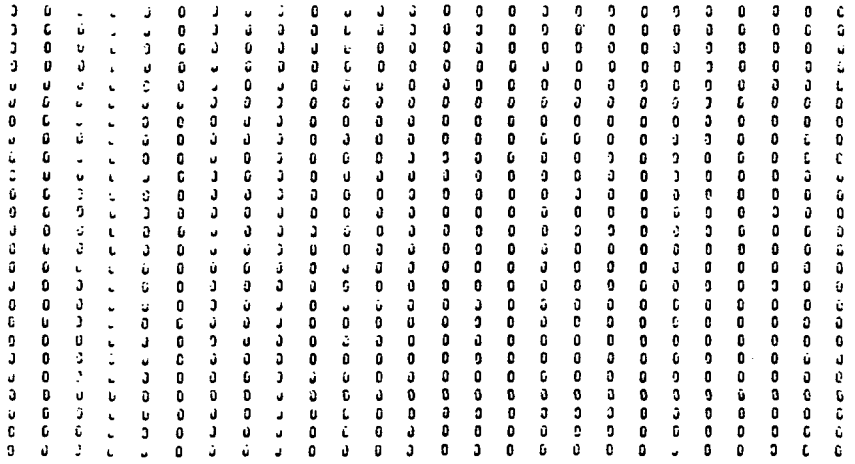

QUADRANT 4, 100 CORRESPONDS TO TWO PI

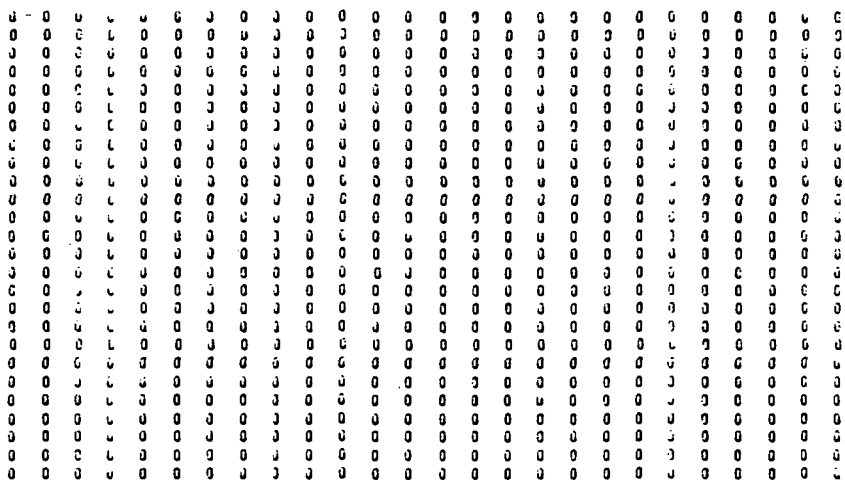

```
RECEIVER TEST CASE *1


DETECTOR COMPUTATIONS.


DETECTOR NO. = 1
RECEIVED SIGNAL BEAM IS SHIFTED X =  0.              AND Y =  0.
WITH RESPECT TO CENTER OF DETECTOR.

LOCAL OSCILLATOR BEAM IS SHIFTED X =  0.             AND Y =  0.
WITH RESPECT TO CENTER OF DETECTOR.

CIRCULAR DETECTOR DIAMETER =  2.07259091E-01

 SIGNAL POWER =  1.5947653E+04
LOCAL OSCILLATOR POWER =  1.2859427E-01
CROSS PRODUCT POWER =  3.6025826E+01
PHASE MATCH EFFICIENCY =  3.5953111E-01 (    -.018 DB )
AVERAGE PHASE SHIFT (RADIANS) =  2.6263201E-01
OPTICAL TRANSMISSION =  9.7581079E-01 (    -.106 DB )
FOCUSING EFFICIENCY =  7.5431726E-01 (   -1.167 DB )
NON-HETERODYNE DETECTION EFFICIENCY =  7.4582903E-01 (   -1.274 DB )
L.O. ILLUMINATION EFFICIENCY =  8.2911054E-01 (    -.814 DB )
MAXIMUM ANTENNA GAIN =  2.3862915E+09 (   93.777 DB )
RECEIVER EFFICIENCY TO I.F. =  4.7204378E-01 (   -3.260 DB )

                        * * * * * * * *
```

APPENDIX D

```
RECEIVER TEST CASE #2
$INP  BETAL(1) = 53.975,2.621, M(1) = 0.,..., MAG(1) = 0.,1., IFLG1(1) = 0,0,
N(1)  = -1.,-1, M(1) = 1,13,  XLINV(1) = 0., -9.4356957-4,
RADS(1) = 0., -1028., 0., 52.83152, 34.0868, 3*0., -105.12044, -161.5964,
RADS(11) = 3*0., 1163.18358, 668.2130+, 0., -105.1204+, -161.5694, 0., 0.,
TS(1) = 0., -514., -32.1, -2., -910., 0., 0., -193., -2.,0.,
TS(11) =  -100.3, 0., 0., -2., -392., -193., -2.,0., -100.3, 0.,
XMUS(1) = 1., -1., -1., -4.00062, 4*-1., -4.00062, 4*-1.,
XMUS(14)=-4.00062, -1., -1., -4.00062, 3*-1.,
SKAPA(2) = 0.,
PZERO(1) = -1.-6, 1.-3,
ZOMEGA = 1.525,
$END
```

* * * * * LACOMA - LASER COMMUNICATOR ANALYSIS PROGRAM * * * * *

* * * * * PAGOS CORPORATION * * * * *

RECEIVER TEST CASE *2

RECEIVED SIGNAL OPTICAL DATA.

N -12 BETA0 5.397500J0E+01 H 0. PZERO -1.0.000000E-06

M 1 XLINV 0. MAG 0. IFLG1 0

SURFACE PARAMETERS

SURF. NO.	CURVATURE RHOS	SEPARATION TS	INDEX XMUS	OBSCURATION DATA BETAPX	OBSCURATION DATA BETAPY	VIGNETTING DATA BETASX	VIGNETTING DATA BETASY
1	0.	0.	1.000000	0.	0.	0.	0.
2	-9.7276265E-04	-5.1400000E+02	-1.000000	0.	0.	0.	0.
3	0.	-3.2100000E+01	-1.000000	0.	0.	0.	0.
4	1.6938849E-02	-2.0000000E+00	-4.000620	0.	0.	0.	0.
5	2.9336869E-02	-9.1000000E+02	-1.000000	0.	0.	0.	0.
6	0.	0.	-1.000000	0.	0.	0.	0.
7	0.	0.	-1.000000	0.	0.	0.	0.
8	0.	-1.9300000E+02	-1.000000	0.	0.	0.	0.
9	-9.5128978E-03	-2.0000000E+00	-4.000620	0.	0.	0.	0.
10	-6.1862567E-03	0.	-1.000000	0.	0.	0.	0.
11	0.	-1.0030000E+02	-1.000000	0.	0.	0.	0.
12	0.	0.	-1.000000	0.	0.	0.	0.

SURFACE	SKAPA	ASPHERIC COEFFICIENTS ALPHA	BETA	GAMMA	DELTA	EPSILON
2	0.	0.	0.	0.	0.	0.

FIELD ANGLE = 0.

LOCAL OSCILLATOR OPTICAL DATA.

M -8 BETAJ 2.62100000E+06 H 0. PZERO 1.0.0000000E-03

M 13 XLINV -9.4056957JE-04 MAG 0. IFLG1 0

SURFACE PARAMETERS

SURF. NO.	CURVATURE RHOS	SEPARATION TS	INDEX XMUS	OBSCURATION DATA BETAPX	BETAPY	VIGNETTING DATA BETASX	BETASY
13	0.	0.	-1.000000	0.	0.	0.	0.
14	9.4056957E-04	-2.0000000E+00	-4.000620	0.	0.	0.	0.
15	1.4955287E-03	-3.9200000E+02	-1.000000	0.	0.	0.	0.
16	0.	-1.9300000E+02	-1.000000	0.	0.	0.	0.
17	-9.5168978E-03	-2.0000000E+00	-4.000620	0.	0.	0.	0.
18	-6.1892908E-03	0.	-1.000000	0.	0.	0.	0.
19	0.	-1.0130000E+02	-1.000000	0.	0.	0.	0.
20	0.	0.	-1.000000	0.	0.	0.	0.

FIELD ANGLE = 0.

NXY = 25 NDET = 1 NFRS = 26
DELFS = 0. ZOMEGA = 1.62500000E+00 VLAMDA = 1.96113850E-02

DETECTOR DATA.

DETECTOR NO. 1 IDETEC = 1 0 0 0 0

PARAXIAL RAY TRACE - RECEIVED SIGNAL OPTICS.

BETA	B	ALPHA	A
5.3975[illegible]E+01	0.	0.	1.85270959E-02
5.3975[illegible]E+01	-1.05309728E-01	0.	1.85270959E-02
2.27377675E-13	-1.05009728E-01	9.52292728E+00	1.85270959E-02
-3.37[illegible]E+0[illegible]	-2.96567218E-01	1.01176471E+01	5.93495660E-01
-3.519[illegible]E+0[illegible]	1.32125346E-02	1.04143489E+01	-3.23266946E-01
8.5[illegible]E+01	1.32125346E-02	-2.83758572E+02	-3.23266946E-01
8.5[illegible]E+01	1.32125346E-02	-2.83758572E+02	-3.23266946E-01
8.5[illegible]E+01	1.32125346E-02	-2.83758572E+02	-3.23266946E-01
1.1[illegible]E+01	-3.02329449E-01	-3.46149093E+02	9.55741745E+00
1.[illegible]E+01	-3.98720322E-02	-3.41371125E+02	3.21863129E+00
1.[illegible]E+01	-3.98720322E-02	-3.41371125E+02	3.21863129E+00
8.[illegible]E-01	-3.98720322E-02	-1.85424068E+01	3.21863129E+00

PARAXIAL ENTRANCE PUPIL POSITION T(0) = -0. TEXIT= -1. [illegible]E+02

INVERSE OBJECT DISTANCE XLINV = 0.

FOCAL LENGTH = 5.[illegible]E+02 BACK FOCAL LENGTH = -1.09171853E+02

TS(N-1) = -1.09171853E+02 FL = 5.4044175[illegible]E+02

PARAXIAL RAY TRACE - LOCAL OSCILLATOR OPTICS.

BETA	B	ALPHA	A
2.621[illegible]E+JC	0.	0.	3.81533766E-01
2.621[illegible]E+JC	7.39722595E-03	0.	3.81533766E-01
2.624598J4E+JC	-4.38301631E-03	1.90737319E-01	3.80677257E-01
9.[illegible]3648E-01	-4.399J1631E-03	1.49416222E+02	3.8J677257E-01
5.712J50J7E-02	-6.01358329E-03	2.22886933E+02	-5.99153915E+J0
5.41141755E-J2	-5.J1459053E-03	2.19896627E+02	-1.89768283E+J0
5.41141755E-J2	-5.J1459053E-03	2.19896627E+02	-1.89768283E+00
-4.46849255E-01	-5.01459J53E-03	2.95590392E+01	-1.89768283E+00

PARAXIAL ENTRANCE PUPIL POSITION T(0) = -0. TEXIT= -1.15876385E+02

INVERSE OBJECT DISTANCE XLINV = -9.40569570E-04

FOCAL LENGTH = 5.22674781E+02 BACK FOCAL LENGTH = -1.07913448E+01

TS(N-1) = -1.08589893E+02 FL = -3.61664382E+02

RECEIVER TEST CASE #2

CHIEF RAY DATA FOR RECEIVED SIGNAL.

FIELD ANGLE (RADIANS) = 0.00000000

CHIEF RAY COORDINATES ON SURFACE N

X	Y	Z
0.	0.	0.

DIRECTION COSINES ON SURFACE N-1

L	M	N
0.	0.	-1.00000000E+00

RADIUS RW AND POSITION TR OF EXIT PUPIL

RW	TR
-3.11689258E+00	-1.06060960E+02

TILT AND DISPLACEMENT OF EXIT PUPIL IN X- AND Y-DIRECTIONS

XTILT	YTILT	XDISP	YDISP
0.	0.	0.	0.

WAVEFRONT ERROR INFORMATION

VARIANCE = 2.31695638E-02
RMS = 3.55589700E-02
WAVELENGTH = 1.06113850E-02
MAXIMUM UNNORMALIZED ERROR= 0.
MINIMUM UNNORMALIZED ERROR=-8.11953341E-04
MAXIMUM NORMALIZED ERROR= 0.
MINIMUM NORMALIZED ERROR=-7.65177534E-02
APPROXIMATE STREHL RATIO = 9.50081996E-01

RECEIVER TEST CASE *2

CHIEF RAY DATA FOR LOCAL OSCILLATOR.

FIELD ANGLE (RADIANS) = 0.0000000

CHIEF RAY COORDINATES ON SURFACE N

X	Y	Z
0.	0.	0.

DIRECTION COSINES ON SURFACE N-1

L	M	N
0.	0.	-1.0000000E+00

RADIUS RW AND POSITION TR OF EXIT PUPIL

RW	TR
-7.2713567[illegible]E+01	-1.1587638[illegible]E+02

TILT AND DISPLACEMENT OF EXIT PUPIL IN X- AND Y-DIRECTIONS

XTILT	YTILT	XOISP	YOISP
0.	0.	0.	0.

WAVEFRONT ERROR INFORMATION

VARIANCE = 2.42966574E-05
RMS = 3.6415494[illegible]E-03
WAVELENGTH = 1.0611385[illegible]E-02
MAXIMUM UNNORMALIZED ERROR= 3.72142444E-10
MINIMUM UNNORMALIZED ERROR=-8.63965902E-07
MAXIMUM NORMALIZED ERROR= 3.50731105E-08
MINIMUM NORMALIZED ERROR=-8.16072456E-05
APPROXIMATE STREHL RATIO = 9.99999348E-01

RECEIVER TEST CASE #2

DETECTOR COMPUTATIONS.

DETECTOR NO. = 1
RECEIVED SIGNAL BEAM IS SHIFTED X = 0. AND Y = 0.
WITH RESPECT TO CENTER OF DETECTOR.

LOCAL OSCILLATOR BEAM IS SHIFTED X = 0. AND Y = 0.
WITH RESPECT TO CENTER OF DETECTOR.

CIRCULAR DETECTOR DIAMETER = 1.29624814E-01

SIGNAL POWER = 8.21899L5E-07
LOCAL OSCILLATOR POWER = 1.2831695E-05
CROSS PRODUCT POWER = 2.8425164E-05
PHASE MATCH EFFICIENCY = 9.9621555E-01 (-.032 DB)
AVERAGE PHASE SHIFT (RADIANS) = 9.3388E54E-02
OPTICAL TRANSMISSION = 9.987291CE-01 (-.006 DB)
FOCUSING EFFICIENCY = 8.2294493E-01 (-.846 DB)
NON-HETERODYNE DETECTION EFFICIENCY = 8.2189905E-01 (-.852 DB)
L.O. ILLUMINATION EFFICIENCY = 8.7864877E-01 (-.562 DB)
MAXIMUM ANTENNA GAIN = 1.0214119E+09 (90.092 DB)
RECEIVER EFFICIENCY TO I.F. = 6.2373198E-01 (-2.008 DB)

* * * * * * * *

```
MULTIPLE DETECTORS
$INP
NDET = 4,
IDETEC(1,1) = 1,0,0,0,0,
IDETEC(1,2) = 2,0,0,0,0,
IDETEC(1,3) = 1,0,0,10,0,
IDETEC(1,4) = 2,0,0,10,0,
$END
```

```
 MULTIPLE DETECTORS


 DETECTOR COMPUTATIONS.


 DETECTOR NO. = 1
 RECEIVED SIGNAL BEAM IS SHIFTED X =  0.              AND Y =  0.
 WITH RESPECT TO CENTER OF DETECTOR.

 LOCAL OSCILLATOR BEAM IS SHIFTED X =  0.              AND Y =  0.
 WITH RESPECT TO CENTER OF DETECTOR.

 CIRCULAR DETECTOR DIAMETER =  1.29624814E-01

 SIGNAL POWER =  8.21899[illegible]3E-07
LOCAL OSCILLATOR POWER =  1.2830695E-05
CROSS PRODUCT POWER =  2.642516[illegible]4E-06
PHASE MATCH EFFICIENCY =  9.9621559E-01 (    -.002 DB )
AVERAGE PHASE SHIFT (RADIANS) =  9.3388654E-02
OPTICAL TRANSMISSION =  9.8872910E-01 (    -.006 DB )
FOCUSING EFFICIENCY =  8.2294493E-01 (    -.846 DB )
NON-HETERODYNE DETECTION EFFICIENCY =  8.2189905E-01 (    -.852 DB )
L.O. ILLUMINATION EFFICIENCY =  8.7864877E-01 (    -.562 DB )
MAXIMUM ANTENNA GAIN =  1.0214119E+09 (   90.092 DB )
RECEIVER EFFICIENCY TO I.F. =  6.2973198E-01 (   -2.008 DB )

                        * * * * * * * *


 DETECTOR NO. = 2
 RECEIVED SIGNAL BEAM IS SHIFTED X =  0.              AND Y =  0.
 WITH RESPECT TO CENTER OF DETECTOR.

 LOCAL OSCILLATOR BEAM IS SHIFTED X =  0.              AND Y =  0.
 WITH RESPECT TO CENTER OF DETECTOR.

 RECTANGULAR DETECTOR DIMENSIONS ARE X =  1.29624814E-01 AND Y =  1.29624814E-01

 SIGNAL POWER =  8.2926663E-07
LOCAL OSCILLATOR POWER =  1.7861969E-05
CROSS PRODUCT POWER =  2.6546892E-06
PHASE MATCH EFFICIENCY =  9.3992926E-01 (    -.027 DB )
AVERAGE PHASE SHIFT (RADIANS) =  5.4334257E-02
OPTICAL TRANSMISSION =  9.9872910E-01 (    -.006 DB )
FOCUSING EFFICIENCY =  8.3032189E-01 (    -.808 DB )
NON-HETERODYNE DETECTION EFFICIENCY =  8.2926663E-01 (    -.813 DB )
L.O. ILLUMINATION EFFICIENCY =  7.9052018E-01 (   -1.021 DB )
MAXIMUM ANTENNA GAIN =  1.0214119E+09 (   90.092 DB )
RECEIVER EFFICIENCY TO I.F. =  4.5783655E-01 (   -3.393 DB )

                        * * * * * * * *


 DETECTOR NO. = 3
 RECEIVED SIGNAL BEAM IS SHIFTED X = -6.48124670E-02 AND Y =  0.
 WITH RESPECT TO CENTER OF DETECTOR.

 LOCAL OSCILLATOR BEAM IS SHIFTED X = -6.48124070E-02 AND Y =  0.
 WITH RESPECT TO CENTER OF DETECTOR.

 CIRCULAR DETECTOR DIAMETER =  1.29624814E-01

 SIGNAL POWER =  3.6728301E-07
LOCAL OSCILLATOR POWER =  1.2681518E-05
```

```
CROSS PRODUCT POWER =  9.2049442E-07
PHASE MATCH EFFICIENCY =  5.9923812E-01 (    -.222 DB )
AVERAGE PHASE SHIFT (RADIANS) = -2.6784753E-02
OPTICAL TRANSMISSION =  9.9872910E-01 (    -.006 DB )
FOCUSING EFFICIENCY =  3.6775039E-01 (   -4.344 DB )
NON-HETERODYNE DETECTION EFFICIENCY =  3.6728301E-01 (   -4.359 DB )
L.O. ILLUMINATION EFFICIENCY =  7.1173252E-01 (   -1.477 DB )
MAXIMUM ANTENNA GAIN =  1.0214119E+09 (   90.092 DB )
RECEIVER EFFICIENCY TO I.F. =  6.6808747E-02 (  -11.752 DB )

                        * * * * * * * *


 DETECTOR NO. = 4
 RECEIVED SIGNAL BEAM IS SHIFTED X = -6.4812407DE-02 AND Y =  0.
 WITH RESPECT TO CENTER OF DETECTOR.

 LOCAL OSCILLATOR BEAM IS SHIFTED X = -6.4812407JE-02 AND Y =  0.
 WITH RESPECT TO CENTER OF DETECTOR.

 RECTANGULAR DETECTOR DIMENSIONS ARE X =  1.29624814E-01 AND Y =  1.29624814E-01

 SIGNAL POWER =  4.7612335E-07
LOCAL OSCILLATOR POWER =  1.7595453E-05
CROSS PRODUCT POWER =  1.2503753E-06
PHASE MATCH EFFICIENCY =  5.2912031E-01 (    -.201 DB )
AVERAGE PHASE SHIFT (RADIANS) = -1.6887601E-03
OPTICAL TRANSMISSION =  9.9872910E-01 (    -.006 DB )
FOCUSING EFFICIENCY =  4.7572923E-01 (   -3.217 DB )
NON-HETERODYNE DETECTION EFFICIENCY =  4.7612335E-01 (   -3.223 DB )
L.O. ILLUMINATION EFFICIENCY =  6.9650314E-01 (   -1.634 DB )
MAXIMUM ANTENNA GAIN =  1.0214119E+09 (   90.092 DB )
RECEIVER EFFICIENCY TO I.F. =  8.8812059E-02 (  -10.515 DB )

                        * * * * * * * *
```